Study of Natural Ventilation Design by Integrating the Multi-zone Model with CFD Simulation

by

Gang Tan

M.S. Tsinghua University
Beijing, China, 2001

Submitted to the Department of Architecture in
Partial Fulfillment of the Requirements for the Degree of
Doctor of Philosophy in the Field of Architecture: Building Technology

at the

Massachusetts Institute of Technology

February 2005

Signature of Author .....
Department of Architecture
January 7, 2005

Certified by..... .....
Leon R. Glicksman
Professor of Building Technology and Mechanical Engineering
Thesis supervisor

Accepted by .....
Stanford Anderson
Head, Department of Architecture
Chairman, Departmental Committee on Graduate Students

Thesis Committee:
Leon R. Glicksman, Professor of Building Technology and Mechanical Engineering
Leslie K. Norford, Professor of Building Technology
Ain A. Sonin, Professor of Mechanical Engineering

Study of Natural Ventilation Design by Integrating the Multi-zone Model with CFD Simulation

by
Gang Tan

Submitted to the Department of Architecture
on January 7, 2005 in Partial Fulfillment of the
Requirements for the Degree of Doctor of Philosophy
in the field of Architecture: Building Technology

Abstract

Natural ventilation is widely applied in sustainable building design because of its energy saving, indoor air qualify and indoor thermal environment improvement. It is important for architects and engineers to accurately predict the performance of natural ventilation, especially in the building design stage. Unfortunately, there is not any good public tool available to predict the natural ventilation design. The integration of the multi-zone model and the computational fluid dynamics (CFD) simulation provides a way to assess the performance of natural ventilation in whole buildings, as well as the detailed thermal environmental information in some particular space.

This work has coupled the multi-zone airflow model with the thermal model. A new program, called MultiVent, has been developed with a web-server that can provide on-line calculation for the public. The MultiVent program can simultaneously simulate the indoor air temperature and airflow rate with known indoor heat sources for buoyancy dominated, buoyancy-wind combined and wind dominated cases.

To properly apply the MultiVent program to the natural ventilation design, two configurations in naturally ventilated buildings should be carefully studied: the atrium and large openings between the zones. A criterion has been set up for dividing the large opening and the connected atrium space into at least two sub-openings and sub-zones.

The results of the MultiVent calculation can provide boundary conditions to the CFD simulation for some particular zone. In order to correctly simulate the particular space with CFD, the location and conditions at the integrating surface (boundary surface) have been studied. This work suggested that the simulation zone should include part of the connected atrium space when the occupied room is simulated with CFD. There are two options to integrate the MultiVent and CFD simulation through different boundary conditions: velocity (mass) integration and pressure integration. The case studies of this work showed that both of them can generate good CFD simulation results.

Thesis Supervisor: Leon R. Glicksman
Title: Professor of Building Technology and Mechanical Engineering

Acknowledgements

The author would like to express his gratitude to those whose support was essential for the completion of this thesis.

I am deeply in debt to Professor Leon R. Glicksman for his sound guidance and supervision. His knowledge and smart ideas have always helped me building and finishing my research approaches. My thanks extend for this wealth of enthusiasm and insight that has been a continual source of inspiration for this work. I feel grateful to have this opportunity to work on this thesis under his supervision.

I would like to thank my thesis committee members, Professor Leslie K. Norford and Ain A. Sonin, for providing me with valuable advice and direction to improve the thesis. My cordial thanks extend to Professor Norford for his advice and help while I was working as his teaching assistant. I would also express my sincere gratitude to Professor Qingyan Chen from Purdue University for his advice and kind help.

To Christine Walker, who worked on the Luton model building experiment, I am grateful her cooperation and sharing of results. Also I want to thank her for the comments on my thesis writing.

I thank Lara Greden, Matthew Lehar, Zhiqiang Zhai, Yi Jiang, Yang Gao and Jinchao Yuan, for their time and knowledgeable help in natural ventilation studies, CFD simulation and thesis preparation. My other co-workers and friends at M.I.T. have given advice and made this a more rewarding experience. My special thanks are to Renee A. Caso, Kathleen Ross and Nancy Dalrymple for their considerate and kind supports.

My sincere love and thanks to my parents, Xianying Fu and Chuanrong Tan, my parents-in-law, Wuming Chen and Shaocheng Chen, I am thankful their support for all these years. Finally, I would like to express the deepest love and gratitude to my wife, Guo Chen, for her love and tireless support.

Dedication

To my wife and my parents.

Contents

Chapter 1

Introduction

1.1 Sustainable building design and natural ventilation

With the modern technology development, the world has achieved significant changes: prospective life increase, convenient and fast transportation, plenty of food and industrial products. However, as we enjoy the progress brought about by technology achievements, we also have to face all the "side effects" of this development: fast population growth, resource limitations, and environmental pollution. More and more people understood that we must transfer our development style into sustainability. In simple words, sustainable development is the challenge of meeting growing human needs for natural resources, industrial products, energy, food, transportation and effective waste management while conserving and protecting environmental quality and the natural resource base essential for future life and development [1].

Buildings provide shelter to people. They consume a lot of materials, a large portion of energy (see Table 1.1) and produce much waste when they are destroyed. Thus, the sustainability of buildings is imperative. The concept of sustainable buildings is a comprehensive idea that reflects each stage of the whole life of a building.

Table 1.1 U.S. residential and commercial buildings total primary energy consumption (quads and percent of total)*

Year	Natural Gas		Petroleum		Coal		Renewable		Electricity	
1980	7.52	28%	3.04	11%	0.15	1%	0.88	3%	14.95	56%
1990	7.22	25%	2.17	7%	0.16	1%	0.68	2%	19.13	65%
2000	8.42	22%	2.22	6%	0.10	0%	0.57	2%	26.30	70%
2001	8.27	22%	2.21	6%	0.10	0%	0.55	1%	26.45	70%
2005	9.07	23%	2.15	5%	0.11	0%	0.58	1%	28.39	70%
2010	9.45	22%	2.14	5%	0.11	0%	0.58	1%	30.69	71%
2020	10.41	22%	2.06	4%	0.12	0%	0.59	1%	34.89	73%
2025	10.95	22%	2.03	4%	0.12	0%	0.60	1%	37.14	73%

**Source: Building Energy Databook: 1.1 Building Sector Energy Consumption. Web link: http://buildingsdatabook.eren.doe.gov/frame.asp?p=tableview.asp&TableID=505&t=pdf. The data of year 2005, 2010, 2020 and 2025 are estimated based on the past years.*

In the traditional building construction process, we build a building at a new place by using materials from cutting trees, producing bricks and concrete. During construction, a

lot of energy, such as electricity, is consumed. After construction, a constant energy flow is still provided into the building to meet people's work and comfort requirement. When the building finishes its task, it is destroyed and buried into a hole.

Comparing with the traditional construction process, a sustainable building construction process would create new buildings from the old, and would be self-powered, emitting no pollutants. Unfortunately, we are fairly far away from a truly sustainable construction process. The US Green Building Council sees five basic components of the green design, which they have included in the LEED Rating System. They are: sustainable site design, water efficiency, energy and atmosphere, materials and resources, and indoor environmental quality. So the Green Design might be considered as a way move to a more sustainable design.

After the energy crisis of 1970's, more and more people tried to find and use more renewable energy. Natural ventilation is one type of renewable/natural energy, which can reduce the energy consumption of HVAC systems in buildings, especially for buildings located in temperate weather areas, such as those in the United Kingdom (see Figure 1.1). Furthermore, natural ventilation is a promising strategy for improving the indoor air quality while reducing Sick Building Syndrome (SBS).

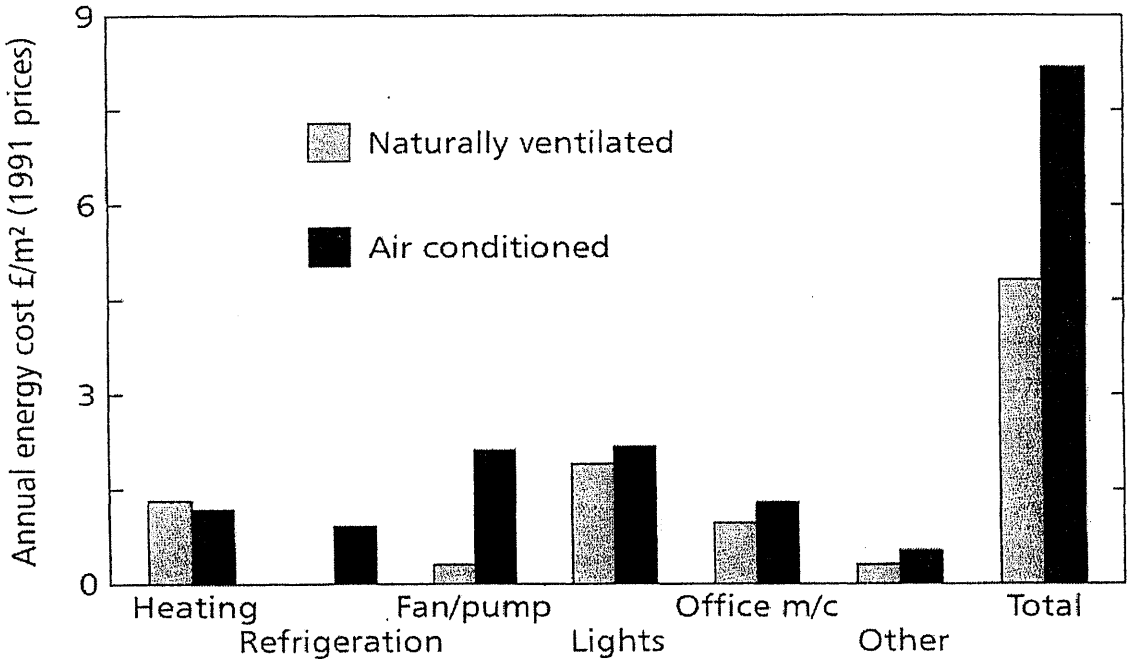

Figure 1.1 Energy costs in U.K. commercial buildings: Benefits of natural ventilation (by Q.Y. Chen)

Natural ventilation uses the buoyancy force induced by the temperature difference between inside and outside air temperatures or wind pressure force generated by the outside wind [2]. In order to maintain a satisfactory indoor environment, natural and mechanical systems can be combined in hybrid ventilation systems as described in IEA Annex 35 [3]. Some people have summarized several advantages of natural ventilation as (http://www.sunnorth.com/ventilation-info.html):

- 85% reduction in cost of electricity
- Reduced dust that comes from air-supply ducts
- Reduced heating cost if combined with a heat exchanger
- Reduced operating costs
- Reduced noise level that comes from the fan-cool unit in air-conditioning system
- Improved odor control for most conditions with total fresh air supply
- Ventilation functions in the event of a power failure
- Summer ventilation rates can be high

In summer, a night cooling method is widely used in hot climate areas. Compared with mechanical ventilation, natural ventilation has a much higher air exchange rate. For instance, the air exchange rate of natural ventilation generally can reach 10~20 ACH (air exchange rate per hour), while most mechanical ventilation only provides 3~5 ACH for commercial or residential buildings. For air to move into and out of a building, a pressure difference between the inside and outside of the building is required. Wind can blow air through openings in the facade on the windward side of the building, and suck air out of openings on the leeward side and the roof. This is due to the high pressure at the windward side and low pressure at the leeward side that can be understood by using fluid dynamics analysis. To increase the airflow rate induced by wind, designers should carefully consider at least two factors: orientation and floor plan. The orientation of the building determines the wind pressure distribution around the building facades, which can optimize the wind force. In addition to the strength of the wind force between the windward and leeward sides of the building, the resistance of the flow path in the building will significantly affect the airflow rate. Therefore, large size openings can often be found in naturally ventilated buildings.

In other word, when designing with natural ventilation in mind, an architect and/or engineer must have separate strategies for winter and summer. In winter, only small airflows are needed for cooling, or the building needs heating. However, in summer it works best to move the ambient cooler air collected at night passing through the building. Rooms should ideally all have inlet and outlet openings, preferably located on opposite sides and/or opposing pressure zones, such as the leeward and windward walls, or a

windward wall and the roof. Of course, these inlet and outlet openings may simply be accounted for with operable windows.

When utilizing operable windows, it's important to distinguish whether the windows provide single-sided or cross ventilation to spaces. Then, there is also a choice among horizontal pivot windows, vertical pivot windows, or casement windows. Most engineers believe that horizontal pivot windows offer the best capacity for ventilation because they can provide the most efficient opening area and the lowest flow resistance.

The buoyancy force is another way to promote the airflow rates of natural ventilation. In order to enhance the stack effect, an atrium and/or a chimney can be used because the pressure difference induced by buoyancy is proportional to the height of the building. In addition to the height, buoyancy force also depends on the temperature difference between inside and outside of buildings. As we know, buoyancy pressure can be simply written as:

$$P_S = \rho g h \Delta T /(T + 273) \tag{1-1}$$

where, P_S is the buoyancy (stack) pressure (Pa), ρ is the air density (kg/m^3), T is the air temperature (^oC), ΔT is the air temperature difference between inside and outside of the building (^oC).

The airflow rate can be calculated by using the pressure difference. Equation (1-2) shows a widely used power-law formula [4] to calculate airflow as:

$$F = C_d A(\frac{\Delta P}{2\rho})^n \tag{1-2}$$

where, F is the airflow rate (kg/s), C_d is the discharge coefficient of the opening that describes the flow resistance of the opening, A is the area of the opening (m^2), and ΔP is the pressure drop at the opening (Pa).

It is obvious that there is an interactive effect between the indoor air temperature and the airflow rate. If the indoor air temperature has a larger difference comparing with outside air temperature, the airflow rate will be greater. However, if the airflow increases, the indoor air temperature will drop and thus decrease the air temperature difference since generally the heat source inside the building is relatively constant. Therefore, when we

predict natural ventilation performance, we need to iterate the indoor air temperature and airflow rate.

Figure 1.2 shows an example building located in Luton, UK, which applies the buoyancy ventilation, cross ventilation and hybrid ventilation strategies with the concrete floor thermal mass.

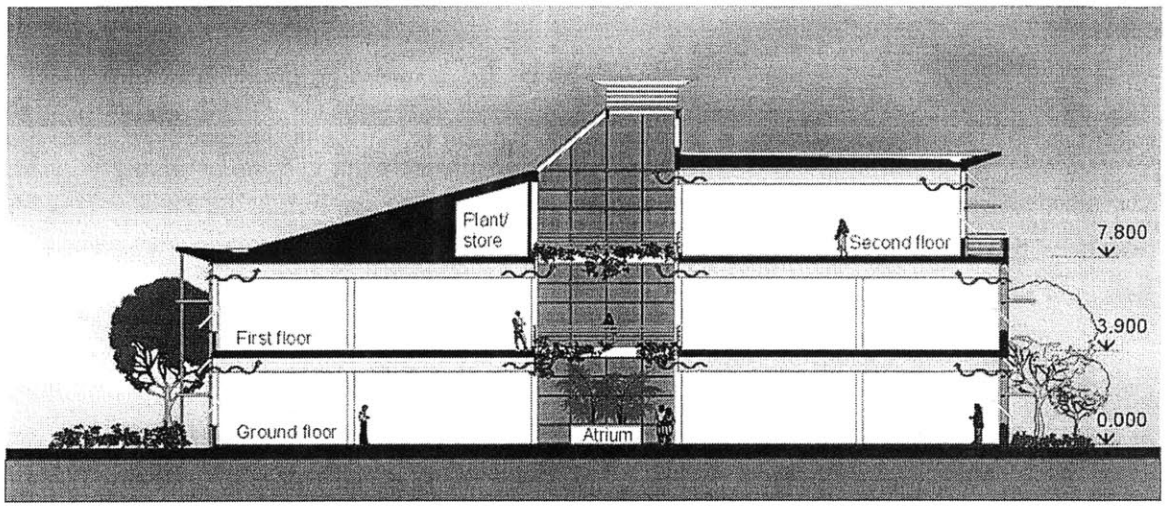

Figure 1.2 A naturally ventilated building in Luton, UK, by Vincent and Gorbing Limited

1.2 Research on natural ventilation

1.2.1 Obstacles in natural ventilation prediction

Natural ventilation is currently widely studied and applied in newly-built buildings, especially in the buildings designed with sustainable (or green) concepts. However, natural ventilation is much more difficult than the mechanical ventilation system to accurately predict its performance. There are three main factors impacting the prediction:

- Geometric dimensions and configurations of the naturally ventilated buildings
- Fluctuations of the driving forces in natural ventilation
- Uncertainty of people's preference on temperature and airflow movement

First, the typical naturally ventilated buildings, especially for commercial use, often have large-scale dimensions and numerous rooms. There is also an atrium that interconnects several floors. This will cause a heavy calculation burden for natural ventilation prediction with computational fluid dynamics (CFD) tools.

As we know, the driving forces of natural ventilation, buoyancy or/and wind, are not as easy as mechanical ventilation to describe because the outside wind has a fluctuating direction and magnitude. These fluctuating characteristics would definitely affect the movement and distribution of particles or VOCs (volatile organic compound) in naturally ventilated buildings. Some recent research was shown that the fluctuating characteristics of natural ventilation could affect its mean airflow rate [5, 6]. People also found that the natural wind's frequency energy spectrum follows the rule of 1/f (f is the fluctuating frequency of the wind velocity), which has this similar rule of 1/f in the frequency energy spectrum as human being heartbeats [7, 8]. The impacts of airflow velocity's frequency on human thermal sensation were studied by previous research of others. It was found that the frequency between 0.3Hz and 0.5 Hz has the strongest cooling effect, and the energy of natural wind mainly lies in the low frequency 0~0.5Hz, i.e. the essence of natural wind makes humans feel cooler and more comfortable in the neutral-warm environment [9, 10]. Besides the fluctuation of outside wind, the buoyancy force is not as constant as we expected, although it seems steadier than outside wind, because the heat transfer from heat sources to indoor air varies with time.

In addition, some unpredictable parameters may be introduced into the natural ventilation prediction, such as the preference of occupants, the strength of internal heat sources and their locations in buildings, and the opening status of the windows and doors. For the occupied naturally ventilated buildings, it is very difficult to control the performance of natural ventilation. Several research studies on control strategies and systems have been carried out. Passen [11] has studied the strategies of building energy savings by using the controlled natural ventilation windows.

Admittedly, some other factors in natural ventilation also will affect our prediction for natural ventilation. For instance, the terrains around the building location and the heights of the surrounding buildings definitely have strong impacts on the natural ventilation performance, particularly for the wind-driven ventilation. The shielding effects of these adjacent buildings on wind pressure differences between windward and leeward walls of the shielded building also have been studied by Aynsely [12], which is important to accurately predict the wind-driven natural ventilation.

1.2.2 Current prediction methods for natural ventilation

There are many difficulties in predicting natural ventilation, but a lot of research has been carried out to make people understand more about natural ventilation. In summary, there are four methods for studying natural ventilation:

1. Model/field experimental methods

Field experiments can provide time-average airflow rates passing through a naturally ventilated building. Due to the complexity of a naturally ventilated building, it is not easy to get good measurements from field tests. Tsutsumi et al [13] has carried out a full-scale measurement of indoor thermal factors in a house, which was compared with numerical simulation. In this measurement, the air flow speed, air temperature, wet bulb temperature, and globe temperature in the house were recorded.

Compared to a field experiment, a model experiment is much more controllable and reliable for studying natural ventilation. In order to investigate the wind pressure coefficients around buildings, people have built model buildings and put them into a wind tunnel to measure the pressures surrounding the building. Jozwiak [14] presented wind tunnel investigations to the aerodynamic interference effects on the pressure distribution on a building adjacent to another one. In this test, a model, made to 1:100 scale, was set up behind a turbulent flow development system.

The experiments also can be designed to study particular parts of a natural ventilation building. Flourentzou [15] has measured the discharge coefficients by setting up model experiments of windows. This study was undertaken to improve our knowledge on velocity and discharge coefficients when measured in real buildings. It provides additional detailed information on the velocity coefficients, jet contraction coefficients and discharge coefficients.

2. Analytical methods

Natural ventilation can be predicted via analytical or empirical calculations. Assumptions are generally made in order to simplify the problem and derive simplified equations that govern the complex phenomena. These methods are generally applied to simple-

geometry buildings, e.g. single-sided ventilation and one-zone buildings with two openings.

There are many models based on simple analytical formulas. For instance, Chen [16] et al has developed a simple multi-layer stratification model for displacement ventilation (in buoyancy ventilation) in a single-zone building driven by a heat source distributed uniformly over a vertical wall. Theoretical expressions for the stratification interface height and ventilation flow rate were obtained, which was then compared with those obtained by an existing model, resulting in a good agreement with the experiment measurements.

Although some analytical methods have the advantage of simple calculations, they are only suitable to deal with small or single-zone buildings. In general conditions, the analytical methods need not include a network for calculation, thus it converges very quickly when compared with the multi-zone model.

3. Multi-zone model methods

With the design of natural ventilation systems for passive cooling (cool the building with natural forces, such as wind and buoyancy effects, without any mechanical system assistance) in buildings, engineers and architects are interested in the prediction of ventilation rates as a function of position and size of the ventilation openings. In common use, there are relatively detailed (i.e. multi-zone) ventilation models which rely on the Bernoulli algorithm to describe airflow through openings.

The multi-zone model provides a simple method, compared with computation fluid dynamics method. It takes a room (space) within a building as one homogeneous node with a uniform temperature and pressure that is connected to others by openings between rooms and/or openings to the outside. This approach is user-friendly in terms of problem definition, straightforward internal representation and calculation procedure. These advantages allow the prediction of bulk flow through the whole building driven by wind, buoyancy or mechanical systems. However, a multi-zone model cannot represent detailed temperature and airflow distributions within a single space, due to its 'well-mixed' assumption.

The multi-zone model has advantages with its ease of use, straightforward application and fast convergence. Several commercial programs based on the multi-zone model are

available, such as COMIS [17] and CONTAM [18]. Although these programs have not focused on the prediction of natural ventilation, they contain excellent methods to model and solve the mass and energy balance equations for multi-zone buildings. When applying CONTAM, the user must specify the temperatures to calculate the buoyancy driven ventilation. However, indoor air temperature is usually unknown. For natural ventilation, the temperature is a function of the airflow rate. Thus current multi-zone programs cannot directly deal with buoyancy driven ventilation in most cases.

A noticeable attempt to simultaneously simulate the energy use and inter-zonal airflow in a building is integration of CONTAM and TRNSYS [19]. TRNSYS [20] is a transient system simulation program with a modular structure that was designed to solve the complex energy system problems by breaking the problem into a series of smaller components. Each small component can be solved independently and thus be coupled with other components into a large component system. The large system therefore can be calculated. By including both the energy and airflow modeling as separate entities inside the TRNSYS program, McDowell et al [19] attempted to iterate both of them to a solution and then pass the information to the other model, which then iterates to a solution before passing the information back. This process would continue until both models reach a satisfactory solution. The preliminary results of this study have developed a feasible method for investigating the combination of the TRNSYS and CONTAM modeling programming. However, this work is still under progress and hasn't provided a public available software package for energy and airflow simulation. Additionally, the integration of the CONTAM and TRNSYS might be too complicated for general unprofessional users and too huge for the applications in the building design stage.

4. Computational fluid dynamics methods

The computational fluid dynamics (CFD) method solves numerically a set of partial differential equations for the conservation of mass, momentum (Navier-Stokes equations), energy, and species concentrations. This solution can provide the distributed air temperature, velocity and contaminant concentration within individual spaces and throughout an entire building. For a typical building, the dimension of the rooms and air supplying velocity generally generate an indoor airflow's Reynolds number that is in the transient or turbulent range. In order to solve the Navier-Stokes equations, turbulence models need to be introduced. The turbulence modeling method should be considered as an engineering approximation [21].

Currently, the CFD method is used extensively in the analysis of airflow, temperature and contaminant distributions [22]. As mentioned above, the CFD method can provide detailed thermal environment and contaminant information. In recent years, CFD has become a more reliable tool for the evaluation of indoor thermal comfort and air quality. However, the application of CFD to the real building design has been limited as it requires excessive computer resource and long running time. For example, a naturally ventilated building with dimentions of 30m×30m×20m may need approximately 2×10^6 grids. Thus it would require around 100 hours of computation time using the CFD calculation with k-ε model. Jiang [23] compared the computing costs of different CFD methods and found that for building simulation, the RANS (Reynolds-averaged Navier-Stokes) method needs at least several hours, the LES (Large eddy Simulation) method needs several days to 30 years, while the DNS (Direct numerical simulation) method needs around 10^5 years.

The work to integrate the CFD simulation (airflow simulation) with the energy simulation also has been extensively carried out during the recently years. Zhai [24] has done significant contributions in the attempt of integrating the CFD simulation with the energy simulation program (e.g. EnergyPlus [25]) by providing different coupling methods. Negrao [26] also has integrated the CFD simulation with building thermal simulation in order to improve the evaluation of building energy consumption and indoor air quality. The integration work of Negrao has focused on the CFD boundary conditions where the interactions of the building thermal simulation and CFD take place.

1.3 Objectives of present study

The previous section discussed the current available methods for studying natural ventilation. Our goal is to develop a method for engineers and architects to correctly predict natural ventilation, especially in the design stage. This method should have the characteristics of relative simplicity, easy of use, and provide some detailed information of interest in several zones.

A combination of the multi-zone model and the CFD method can provide complementary information about a building and save significant computer resources and time. The integration of the multi-zone model and CFD has therefore been investigated by several studies [27]. Gao [28] developed three strategies for coupling the multi-zone model with CFD:

- Virtual coupling by extracting CFD information

The so-called "virtual coupling" is a manmade coupling procedure between CFD simulation and CONTAM multi-zone simulation. Strictly speaking, it is not a real coupling. This coupling strategy generates an outside wind pressure field by CFD simulation and provides to the CONTAM simulation as input wind pressure.

- Quasi-dynamics coupling of CFD into CONTAM
  To improve the calculation results of the CONTAM program, CFD simulation is applied to simulate one zone of multi-zone model's network, which therefore provides more reliable information of the airflow field and the air partition through exits.
- Dynamic coupling of CFD into CONTAM
  Similar as the quasi-dynamic coupling method, the CFD domain substitutes a particular zone of the multi-zone model's network. The dynamic coupling method requires a mutual feedback between the CONTAM and CFD simulations.

Gao's work mainly have been focused on the mechanical ventilation. From the simulation results obtained by Gao, the 'quasi-dynamic' coupling strategy can significantly alter the airflow pattern in multi-zone-only simulations and enhance the accuracy of the airflow obtained by calculations with the multi-zone model. The so-called 'quasi-dynamic' coupling means transferring results of CFD simulation once back to the multi-zone model (e.g. CONTAM) and re-run the multi-zone model simulation. Therefore, there are two data transfers: first from the multi-zone model calculation to CFD, and second from the CFD to the multi-zone simulation. Hence, there is only single iteration between the multi-zone model and CFD simulation. However, this iteration can only improve the multi-zone model's calculation for certain local resistances, such as the resistance changes due to furniture. In order to simplify the simulation and reduce time cost, the objective of this thesis is to predict natural ventilation by transferring data from the multi-zone model to CFD without iterating these two models, because our goal is first focused on the performance prediction of the whole building. The multi-zone model would predict overall airflow and average temperature in each zone, while the CFD would be applied to few particular zones to give detailed temperature and airflow behavior. The latter is needed to establish comfort conditions within the space. However, studies are lacking for applications of the integrated program to natural ventilation prediction because natural ventilation has special characteristics that differ from mechanical ventilation.

The overall objective of this thesis is to develop a simple and easy to use multi-zone model program, which focuses on natural ventilation and investigates strategies to couple

the multi-zone model results with CFD simulation for particular zones. More specially, this study's aim is to:

- Develop a multi-zone model program, MultiVent (multi-zone model program for natural ventilation) that can be applied to both buoyancy and combined wind-buoyancy ventilation. Compared with other multi-zone model programs, such as CONTAM, MultiVent couples the multi-zone airflow model with the thermal model. Thus it can simultaneously predict the temperature and airflow in each zone.
- Validate the MultiVent program by comparing it with full CFD simulation, for both buoyancy and combined wind-buoyancy ventilation. General methods for MultiVent applied to four types of naturally ventilated buildings will be investigated and summarized for architects as user guides.
- Build a web-based interface for MultiVent, so that users can solve their natural ventilation problems via internet. Four typical building scenarios are available for users to choose and the MultiVent automatically divides the zone and generates the network for these cases. Virtual graphs for the simulation results of these typical cases are provided.
- Investigate the strategies for coupling the MultiVent calculation results to CFD simulation. Both velocity and pressure boundary integration methods will be studied and summarized.

1.4 Structure of the thesis

The thesis is organized as follows:

- Chapter 2 introduces the fundamentals of the multi-zone model and an example program of multi-zone model, CONTAM, which include the theoretical background, the mathematical methods, the application cases, and the limitations of CONTAM.
- Chapter 3 introduces the fundamentals of computational fluid dynamics, which include the governing equations of fluid dynamics, the turbulence models and a widely used example code PHOENICS. The validation of PHOENICS in air-conditioned indoor environment and natural ventilation is presented.
- Chapter 4 illustrates the development of the MultiVent code. It presents the theories, solution methods and interfaces of the MultiVent. In this chapter, the

MultiVent is validated for typical naturally ventilated buildings under buoyancy and combined wind-buoyancy ventilation.

- Chapter 5 introduces the on-line calculation service of the MultiVent. It shows the structure and management of the web-server. The main functions of the on-line calculation service are also described.
- Chapter 6 investigates the integration strategies between the MultiVent and CFD simulation (PHOENICS) in buoyancy ventilation. It optimizes the integration boundary surface and helps to properly choose the integrating zone. The integration boundary condition, both velocity and pressure boundary conditions, are studied. Applications to the typical cases are presented.
- Chapter 7 generalizes the integration strategies for natural ventilation. The generalized strategies for large opening and atrium are studied and summarized. These assist to correctly simulate natural ventilation by integrating the multi-zone model and CFD.
- Chapter 8 summarizes the conclusions arising from the study and recommends future research topics.

Chapter 2

Multi-zone Model

2.1 Introduction of multi-zone model

As discussed in previous section, there are at least two methods for characterizing indoor air flow rates: air flow field measurements, such as using tracer gas techniques; and mathematical models to simulate the indoor airflow including, at least, an analytical model, a multi-zone model and a CFD model.

The field measurement can directly tell us the performance of the ventilation, no matter mechanical or natural ventilation system. Measurements based on tracer gas techniques can determine the air flows between the inside and the outside of the building, as well as inter-zonal air flows. However, because tracer gas measurements reflect the prevailing leakage and weather conditions at measurement time, their use in characterizing general building leakage is limited. In addition, the tracer gas measurement is difficult to be applied to wind-driven natural ventilation because wind has fluctuation and natural ventilation has very high air exchanging rates. Since there is different for each building design, it is difficult to use the measurement results in the design of new buildings. To describe indoor air flows for any/general leakage and weather conditions, a number of mathematical models describing inter-zonal air flow have been developed. In addition to air flows, these mathematical models can also simulate the thermal environment and indoor contaminant transport, in bulk or in details.

The multi-zone model is developed from the node (the simple network prediction model) model [29]. Multi-zone modeling is a way to determine the air flows in a complex ventilated building subject to internal and external loads, so it is extensively used in ventilation. The multi-zone model is capable of predicting air flow and pressure distribution within a building by dividing it into an arbitrary number of zones and flow paths. Air flows and their distribution in a given building are caused by pressure differences that can be induced by wind, buoyancy effect, mechanical force, or a combination of these factors. Building-related properties such as the distribution of openings in the building shell, inner pathways, and occupant activity can also create indoor pressure differences. However, these local and small pressure differences inside the building, especially in a large room, will not be considered when we design the

program MultiVent to calculate natural ventilation because these factors do not strongly affect the overall air flow rates.

The macroscopic models mainly include multi-zone and zonal models. The main differences between multi-zone and zonal models are the zone divisions and mathematical fluid models. The multi-zone model requires the user to identify and describe all the zones (rooms) of interest and the links (e.g. flow paths) between those zones (and with the outside air). The network of links is described by a series of flow equations which are solved simultaneously to provide air flow rates between rooms. Assuming that air flow patterns are unaffected by any contaminant present, a mass balance calculation in each zone at each time step can be included in a multi-zone model to predict the variation of concentrations with time. In our newly developed multi-zone model, an energy conservation equation of each zone is introduced and solved at each time step in order to predict the variation of indoor air temperature. Thus, we can predict natural ventilation with this energy equation.

The multi-zone model uses average or representative values for the parameters describing the conditions in a single zone (pressure, temperature, etc.). While they may be used to predict air flows into and out of a room and the mean pollutant concentration within a room, they can not resolve air flow patterns or temperature distributions or pollutant concentrations within a room. If knowledge of such distributions is important, then the multi-zone model will not be enough. In this thesis study, the multi-zone model will be combined with computational fluid dynamics method to provide a strategy for simulating natural ventilation, which can calculate the overall flows in few minutes and simulate detailed distributions in zones of interest.

Comparing with the multi-zone model, zonal models may be used where it is required to model distributions within a single zone. Zonal model's complexity lies between multi-zone models and computational fluid dynamics. In a zonal model, a space such as an individual room is divided into a small number (tens to hundreds) of zones, each of which has single representative values for pressure, temperature and pollutant concentrations. However, in order to describe the flow characteristics of the sub-zones in a single room, the zonal model must include some models more specific than the flow and mass models used in the multi-zone model. For instance, the models may need to describe: wall anisothermal horizontal jet, wall thermal plume derived from a local heat source, and thermal boundary layer [30]. From this point of view, the zonal model is much more complex than a multi-zone model while it cannot be as widely applied as CFD. The published details of current zonal models suggest they have only been applied to single

rooms with a limited set of driving forces [30]. A zonal model, POMA, has been developed [31]. It can predict the airflow pattern and temperature distribution in naturally or mechanically ventilated rooms. POMA's prediction has been compared with existing information in the literature, which showed that the model is a feasible approach for simulation from an engineering view point.

Combining the capabilities of low and high resolution models offers the potential to use higher resolution when appropriate and low resolution for the rest of a building. For example, some researchers have succeeded in coupling multi-zone models with CFD [23], but the combined models still suffer from the difficulties that the multi-zone model cannot predict buoyancy domain natural ventilation. Due to the problems of zonal model, such as complexity and the completeness of sub-models, this thesis will integrate multi-zone model with CFD for natural ventilation prediction.

2.2 An example multi-zone model program-CONTAM

2.2.1 Overview

CONTAM is one of the most recently developed air flow models. It is one of the few multi-zone model programs available to the public. It can be used as a stand-alone program with input and output features, or as an infiltration module that can be integrated into the thermal building simulation program. For example, as discussed in previous section, McDowell et al [19] have tried to integrate the CONTAM as an infiltration module into the energy simulation program TRNSYS.

The objectives of CONTAM are designed to determine: *airflows*-infiltration, exfiltration, and room-to-room (or zone-to zone) airflows in building systems; *contaminant concentrations*-the dispersal of airborne contaminants transported by these airflows and transformed by a variety of processes.

CONTAM can be used to predict the airflow in order to assess the adequacy of ventilation rates in a building, to determine the variations in ventilation rates over time according to different requirements, to predict the overall airflow distribution throughout the buildings.

CONTAM has a graphical input and output interface, which is very user-friendly (see Figure 2.1). The user can schedule the occupants' movement within a building, and

account for either steady-state or varying weather conditions. Weather conditions consist of ambient temperature, barometric pressure, wind speed and direction as well as ambient contaminant concentrations. However, up to July 2004, CONTAM still cannot set the indoor air temperature as a variable. It only can set the indoor air temperature as constant or scheduled known values. For natural ventilation, it is very important to predict the indoor air temperature as a function of user inputs such as the internal loads and weather conditions. From temperature predictions, a designer can assess his/her natural ventilation design and improve it.

The multi-zone model has been extensively evaluated with both analytical solutions and experimental data [32]. From these evaluations, it can see that the multi-zone model can be applied to ventilation prediction at least from an engineering point of view.

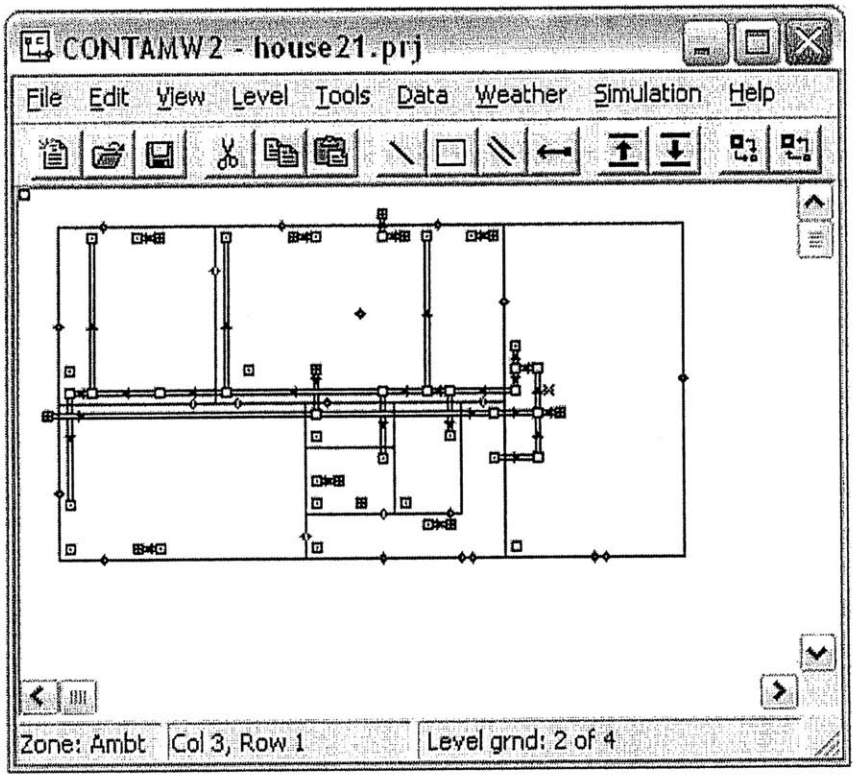

Figure 2.1 Interface of program CONTAM (form NIST) [18]

2.2.2 Theoretical background of CONTAM

The theories in CONTAM can be described in following several parts.

- Airflow analysis

Over the years, many methods including analytical, multi-zone and zonal models have been developed to simulate the airflow in buildings. Feustel et al has reported over 50 different computer programs for multi-zone airflow analysis [33].

Infiltration is the result of air flowing through openings, large and small, intentional and accidental, in the building envelope. CONTAM uses flow elements to describe the airflow characteristics of openings between zones and the outdoors, and between interior zones. There are several options to describe these airflow characteristics: power law models, orifice models, quadratic models, stairwell and shaft models, and two-way flow models. Each model requires specific data to describe the airflow characteristics of the opening.

Flow within each airflow element is assumed to be governed by Bernoulli's equation:

$$\Delta P = (P_1 + \frac{\rho V_1^2}{2}) - (P_2 + \frac{\rho V_2^2}{2}) + \rho g(z_1 - z_2) \qquad (2\text{-}1)$$

where

ΔP =total pressure drop between points 1 and 2

P_1, P_2 =entry and exit static pressures

V_1, V_2 =entry and exit velocities

ρ =air density

g =acceleration of gravity (9.81 m/s^2)

z_1, z_2 =entry and exit elevations.

However, the pressure drops of the airflow through an opening with local resistance will be governed by the formula of $\Delta P = \zeta(\frac{1}{2}\rho V^2)$ with the local resistance coefficient ζ and airflow velocity at opening V.

Pressure terms can be rearranged and a possible wind pressure for building exterior openings added to give

$$\Delta P = P_j - P_i + P_S + P_W \qquad (2\text{-}2)$$

where

P_i, P_j =total pressures at zones i and j

P_S =pressure difference due to density and elevation differences, and

P_W =pressure difference due to wind.

In CONTAM, the zone temperature must be specialized as input for determining P_S. In contrast, the zone temperature and airflow rates are simultaneously calculated in MultiVent.

Many forms of airflow elements are available in CONTAM, such as power-law and quadratic flow elements.

Most infiltration models are based on the following empirical (power-law) relationship between the flow and the pressure difference across a crack or opening in the building envelope. There are three types of expressions of the power-law functions defined in CONTAM:

$$Q = C(\Delta P)^n \tag{2-3}$$

where

Q =volumetric flow rate (m^3/s)

A common variation of the power-law equation is:

$$F = C(\Delta P)^n \tag{2-4}$$

where

F =mass flow rate (kg/s)

A third variation is related to the orifice equation:

$$Q = C_d A \sqrt{\frac{2\Delta P}{\rho}} \tag{2-5}$$

where

Cd =discharge coefficient, and

A =orifice opening area (m^2).

In order to correctly predict the airflow in buildings, several special models have been developed in CONTAM to describe the flow characteristics of the openings. For instance, empirical models of stairwells, cracks, and ducts have been integrated into the model libraries of CONTAM.

- Contaminant and mass analysis

Conservation of contaminant mass for each species (and assuming trace dispersal, i.e., $m_{\alpha,i} \ll m_i$) produces the following basic equation for contaminant dispersal in a building:

$$\frac{dm_{\alpha,i}}{dt} = -R_{\alpha,i}C_{\alpha,i} - \sum_j F_{i,j}C_{\alpha,i} + \sum_j F_{j,i}(1-\eta_{\alpha,j,i})C_{\alpha,j} + m_i \sum \kappa_{\alpha,\beta}C_{\beta,i} + G_{\alpha,i} \qquad (2\text{-}6)$$

where

$m_{\alpha,i}$ =mass of contaminant α in zone i (kg),
$C_{\alpha,i}$ =the concentration mass fraction of contaminant α in zone i,
$R_{\alpha,i}$ =removal coefficient,
$\kappa_{\alpha,i}$ =kinetic reaction coefficient in zone I between species α and β.
$\eta_{\alpha,j,i}$ =filter efficiency of contaminant α in the path from zone j to zone i,
$G_{\alpha,i}$ =generation rate.

CONTAM uses the following formula (ideal gas law) to compute air density ρ:

$$\rho = P/(287.055T)$$

Using reference conditions of standard atmospheric pressure and temperature of 20°C gives ρ_o=1.2041kg/m3.

For a transient solution the principle of conservation of mass states that

$$\frac{dm_i}{dt} = \sum_j F_{j,i} + F_i \qquad (2\text{-}7)$$

where

m_i =mass of air in zone i (kg),
$F_{j,i}$ =airflow rate between zones j and zone i (kg/s),
F_i =non-flow process that could add or remove significant quantities of air from the zone.

Such non-flow processes are not considered in CONTAM and flows are evaluated by sssuming quasi-steady conditions, $dm_i/dt=0$, leads to:

$$\sum_j F_{j,i} = 0 \qquad (2\text{-}8)$$

2.2.3 Mathematical methods of CONTAM

The steady-state flow analysis for multiple zones requires the simultaneous solution of equation (2-8) for all zones. Since airflow analysis functions are usually non-linear, the Newton-Raphson (N-R) method solves the nonlinear problem by an iteration of the solutions of linear equations. In the N-R method a new estimate of the vector of all zone pressures, {P}*, is computed from the current estimate of pressures, {P}, by

$$\{P\}^*=\{P\}-\{C\} \tag{2-9}$$

where the correction vector, {C}, is computed by the matrix relationship

$$\{J\}\{C\}=\{B\} \tag{2-10}$$

where {B} is a column vector with each element given by

$$B_i = \sum_j F_{j,i} \tag{2-11}$$

and {J} is the square (i.e. N by N for a network N zones) Jacobian matrix whose elements are given by:

$$J_{i,j} = \sum_i \frac{\partial F_{j,i}}{\partial P_j} \tag{2-12}$$

where,

$F_{j,i}$ =airflow rate (kg/s) between zones j and zone i,

P_j =pressure (Pa) at mid-point of zone j.

In equation (2-11) and (2-12) $F_{j,i}$ and $\partial F_{j,i}/\partial P_j$ are evaluated using the current estimate of pressure {P}.

CONTAM allows zones with either known or unknown pressures. The constant pressure zones are included in the system of equations and equation (2-10) is processed so as not to change those zone pressures.

Conservation of mass at each zone provides the convergence criterion for the N-R iterations. That is, when equation (2-8) is satisfied for all zones for the current system pressure estimate, the solution has converged. Sufficient accuracy is attained by testing for relative convergence at each zone:

$$\frac{|\sum_j F_{j,i}|}{\sum_j |F_{i,j}|} < \varepsilon \tag{2-13}$$

with a test ($\Sigma|F_{j,i}|<\varepsilon_1$) to prevent division by zero.

Newton's method requires an initial set of values for the zone pressures. These may be obtained by including in each airflow element model a linear approximation relating the flow to the pressure drop in CONTAM:

$$F_{j,i} = c_{j,i} + b_{j,i}(P_j - P_i) \tag{2-14}$$

2.2.4 Applications of CONTAM

CONTAM can be useful in a variety of applications. Its ability to calculate building airflows is useful in assessing the adequacy of ventilation rates in a building, predicting the variation in ventilation rates over time, finding out the distribution of ventilation air within a building, and estimating the impact of envelope air-tightening efforts on infiltration rates. The prediction of contaminant concentrations can be used to determine the indoor air quality performance of buildings before they are constructed or occupied, to investigate the impacts of various design decisions related to ventilation system design and building material selection, to evaluate indoor air quality control technologies, and to assess the indoor air quality performance of existing buildings [31].

To calculate ventilation, users may need to input the information of the boundary conditions to CONTAM program. CONTAM includes the weather data and wind profile information to determine the wind pressure coefficients on the building envelope. For the people activity schedule, CONTAM also gives users way to define information, which will affect the internal heat source variations and the flow path area variations.

There are lots of evaluation cases for CONTAM. Gao [28] verified the CONTAM's applicability through inter-model comparison with other multi-zone models or CFD simulation results. Gao examined three cases: first case is AIVC three-story building using inter-model comparison with COMIS; the second case is French house case using personal exposure prediction within a residential house compared with CFD studies; the third case is a 90-degree planar branch case to testify the limitation of CONTAM multi-zone model in predicting correct airflow pattern. These three case comparisons indicate that CONTAM may provide reasonable results with some limitations, for example, in the case of 90-degree planar branch.

2.3 Discussion

In this chapter, the fundamentals of CONTAM program has been reviewed and discussed. Although there are more than 50 multi-zone models developed that are available for public or not, the basic considerations in most models are very similar. CONTAM is one of the best multi-zone models that are available to public, and has become widely used. The validation cases showed that multi-zone models can simulate the airflow rates with reasonable direction and magnitude.

However, the current multi-zone model programs have limitations when applied to natural ventilation prediction. To design a naturally ventilated building, architects may need to assess their design by estimating the indoor air temperature under natural ventilation. This objective requires that the prediction program can predict the indoor air temperature at the design stage, in which architects roughly know the internal heat sources and typical ambient conditions. Current multi-zone models cannot handle the combined prediction of temperature and airflow. To properly predict the performance of the natural ventilation design, some strategies for applying multi-zone model to natural ventilation prediction need to be investigated.

Of course, the development of the multi-zone models during the past years provided us a high starting point to study the application of multi-zone model to natural ventilation calculation. The reliability of the current multi-zone model suggests a way to predict indoor environment with a fast speed.

Chapter 3

Fundamentals of Computational Fluid Dynamics (CFD)

3.1 Introduction of CFD

To study the details of a turbulent flow, it is sometimes more informative to accurately simulate the flow with a computer than to try to observe it in the laboratory. Computational fluid dynamics (CFD) became popular with the development of turbulence models and computer technology. There are at least two different CFD methods: direct numerical simulation (DNS) and turbulence model approximating modeling (including Reynolds-averaged Navier Stokes (RANS) and large eddy simulation (LES)) [21].

- DNS.

Getting to understand the complicated non-linear dynamics of turbulence is a major scientific and technological challenge. A high-potential tool to improve our understanding is direct numerical simulation (DNS). DNS has shown rapid progress in recent years, due to the improvement in computers and, perhaps even more, due to improvements in numerical algorithms. DNS requires numerically reliable solutions of the unsteady, incompressible Navier-Stokes equations that resolve all dynamically significant scales of motion. DNS directly solves the Navier-Stokes equation without approximation. It requires the use of very fine grid resolutions so that the smallest eddies can be computed; for instance, the Kolmogorov length scale in natural ventilation is about 0.001m [23]. For a small building and its surroundings, DNS may require a grid number of 10^{11} if the building has configurations of 5m×6m×3m (Length×Width×Height). But current available super computers can handle a grid resolution as fine as 10^{8} and thus cannot solve natural ventilation airflows using DNS method.

- LES

In the numerical solution of turbulent flows, it is usual to attempt to simulate averages of the fluid velocity rather than its point-wise values. When the averages chosen are local, the approach is known as Large Eddy Simulation (LES). The main claim for LES is that "LES will simulate the motion of large eddies in a turbulent flow with computational complexity independent of the Reynolds number" [35]. Some research [36] showed that the LES can predict the indoor airflow successfully, and Jiang [23] also

examined the capacity of LES applied to natural ventilation. There has a critical limitation of LES applications in architecture design because it still needs high speed computer or long running time. LES is generally more complex than RANS modeling. Correctly running LES requires high understanding on turbulence model and substantial numerical simulation experiences.

- RANS

Although the full, unsteady Navier-Stokes equations correctly describe nearly all flows of practical interest, they are too complex for practical solution in many cases and a special "reduced" form of the full equations is often used instead - these are the Reynolds-averaged Navier-Stokes (RANS) equations. The solution of the full steady Navier-Stokes equations is sufficiently accurate alone for cases where the fluid flow is laminar. For turbulent flows the Reynolds-averaged form of the equations are most commonly used. The RANS form of the equations introduce new terms that reflect the additional modelling of the small turbulent motions.

Comparing with DNS or LES, the Reynolds-averaged Navier Stokes (RANS) modeling is simple and converges fast. There are lots of models for RANS modeling, yet the simplifying assumptions in RANS limit its applicability. For example, in studying natural ventilation, RANS modeling has shortcomings. Chen [37] compared five different k-ε models of RANS modeling for indoor airflows. All of the models failed to predict the secondary recirculation of indoor airflow. However, RANS can predict the main characteristics of the airflow in building, no matter it is mechancially ventilated or naturally ventilated. RANS does provide most of the information about the airflow to us. In addition, its advantages of relative simple and low computer requirement support the suitability for architecture design application. A building design does not need as accurate simulation as high-technology application (i.e. airplane wing design).

3.1.1 Governing equations of fluid dynamics

Incompressible turbulent flows are governed by the conservation laws for mass and momentum, the Navier-Stokes equations.

- Continuity equation

Let dV be an elemental control volume bounded by a surface dS. In an incompressible flow, the entering mass flux through dS is equal to the leaving mass flux through dS. This condition is satisfied if

$$\nabla \cdot u = 0 \tag{3-1}$$

where, u is the velocity.

- Momentum equations

The principle of conservation of momentum is an alternative statement of Newton's second law. The forces F acting at the boundaries of an elemental control volume dV are equal to the product of mass times acceleration of the flow through dV. The main aerodynamic forces are the static pressure p and the viscous stress τ. The product mass times acceleration is equal to the rate of momentum accumulation in dV minus the momentum flux imbalance through dS. This gives

$$\frac{\partial}{\partial t}u + u \cdot \nabla u = -\frac{1}{\rho}\nabla p + \frac{1}{\rho}\nabla \cdot \tau \tag{3-2}$$

where, ρ is the density (constant for imcompressible fluid). In a Newtonian fluid, the viscous stress is a function of the molecular viscosity μ and of the velocity gradient, according to Stokes' hypothesis: $\tau = \mu(\nabla u - u\nabla)$. Thus equation (3-2) simplifies to

$$\frac{\partial}{\partial t}u + u \cdot \nabla u = -\frac{1}{\rho}\nabla p + \upsilon \nabla^2 u \tag{3-3}$$

In equation (3-3), $\upsilon = \mu / \rho$ is the kinematic viscosity which depends on the temperature. For air, it can be determined by Sutherland's law and the equation of state. Therefore, the variation of air viscosity (and hence conductivity) with temperature may be empirically described by the Sutherland's Law which states:

$$\frac{\mu}{\mu_0} = (\frac{T}{T_0})^{3/2}\frac{T_0 + S_1}{T + S_1}$$

where m_0 denotes the viscosity at the reference temperature T_0, and S_1 is a constant. For air, S_1 assumes the value 110 degrees Kelvin.

3.1.2 RANS modeling and turbulence models

Equations (3-1) and (3-3) govern incompressible Newtonian flows. The flow field is determined by the solution of the system of equations (3-1) and (3-3). Most industrial and building's flows do not allow a direct solution of the governing equations due to the computer resouce and running time limitation. In fact, in unsteady turbulent flows, flow properties such as the kinetic energy ($0.5u \cdot u$) and heat are transported by turbulence. The turbulent transport occurs on length scales greater than the ones where viscous dissipation and heat conduction occur. It is therefore necessary to average the governing equations to obtain approximate solutions. Here we will introduce RANS modeling first and then discuss several tubulence models, which may be applied for this thesis work.

Airflows in building, such as a jet flow passing a flat plane , is turbulent and the air velocity and pressure depend on space and time. These quantities are the sum of a time mean component and a time dependent fluctuation. For instance, the velocity can be decomposed into:

$$u(x,t) = \overline{u}(x) + u'(x,t) \tag{3-4}$$

In an attached flow, the fluctuation u' is generally smaller in amplitude than the mean value $\overline{u}$. Thus, knowledge of the mean flow may be adequate for indoor airflow design or for a similar practical application [38].

- Time average

Let ϕ be a flow property, $\phi = (u, p)$. Let ϕ be the sum of a time average component and a fluctuation:

$$\phi(x,t) = \phi(x) + \phi'(x,t) \tag{3-5}$$

The time mean is determined by

$$\overline{\phi}(x) = \lim_{T\to\infty} \frac{1}{2T} \int_{T}^{T} \phi(x,t)dt \tag{3-6}$$

Actually, the limitation value in equation (3-6) can be estimated by choosing a time period T that is much longer than the fluctuating time length $\hat{t}$.

As we know, the time mean is a linear operator which has the following properties:

$$\overline{\nabla \cdot \phi} = \nabla \cdot \overline{\phi} \tag{3-7}$$

$$\overline{\nabla \phi} = \nabla \overline{\phi} \tag{3-8}$$

$$\overline{\overline{f} \cdot g} = \overline{f} \cdot \overline{g} \tag{3-9}$$

$$\overline{\overline{f} \cdot g'} = \overline{f} \cdot \overline{g'} = 0 \tag{3-10}$$

$$\overline{f + g} = \overline{f} + \overline{g} \tag{3-11}$$

$$\overline{f \cdot g} \neq \overline{f} \cdot \overline{g} \tag{3-12}$$

- Reynolds averaged continuity equation

Let the flow velocity ***u*** be the sum of the time mean component and of a fluctuation about the mean:

$$u = \overline{u} + u' \tag{3-13}$$

Replacing equation (3-13) in equation (3-1) gives

$$\nabla \cdot (\overline{u} + u') = 0 \tag{3-14}$$

Equation (3-14) is the accurate instaneous continuity equation. Time averaging equation (3-14) and making use of equations (3-7), (3-10) and (3-11) gives

$$\overline{\nabla \cdot (\overline{u} + u')} = 0 \tag{3-15}$$

$$\nabla \cdot (\overline{u} + \overline{u'}) = 0 \tag{3-16}$$

$$\nabla \cdot \overline{u} = 0 \tag{3-17}$$

Equation (3-17) is the Reynolds averaged continuity equation. Taking equation (3-17) away from equation (3-14) the continuity equation for fluctuating velocity is obtained

$$\nabla \cdot u' = 0 \tag{3-18}$$

- Reynolds averaged momentum equation

The Reynolds averaged momentum equation is derived along the same lines as the Reynolds averaged continuity equation. The density ρ is constant in an incompressible

flow and the unsteady kinematic viscosity component is often negligible, so that $\upsilon = \bar{\upsilon}$. The time averaging equation (3-3) gives

$$\frac{\partial}{\partial t}(\bar{u}+\overline{u'}) + \bar{u}\cdot\nabla\bar{u} = -\frac{1}{\rho}\nabla(\bar{p}+\overline{p'}) + \upsilon\nabla^2(\bar{u}+\overline{u'}) - \overline{u'\cdot\nabla u'} \tag{3-19}$$

The first term on the left hand side is time averaged, thus independent of time. Furthermore, the time average of a velocity fluctuation $\overline{u'}$ is nil, from equation(3-10). The first term therefore drops out and the Reynolds averaged momentum equation is time independent. The second term on the left hand side and the last term on the right hand side come from the Reynolds average of $u\cdot\nabla u$. This term was simplified by replacing equation (3-13) and noting that the cross products $u'\cdot\nabla\bar{u}$ and $\bar{u}\cdot\nabla u'$ drop out, due to equation (3-10). The pressure term on the right hand side simplifies as $\overline{p'=0}$ and similarly $\overline{u'}=0$ in the second right hand side term. The simplified Reynolds averaged momentum equation is

$$\bar{u}\cdot\nabla\bar{u} = -\frac{1}{\rho}\nabla\bar{p} + \upsilon\nabla^2\bar{u} - \overline{u'\cdot\nabla u'} \tag{3-20}$$

Equation (3-18) can then be added to the last term on the right hand side

$$\overline{u'\cdot\nabla u'} = \overline{u'\cdot\nabla u'} + \overline{u'\nabla\cdot u'} = \nabla\cdot\overline{u'u'} \tag{3-21}$$

to obtain

$$\bar{u}\cdot\nabla\bar{u} = -\frac{1}{\rho}\nabla\bar{p} + \upsilon\nabla^2\bar{u} - \frac{1}{\rho}\nabla\cdot t \tag{3-22}$$

where $t = -\overline{\rho u'u'}$ is the Reynolds stress tensor. This represents the mean rate of momentum transfer through the control volume boundaries, due to turbulence. This term is unknown and is a function of the turbulence statistics.

The system of Reynolds averaged Navier-Stokes equations is indeterminate as the Reynolds stress is an additional unknown with respect to the Navier-Stokes equations. This requires the addition of a relationship to model t as a function of the mean flow variables $(\bar{u}, \bar{p}, \rho, \upsilon)$. Finding this relationship is termed performing turbulence closure on the Reynolds averaged equations.

After we derived above formulas, we may apply turbulence models to solve the Navier-Stokes equations. There are two approaches to turbulence modeling. Both Reynolds [39] and Prandtl [40] regarded turbulence as an expression of the near-random intermingling of sizeable fragments of unlike fluid, which, during a succession of brief encounters, tended to equilibrium. However, their concept found no place in the family of turbulence models springing from Kolmogorov's [41] proposal to attend only to statistical measures of the turbulent motion, such as energy and frequency.

The intermingling-fragments idea was nevertheless preserved in the models of Spalding[42] and Magnussen [43] ("eddy-break-up" and "eddy-dissipation", respectively) which are still used for combustion simulation. It also featured in Spalding's [44] "two-fluid" model of turbulence; and it is essential to the "multi-fluid" models of turbulence (Spalding, 1996) [45] which are not the subject of this thesis.

3.2 A CFD program-PHOENICS

3.2.1 Overview

PHOENICS [46] is a general-purpose software package which predicts quantitatively how fluids (air, water, oil, etc) flow in and around engines, process equipment, buildings, natural-environment features, and so on, the associated changes of chemical and physical composition, and the associated stresses in the immersed solids.

PHOENICS has been continuously marketed, used and developed since 1981, and still possesses many features not yet adopted by later competitors, for example, the parabolic option, simultaneous solid-stress analysis, the multi-fluid turbulence model, and many others.

PHOENICS is applied by engineers to the design of equipment, architects to the designing of buildings, environmental specialists to the prediction, and if possible control, of environmental impact and hazards. PHOENICS is used in this work as the CFD simulation program to integrate with the MultiVent program, and also provides full simulations for the whole building.

3.2.2 Main models in PHOENICS applied to this work

There are more than ten turbulence models available in PHOENICS. These models have different applications and limitations. The most widely used k-ε model and RNG k-ε model are discussed in followings.

- k-ε Model

The k- ε turbulence model proposed by Harlow and Nakayama in 1968 is by far the most widely-used two-equation eddy-viscosity turbulence model, mainly because the ε (energy dissipation) was long believed to require no extra terms near walls. The popularity of the model, and its wide use and testing, has thrown light on both its capabilities and its short-comings, which are well-documented in literatures. PHOENICS provides the standard high-Reynolds-number form of the k- ε model, as presented by Launder and Spalding [47], which includes buoyancy effects.

For high turbulence Reynolds numbers, the standard form of the k- ε model may be summarized as follows, with t denoting differentiation with respect to time, and x_i denoting differentiation with respect to distance x:

$$\frac{\partial(\rho \cdot k)}{\partial t} + \frac{\partial(\rho \cdot u_i \cdot k - (\rho \cdot \mu_t / \sigma_k) \cdot \frac{\partial k}{\partial x_i})}{\partial x_i} = \rho \cdot (P_k + G_h - \varepsilon) \tag{3-23}$$

$$\frac{\partial(\rho \cdot \varepsilon)}{\partial t} + \frac{\partial(\rho \cdot u_i \cdot \varepsilon - \frac{\rho \cdot \mu_t}{\sigma_\varepsilon} \cdot \frac{\partial \varepsilon}{\partial x_i})}{\partial t} = (\rho \cdot \frac{\varepsilon}{k}) \cdot (C_1 \cdot P_k + C_3 \cdot G_h - C_2 \cdot \varepsilon) \tag{3-24}$$

$$\mu_t = C_\mu \cdot k^2 / \varepsilon \tag{3-25}$$

where, k is the turbulent kinetic energy; ε is the dissipation rate; ρ is the fluid density; and μ_t is the turbulent kinetic viscosity.

The item P_k is the volumetric production rate of k by shear forces. It is calculated from:

$$P_k = \mu_t \cdot (u_{i,j} + u_{j,i}) \cdot u_{i,j} \tag{3-26}$$

And the item G_h is the volumetric production rate of k by gravitational forces interacting with density gradients that can be calculated as:

$$G_h = -\mu_t \cdot g_i \cdot (\frac{\partial \rho}{\partial x_i} / (\rho \cdot \sigma_p)) \tag{3-27}$$

where, g_i is the gravitational constant and σ_p is the turbulent Prandtl number.

The item G_h is negative for stably-stratified (dense below light) layers, so that k is reduced and turbulence damped. G_h is positive for unstably-stratified (dense above light) layers, in which therefore k increases at the expense of gravitational potential energy.

With the Boussinesq approximation, in which the variations in density are expressed by way of variations in enthalpy, equation (3-27) reduces to:

$$G_h = \mu_t \cdot \beta \cdot g_i \cdot (\frac{\partial h}{\partial x_i} / (C_p \cdot \sigma_p)) \tag{3-28}$$

where, h is the enthalpy, C_p is the specific heat at constant pressure, and β is the volumetric coefficient of expansion.

In PHOENICS, the following constants are normally used:
$\sigma_k = 1.0$, $\sigma_\varepsilon = 1.314$, $C_\mu = 0.09$, $C_1 = 1.44$, $C_2 = 1.92$, $C_3 = 1.0$.

The constant C_3 has been found to depend on the flow situation. It should be close to zero for stably-stratified flow, and to 1.0 for unstably-stratified flows.

The k- ε model presented above is applicable only in regions where the turbulence Reynolds number is high. Near walls, where the Reynolds number tends to zero, the model requires the application of so-called 'wall functions' or alternatively, the introduction of a low-Reynolds- number extension.

It should be mentioned that the standard form of the k-ε model has been found to perform less than satisfactorily in a number of flow situations, including: separated flows, buoyancy, streamline curvature, and swirl, etc.

Nevertheless because the k- ε model is so widely used, variants and/or modifications aimed at improving its performance abound in the literatures. The most well-known include:
(a) The RNG k- ε model, Chen-Kim and Yap variants for use in separated flows; and
(b) The ad-hoc Richardson-number modification of Launder et al [48] for curvature, swirl and rotation.

- RNG k- ε model

ReNormalisation Group (RNG) methods provide a general set of rules which allow physical problems to be expressed in terms of equations governing the large-scale, long-time behavior of the system. The RNG method can be applied to any scale invariant phenomenon which has no externally imposed characteristic length and time scale. Yakhot and Orszag (simply named YO later) [49] derived a k-ε model based on Renormalization Group (RNG) methods. In their approach, RNG techniques have been used to develop a theory for the large scales in which the effects of the small scales are represented by modified transport coefficients.

The RNG procedure employs a universal random force that drives the small-scale velocity fluctuations and represents the effect of the large scales (including initial and boundary conditions) on the eddies in the inertial range (see for example Hinze [50]). This force is chosen in such a way that the global properties of the resulting flow field are the same as those in the flow driven by the mean strain.

The equations of motion for the large-scale field are derived by averaging over an infinitesimal band of small scales to remove them from explicit consideration. The removal process is iterated until the infinitesimal corrections to the equations accumulate to give finite changes.

The current implementation of the RNG model uses the same equation as the standard k-e model for the turbulent viscosity with the exception that the constant Cμ has an adjusted value.

The range of scales of the effective excitation in turbulence lie between the low, energy containing wave number $k_0 = 2^{\pi/L}$ and the high wave number viscous cutoff Λ. The RNG method removes a narrow band of modes near Λ by expressing them in terms of lower modes in the range $k_0 < k < \Lambda e^{-l}$. Having removed this band of modes the equations of motions for the remaining modes is a modified system of Navier-Stokes equations in which the eddy viscosity, force and non-linear coupling have all been affected. In turn, further modes are iteratively removed from the dynamics. Thus the RNG method produces a form of the Navier-Stokes equation which allows the computation on coarser grids.

Some special comments on the k- ε model are provided in the CHAM's guide [46] as: "Quite recently Smith and Reynolds [51] identified several problems with YO's original derivation of the ε-equation. This led Yakhot and Smith [52] to reformulate the derivation of this equation, which resulted in:

a). A re-evaluation of the constant controlling the production of ε; and

b). The discovery of an additional production term in the ε-equation which becomes significant in rapidly-distorted flows and flows removed from equilibrium."

Although RNG methods were unable to close the additional production term, Yakhot et al[53] developed a model for the closure of this term. The resulting high-Reynolds-number form of the RNG k- ε model proved successful for the calculation of a number of separated flows, and it is this version of the model that has been provided in PHOENICS. However, the user is advised that the model results in substantial deterioration in the prediction of plane and round free jets in stagnant surroundings.

The RNG k-ε model differs from the standard high-Reynolds-form of the k- ε model in that:

(a) The following model constants take different values: $\sigma_k = 0.7194$, $\sigma_\varepsilon = 0.7194$, $C_{1\varepsilon} = 1.42$, $C_{2\varepsilon} = 1.68$, $C_\mu = 0.0845$, and

(b) The dissipation-rate transport equation includes an additional source term per unit volume:

$$S_\varepsilon = -\rho \cdot \alpha \cdot \varepsilon^2 / k \tag{3-29}$$

where,

$$\alpha = C_\mu \cdot \zeta^3 \cdot (1 - \frac{\zeta}{\zeta_0}) / (1 + \beta \cdot \zeta^3) \tag{3-30}$$

and, $\zeta_0 = 4.38$, $\beta = 0.012$.

The dimensionless parameter ζ is defined by:

$$\zeta = S \cdot k / \varepsilon \tag{3-31}$$

where, $S^2 = 2 \cdot S_{i,j} \cdot S_{i,j}$ and $S_{i,j} = 0.5 \cdot (du_i / dx_j + du_j / dx_i)$.

In PHOENICS terms, it may be noted that S is simply the square root of the generation function. The additional source term (3-29) becomes significant for flows with large strain rates, i.e. when $\zeta >> \zeta_0$. The parameter ζ is a measure of the ratio of the turbulent to mean time scale.

3.3 Validation of PHOENICS

PHOENICS is widely applied to indoor environment prediction. It has been extensively validated by many users and by the developing group. A displacement ventilation case is used here to validate the application of PHOENICS with RNG k-ε model. Studying the displacement ventilation by using CFD simulation has been deeply completed in recent years [54, 55, 56]. The CFD simulation can be used to evaluate the performance of the displacement ventilation system with the evaluation criteria of thermal comfort level and indoor air quality after CFD has been validated by experimental measurements.

Displacement ventilation can generate a stratified flow and represents a typical mixed convection case [54, 57]. In displacement ventilation, the conditioned air is supplied with a temperature slightly lower than the desired room air temperature to the occupied space in low velocities. The supply diffusers are often located at the floor level or low part of the wall. With the buoyancy force from heat sources in room, such as people and equipments, the heated air will rise from low level and finally be exhausted from the top of the room. From this point, we can see that displacement ventilation has advantages of energy saving and no draft. The buoyancy forces in displacement ventilation can also usually be found in natural ventilation.

A model experiment of displacement ventilation case had been monitored in a controlled test chamber at MIT [57]. This experiment was designed to model an office room with two persons, two computers and six roof lights. Figure 3.1 shows the simulated and tested displacement ventilation. The geometrical, thermal, and flow boundary conditions for the diffuser, window and heat sources are listed in the Table 3.1.

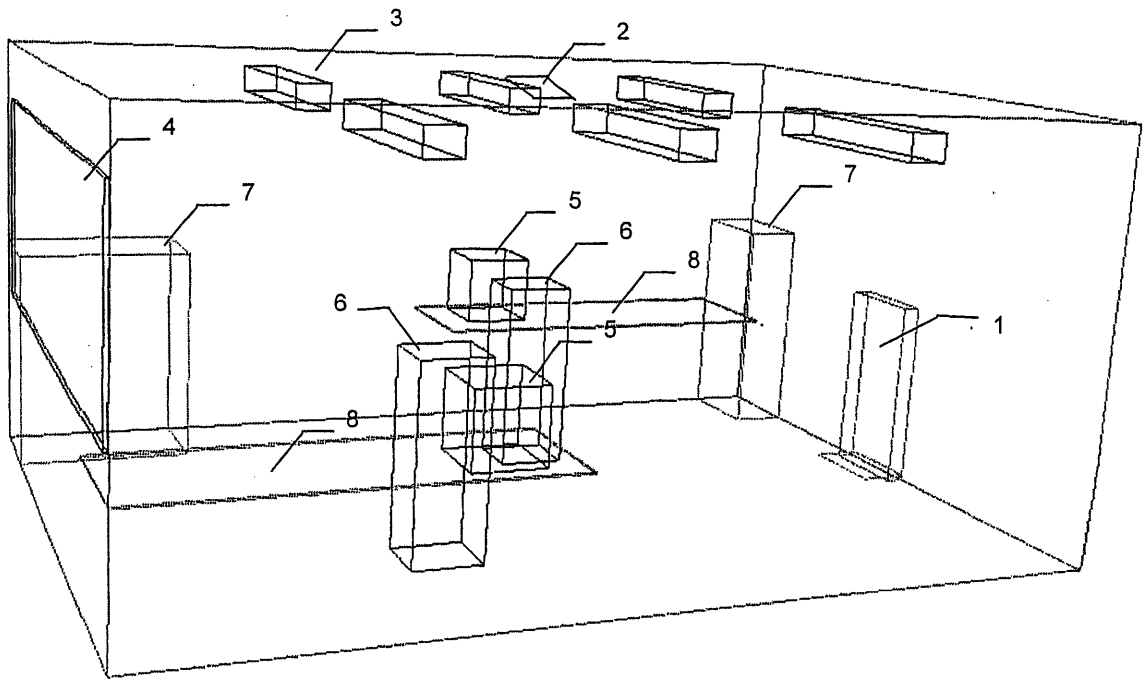

Figure 3.1 The sketch of the displacement ventilation simulated and tested in the chamber (inlet -1, exhaust -2, light -3, window -4, computer -5, person -6, cabinet -7, table -8)

Table 3.1 The geometrical, thermal, and flow boundary conditions for the diffuser, window and heat sources

Inlet diffuser	Size: 0.53mx1.11m	Temperature: 17°C	Velocity: 0.086 m/s
Exhaust	Size: 0.43mx0.43m		
Window	Size: 3.65mx1.16m	Temperature: 27.7oC	
Person	Size: 0.4mx0.35mx1.1m	75W/person	
Computer	Size: 0.4mx0.4mx0.4m	Computer1: 108W Computer2: 173W	
Overhead lighting	0.2mx1.2mx0.15m	34W/each	

The comparison between measured and CFD calculated velocity and air temperature is given in the Figure 3.2 and Figure 3.3, respectively. These figures show a good agreement between the experimental measurements and the CFD simulation for this displacement ventilation case.

As discussed above, there has mechanical force and buoyancy force in displacement ventilation, which is very similar as natural ventilation. For instance, the airflow of displacement ventilation is mainly driven by the buoyancy force that is analogy to the buoyancy-driven natural ventilation. Similarly, the mechanical air supply of displacement ventilation may be analogy to the wind-driven (or combined) natural ventilation. Therefore, although the pure natural ventilation case is not directly validated by CFD simulation in PHOENICS here, PHOENICS program can be used to predict natural ventilation with this validation of the displacement ventilation case and other people's validations [46, 58].

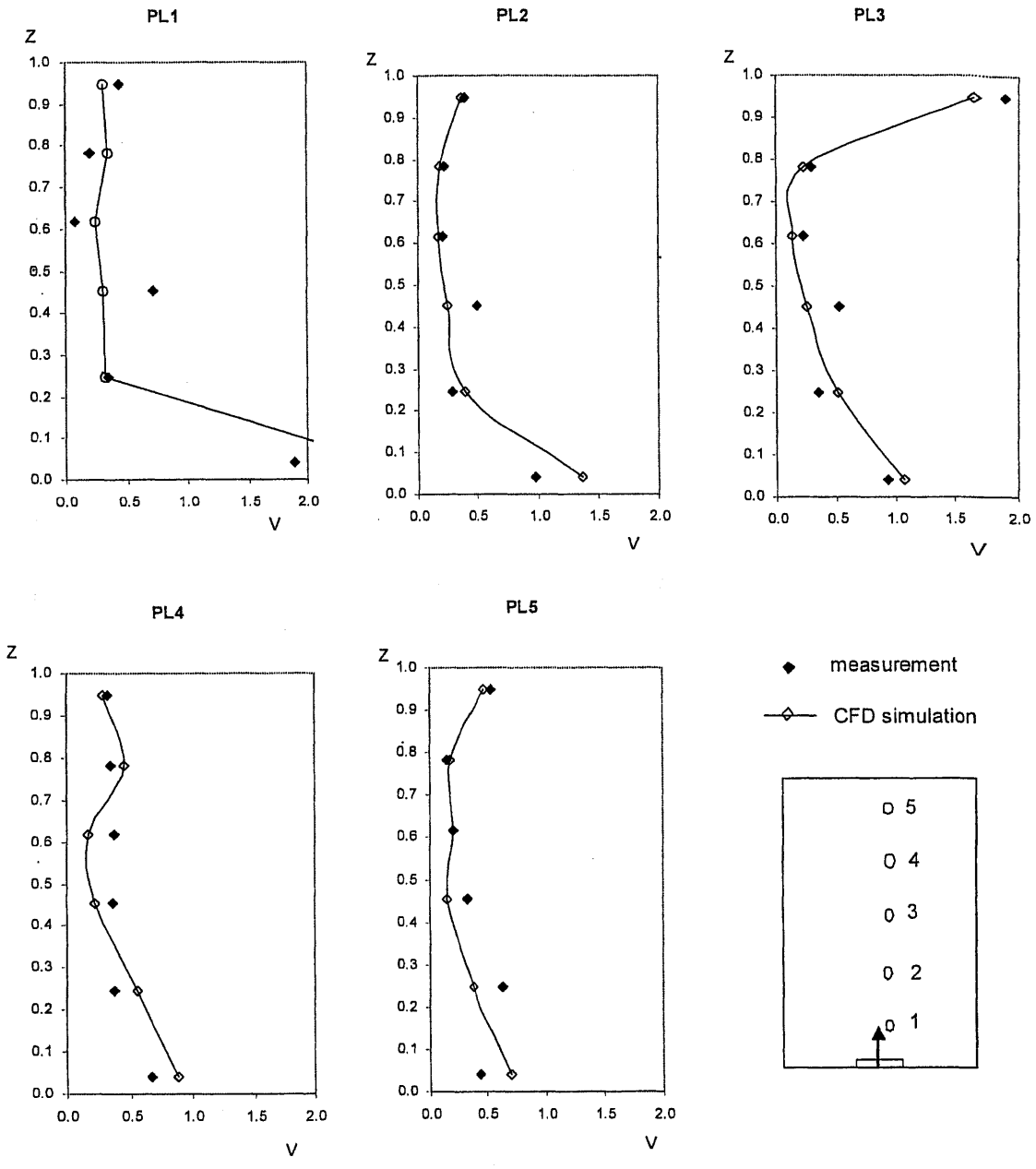

Figure 3.2 The comparison of the velocity profiles at five positions in the room between the simulated and measured data for the displacement ventilation. Z=height/total room height (H), V=velocity/inlet velocity (V_{in}). H=2.43m, V_{in}=0.086m/s.

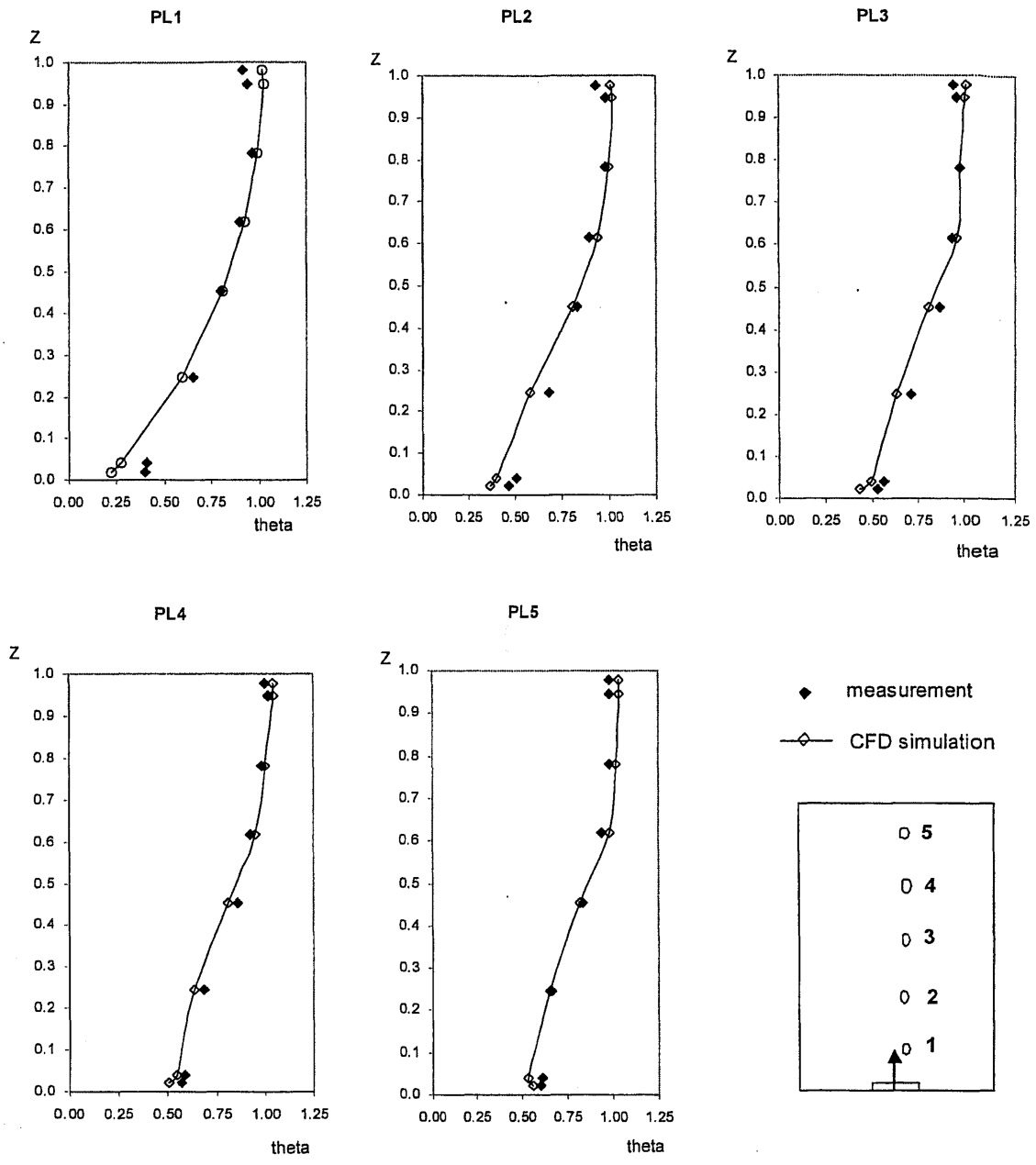

Figure 3.3 The comparison of the temperature profiles at five positions in the room between the simulated and measured data for the displacement ventilation. Z=height/total room height (H), theta=$(T-T_{in})/(T_{out}-T_{in})$. H=2.43m, T_{in}=17°C, T_{out}=26.7 °C.

3.4 Discussion on RNG k-ε model

As discussed in section 3.2, to accurately predict the indoor air velocity, temperature and contaminant concentration, the k-ε turbulence models have been widely applied into CFD simulation because they have the advantages of easy programming and providing reasonable results. During this period, many different modified k- ε models have been developed, such as the RNG k-ε model.

Chen [59] has investigated the applications of several typical k- ε models, including the standard k- ε model, the low-Reynolds-number k- ε model, the two-layer k- ε model, the two-scale k- ε model and the renormalization group (RNG) k- ε model, to the prediction of the indoor airflow. After examining the natural convection, forced convection, mixed convection and impining jet flow, Chen found that the RNG k- ε model performs slightly better than the standard k- ε model, and the two models have similar stability during his computations. The above simulation for the displacement ventilation using the RNG k- ε model in this work also validated the good performance of the RNG k- ε model in prediction of indoor airflow.

However, one thing should be noticed that the RNG k- ε model (or other k- ε models) cannot very accurately predict the turbulent flow around a building under wind-driven natural ventilation. Jiang [23] found that for the single-sided natural ventilation, the LES (large eddy simulation) performs better than the RANS modeling (e.g. k- ε models). However, the LES will cost much more time than the RANS modeling. Therefore, the RNG k- ε model is still chosen as the CFD simulation model in this research because the goal of this research is to provide a fast method to predict the performance of natural ventilation in the design stage with not too high accuracy requirement.

3.5 Conclusions

This chapter gives a simple overview of mathematical and numerical modeling used in CFD, focused on the Reynolds-averaged Navier Stokes (RANS) simulation. The widely applied turbulence models, standard k-ε model and RNG k-ε model in a mature CFD simulation program (i.e. PHOENICS) are introduced. An experimental case, displacement ventilation, is chosen to validate the RNG k-ε model in PHOENICS. More validations of PHOENICS can be gotten in CHAM [46]. Furthermore, the CFD simulation

of natural ventilation when integrated with multi-zone model is very similar to the displacement ventilation case. That is to say, the multi-zone model provides boundary conditions to CFD simulation, which generates the analogy mechanical force as diffuser (inlet). Additionally, the heat sources in natural ventilation building create buoyancy effects just like the buoyancy effects in displacement ventilation.

Although CFD simulation requires significant computing effort, it does provide detailed information and more accurate results. As a result, PHOENICS is appropriate to be integrated with the multi-zone model program (MultiVent) to simulate a particular zone and generate detailed information for building environment design.

Chapter 4

A Newly Developed Multi-zone Model Program- MultiVent

4.1 Objectives and characteristics of MultiVent

A new program of the multi-zone model that couples the airflow model with thermal model for natural ventilation application, called MultiVent, is developed in this work.

When designing a naturally ventilated building, architects need to assess their design, for instance, the thermal comfort conditions in the building. In the design stage, it is impossible to measure the performance of the un-built building. Furthermore, designers may not exactly decide the detailed structures of the building and may not know the exact heat sources' (persons, lights and equipments) locations in the whole building, thus computational fluid dynamics (CFD) may not be able to apply to predicting natural ventilation of the whole building. Besides this, another important reason is that the CFD method costs too much computing time for the whole building simulation. Therefore, the CFD simulation of the whole building is not suitable in early design stage. Alternatively, our strategy of integrating a multi-zone model with CFD can provide a good way to predict natural ventilation as described in follows:

- The multi-zone model calculates the airflow and indoor air temperature for the whole building, which only needs some bulk input parameters, such as the opening areas, the total heat sources in the rooms and the main configurations of the buildings. Detailed information on the building is not required.
- With the bulk airflows and indoor air temperatures from the multi-zone model calculation, architects and engineers can have a basic idea on the future performance of the design and can improve it.
- After understanding the bulk performance of the natural ventilation design, the designers may be interested in some particular spaces and want to know the detailed information on the indoor thermal environment in the spaces. As they are interested in the particular space, designers can do some detailed plan for the particular space and provide it to the CFD simulation.
- Therefore, the results of multi-zone model calculation and the detailed design of the particular space can be combined together to set up the CFD simulation for

this particular space, which provides detailed understanding of the indoor thermal environment in this space. Comparing with the full CFD simulation for the whole building, this integration strategy can save much setting and computing time as well as not require detailed design for the whole building.

With these objectives, the multi-zone model program, MultiVent, should have the following characteristics in order to meet the requirements of architects:

- Simple. The program's theoretical fundamentals should be simple for architects to understand. Complex fluid dynamics would not appear in program.
- Fast. The data inputting and program running for typical buildings should not cost too much time. In the ideal case, the user can finish an integrated simulation in one hour.
- User friendly. The interface should be easy to use and simple for architects.
- Available to public. On-line service will be provided. Thus users can use the program anywhere around the world and not need to install any programs.

MultiVent program has a web-server interface that can provide on-line calculation. Its key mathematical calculation codes are developed in Java language.

4.2 Design of MultiVent

As discussed in previous sections, the multi-zone model is a powerful tool that models airflow and contaminant dispersal in buildings. It is important to realize that this model programmed in MultiVent incorporates assumptions that simplify the model of the real phenomenon. Of course, most assumptions in MultiVent are the same as those in the general multi-zone airflow model, although MultiVent couples the airflow model with the thermal model.

4.2.1 Assumptions in the multi-zone airflow model applied to MultiVent

1. Well-mixed zones

This assumption treats the zone as a single node, in which the air has uniform conditions throughout, consists of temperature, contaminant, pressure and etc.

2. Thermal effects

The model can handle the simplest heat transfer phenomenon: heat sources in the zone directly transfer heat into air without considering the heat transfer process and the effects of thermal mass. The air temperatures in all zones are variables that can vary with the airflows and finally reach the steady state.

3. Airflow paths

The airflow paths are represented by nonlinear mathematical models that are related the pressure drop across the path and geographic characteristics of the flow path.

4. Quasi-state airflows

In each time step, a mass balance in each zone is generated to solve the zone pressures and mass flow rates. That is, this assumption introduces non-real transient solutions that results fast convergence of the program for cases when both the internal temperature and the airflow are initially unknown.

5. Boussinesq assumption

MultiVent assumes the air density meets the Boussinesq assumption. Thus, the air density is determined only by the air temperature, which is different from CONTAM's ideal gas assumption that calculates the air density according to both the pressure and the air temperature. This difference is generated from the different goals of these two programs. MultiVent focuses on natural ventilation, in which the variable temperatures are important while indoor air pressure changes in a relatively very small range. Therefore, MultiVent emphasizes the function of the temperature variation and neglects the change of the pressure because there is no mechanical equipment, such as fans. In contrast, CONTAM was designed mainly for mechanical ventilation, which has much greater pressure differences between zones or ducts.

4.2.2 Theoretical background of MultiVent

The multi-zone airflow model is applied to the MultiVent program. The main governing equations for multi-zone airflow model are listed as followings.

The airflow between two zones through a flow path is given by [4]:

$$F_{j,i} = C_d A(\frac{2\Delta P_{ji}}{\rho})^n \quad (4\text{-}1)$$

where

$F_{j,i}$ =mass flow rate between zone j and i (kg/s),
C_d =discharge coefficient of flow path between zone j and i,
A =effective area of the flow path (m^2),
$\Delta P_{j,i}$ =pressure drop between zone j and i (Pa),
ρ =air density (kg/m^3),
n =power number.

MultiVent applies two types of power-law flow functions for cracks and general openings.

- Cracks

  If any dimension of the opening (flow path), width or height, is less than 10 cm, this opening will be treated as crack in MultiVent if the building is a full scale building. The physical relationship of airflow through cracks that can be converted directly into a power-law airflow element is presented by Clarke [60] as:

  $$F_{j,i} = \rho k a(\Delta P_{j,i})^n \quad (4\text{-}2)$$

  where

  $n = 0.5 + 0.5e^{(-W/2)}$,

  and

  $k = 0.0097 \cdot (0.0092)^n$

  with

  $F_{j,i}$ =mass flow rate between zone j and i (kg/s)
  W =crack width (mm), and
  a =crack length (m),
  ρ =air density (kg/m^3),
  $\Delta P_{j,i}$ =pressure drop between zone j and i (Pa),

- General opening

  For openings with dimensions that exceed the crack definition, the airflows in MultiVent will be calculated in a 0.5 power-law function:

  $$F_{j,i} = C_d A(\frac{2\Delta P_{ji}}{\rho})^{0.5} \quad (4\text{-}3)$$

  where,

  $F_{j,i}$ =mass flow rate between zone j and i (kg/s)

C_d =discharge coefficient of flow path between zone j and i,
A =effective area of the flow path (m^2),
$\Delta P_{j,i}$ =pressure drop between zone j and i (Pa),
ρ =air density (kg/m^3),

Similar to CONTAM, the pressure difference between two zones can be written as:

$$\Delta P_{j,i} = P_j - P_i + P_S + P_W \tag{4-4}$$

where

P_i, P_j =static pressures at midpoint of zones i and j (Pa),
P_S =pressure difference due to density and elevation differences (Pa),
P_W =pressure difference due to wind (Pa).

Thus, the pressure difference between two sides of the opening o (see Figure 4.1), which connects zone j and i, can be derived as:

$$\Delta P_{o,(j,i)} = [P_j - \rho_j g(h_o - h_j)] - [P_i - \rho_i g(h_o - h_j)] + sign(V) \cdot C_W (0.5 \rho V^2) \tag{4-5}$$

where,

P_i, P_j =static pressures at midpoint of zones i and j (Pa),
ρ_i, ρ_j =air densities in the zones i and j (kg/m^3),
h_i, h_j =elevation, relative to ground, of the midpoint of zones i and j (m),
h_o = elevation, relative to ground, of the midpoint opening o (m),
V =ambient free wind velocity (m/s),
C_W =pressure coefficient at midpoint of opening o.

In equation (4-5), the sign(V) is defined by the direction of the ambient wind. For instance, as Figure 4.1 shows, the sign(V) should be positive when we calculate the pressure drop at opening o from zone j to zone i, $\Delta P_{o,(j,i)}$. The pressure variations due to density and elevation differences (buoyancy effect) are separately calculated in each zone shown as equation (4-5). For example, when we count from the midpoint of zone j to the midpoint of opening o, the pressure will drop an amount of $\rho_j g(h_o - h_j)$.

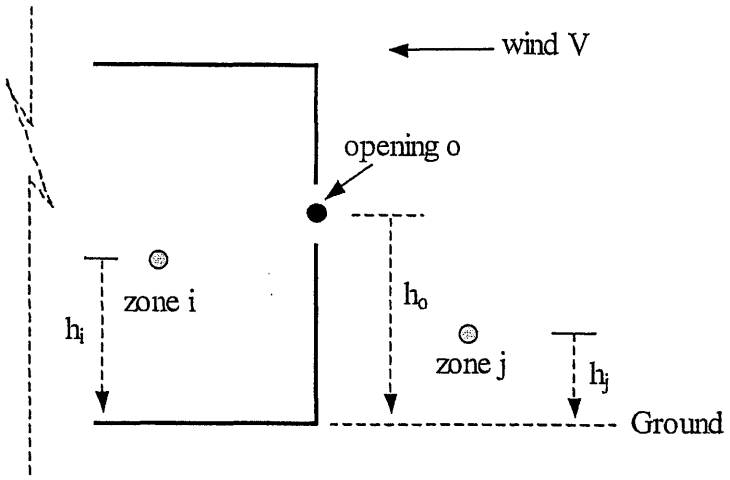

Figure 4.1 Illustration of the pressure difference calculation between two sides of the opening o

To estimate wind pressures, MultiVent applies an empirical equation to calculate the wind pressure coefficient on building envelope [61]:

$$C_p = 1.1198 + 0.1721(zh) - 1.6104(\alpha) - 0.0080(rbh) - 0.2636(far) + 0.1777(sar) - 0.0094(anw) \quad (4\text{-}6)$$

where

C_p	=pressure coefficient,
zh	=height of this point located/height of the building,
α	=wind power coefficient determined by ground roughness,
rbh	=height of the building/average height of surrounding buildings,
far	=width of the windward wall/height of the windward wall,
sar	=width of the side wall/height of the side wall.
anw	=wind direction angle.

The definition of anw (wind direction angle) is illustrated as following Figure 4.2. Thus the value of anw is between 0~180. The angle anw is symmetric to the building's normal surface (see Figure 4.2).

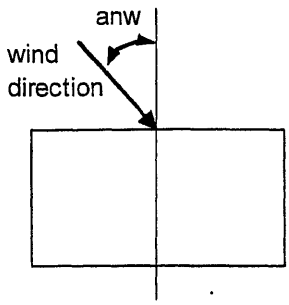

Figure 4.2 Definition of anw in a building (plan view)

In equation (4-6), the parameter of wind power coefficient determined by ground roughness, α, can be chosen in the list of Table 4.1 according to the ASHRAE model [62]. MultiVent estimates the values of the average height of the surrounding buildings (rbh) for different locations shown in Table 4.1

Table 4.1 Values of α and average height of surrounding buildings in MultiVent

Location of building	α	Average height of surrounding buildings (m)
Airport	0.1	2.0
Suburban	0.22	8.0
Urban	0.32	15.0

For mass conservation, we have for each zone by applying the quasi-state assumption:

$$\sum_j F_{j,i} = 0 \tag{4-7}$$

CONTAM assumes that the temperature in all zones is set constant or scheduled by the user. However, the internal heat sources are known while internal temperatures are a function of the resulting airflow rates in natural ventilation. In order to deal with natural ventilation with initially unknown zone temperature, MultiVent introduces an energy balance equation to predict the space temperature as:

$$\frac{d(m_i C_p T_i)}{dt} = \sum_{j,F_{j,i}>0} F_{j,i} C_p \cdot T_j + \sum_{j,F_{j,i}<0} F_{j,i} C_p \cdot T_i + S_Q \tag{4-8}$$

where

C_p =specific heat of air (kJ/kg.°C),

m_i =mass of air in zone i,

T_i =temperature of air in zone i,

t	=time (s),
$F_{j,i}$	=mass airflow rate from zone j to zone i,
S_Q	=heat source in zone i (W).

In the thermal model of the MultiVent, shown as equation (4-8), we only considered the total heat source in the zone, which mainly includes the heat generated by lights, equipments, people and direct solar radiation. The heat transferred into the zone through façade conduction is not considered in this thermal model because the conduction heat may be not as significant as above heat sources. Additionally, the conduction physics is so complicated that it is not worthy to be included into the relative simple simulation program, MultiVent.

4.2.3 Mathematical solution methods of MultiVent

The governing equations of MultiVent consist of the nonlinear and differential equations. We will use Newton-Raphson (N-R) method to solve the nonlinear algorithm equations (4-1)-(4-7) at each time step, and use finite difference method to solve the differential equation (4-8) to find the air temperatures for the next time step.

4.2.3.1 N-R method

First, we recall N-R method and review it.

Considering a series of nonlinear equations:

$$F(x) = 0 \tag{4-9}$$

The N-R solution method will be:

$$x^{m+1} = x^m - (F'(x^m))^{-1} F(x^m) \tag{4-10}$$

where, the $F'(x^m)$ is the value of Jacobi matrix at x^m, and x^m is the value of x at the m^{th} iteration step.

Here we only consider the nonlinear equations, thus the time step is not touched.

At iteration step m, we need to solve the following linear equations first:

$$F'(x^m)\nabla x^m = F(x^m) \tag{4-11}$$

Then, let $x^{m+1} = x^m - \nabla x^m$. The operator ∇ means gradient, which is used to express the change of a vector. It is same as operator Δ when the vector, for example x, only has one element.

During this iteration process, the vector of $F(x^m)$ and matrix $F'(x^m)$ should be calculated for the m^{th} iteration step.

4.2.3.2 Application of N-R method for the multi-zone airflow model in the MultiVent

For the multi-zone airflow model in MultiVent, we have nonlinear equations of pressure P that are implicitly presented in equations (4-7) and (4-1). With the Boussinesq assumption, we may re-write equation (4-7) into only a function of pressures P, just like combination of equations (4-5) and (4-7).

$$F_{j,i} = C_d A\left(\frac{[P_j - \rho_j g(h_o - h_j)] - [P_i - \rho_i g(h_o - h_i)] + sign(V)\cdot C_W (0.5\rho V^2)}{0.5\rho}\right)^n \qquad (4\text{-}12)$$

Therefore, we can derive the N-R method in MultiVent for the iteration step k as follows.

At each iteration step, for example, the k^{th} iteration, we should solve the linear equations:

$$J \cdot \nabla P = B \qquad (4\text{-}13)$$

where,

J =the Jacobi matrix, and $J_{i,j} = \sum_i \frac{\partial F_{j,i}}{\partial P_j} = \sum_i \frac{nF_{j,i}}{\Delta P_{o,(j,i)}}$, $F_{j,i}$ is the airflow rate from zone j to zone i.

B =a column vector, and $B = \sum_j F_{j,i}$.

∇P =the gradient of the zone pressure vector P.

With results of equation (4-13), we get the changes of the pressure vector P, then the new pressures can be calculated for the next iteration step ($k+1^{th}$):

$$P^{k+1} = P^k - \omega \nabla P^k \qquad (4\text{-}14)$$

where,

P =a vector of zone pressures,

ω =the relaxation coefficient that equals to 0.75 in MultiVent.

Iterate this process and stop until following relation is met:

$$\frac{|\sum_j F_{j,i}|}{\sum_j |F_{j,i}|} \le \varepsilon \tag{4-15}$$

where

ε =the error controller that equals to 10^{-6} in MultiVent

To derive the Jacobi matrix of equation (4-13), we have following derivation:

$$\frac{\partial F_{j,i}}{\partial P_j} = \frac{\partial (C_d A(\frac{2\Delta P_{ji}}{\rho})^n)}{\partial P_j} = \frac{\partial (C_d A(\frac{2(P_j - P_i + P_S + P_W)}{\rho})^n)}{\partial P_j} = C_d A \cdot n \cdot (\frac{2(P_j - P_i + P_S + P_W)}{\rho})^{n-1} \frac{2}{\rho}$$

$$= \frac{n \cdot C_d A[\frac{2}{\rho}(P_j - P_i + P_S + P_W)]^n}{(P_j - P_i + P_S + P_W)} = \frac{n \cdot F_{j,i}}{\Delta P_{o,(j,i)}}$$

In addition, we used Gauss-Seidel iteration method with relaxation coefficient ω to solve the linear equation (4-13) in MultiVent.

As we know, the N-R method is quadratically convergent (super-linear convergent) [63]. In addition, the Gauss-Seidel iteration method is convergent because the Jacobi matrix J is a quasi diagonal-dominant matrix. Therefore, the solution methods of the multi-zone airflow model in MultiVent are stable and convergent.

4.2.3.3 Finite difference method for the thermal model in MultiVent

1. Fnite difference method for differential equations

There are two finite difference expressions available to solve differential equations: explicit finite difference and implicit finite difference. Generally, the implicit method is more stable than the explicit method. First, we may investigate the applications of both methods in the well-known parabolic PDE, heat conduction equation:

$$k\frac{\partial^2 T}{\partial x^2} = \frac{\partial T}{\partial t} \tag{4-16}$$

Approximate the derivatives by finite difference schemes and get the explicit expression as:

$$T_i^{k+1} = T_i^k + \frac{k\Delta t}{(\Delta x)^2}(T_{i+1}^k - 2T_i^k + T_{i-1}^k) \tag{4-17}$$

where, the superscript k is the k^{th} time step, and the subscript i is the i^{th} grid along x.

However, in order to keep the stability and convergence of the explicit method in iterations, we may have to follow a relationship between the grid size of dimension scale x and step of time t:

$$\frac{k\Delta t}{(\Delta x)^2} \le \frac{1}{4} \tag{4-18}$$

The implicit method, such as the Crank-Nicolson method, for this heat conduction equation can be written as:

$$T_i^{k+1} = T_i^k + \frac{k\Delta t}{2(\Delta x)^2}(T_{i+1}^k - 2T_i^k + T_{i-1}^k + T_{i+1}^{k+1} - 2T_i^{k+1} + T_{i-1}^{k+1}) \tag{4-19}$$

The implicit method is stable during numerical iterations in general condition. It can generate a linear equation system for temperatures at time step k+1 from equation (4-19). Thus, Gauss-Seidel iteration method can be used to solve this linear equation system.

2. Application of finite difference method for solving MultiVent thermal model

- Explicit difference method

The finite difference method can be applied to dealing with the energy equation (4-8). If we assume the mass of each zone doesn't change in calculation (quasi-steady), we may re-write the equation (4-8) by using explicit difference method as:

$$\frac{m_i C_p (T_i^{k+1} - T_i^k)}{\Delta t^{k+1}} = \sum_j F_{j,i} \cdot C_p \cdot (T_j^k - T_i^k) + S_Q$$

$$T_i^{k+1} = T_i^k + \frac{\Delta t^{k+1}}{m_i}[\sum_{j,F_{j,i}^k>0} F_{j,i}^k \cdot T_j^k + \sum_{j,F_{j,i}^k<0} F_{j,i}^k \cdot T_i^k + S_Q / C_p] \tag{4-20}$$

From the stability analysis of equation (4-18), we find that this criterion actually just needs the coefficient of the temperature change is less or equals to ¼ because this can guarantee the stability if the temperature change magnitude will decrease with the iterations. Similarly, in order to keep the iteration stable, we may apply this criterion to MultiVent and solve equation (4-20). Therefore, we may solve equation (4-20) as

following method (called ED method thereafter):

1). Choose an initial time step Δt^0 equal to 30s.

2). Calculate the air temperature T at time step 1 (T^1). If maximum value of $|T^1-T^0|$ is greater than 1°C, divide the initial time step by 2 and get a new Δt^0. Recalculate the air temperature T^1 until the maximum value of $|T^1-T^0|$ is less than 1°C.

3). At time step k, calculate the new air temperature T^{k+1}, then divide the current time step Δt^k by 2 and get a new time step Δt^{k+1} for next time step. If the new time step Δt^{k+1} is less than 0.1s, we set it equal to 0.1s.

4). Check whether the temperature is converged. If not, repeat step 3) until temperature reaches convergence.

In above method (ED method), we choose the time step range of (0.1s, 30s) as MultiVent's acceptable time step range based on the physical and numerical considerations. Generally, a room has height of 2.8m, the heat source of 100W/m^2. After 30 seconds, the indoor air temperature will increase around:

$$\frac{100W/m^2}{2.8m\times 1.2kg/m^3\times 1005J/kg.^oC}\approx 1^oC \qquad (4\text{-}21)$$

When the indoor air temperature change (increase or decrease) 1°C, the buoyancy pressure between two connected zones will change:

$$\Delta P_S \le 2\frac{\rho gh\Delta T}{(T+273)} = 2\times\frac{1.2kg/m^3\times 9.8N/s^2\times 1^oC}{300^oC}\approx 0.157Pa \qquad (4\text{-}22)$$

Therefore, the pressure just changes a relatively small value that cannot generate a significant change in airflow rates for a time period of 30 seconds. From the numerical consideration, we know that we need to meet the inequality (4-18) in order to keep stable when we calculate the iterations between the air temperature and the airflow using the explicit difference method. Thus, we choose 0.1s as the minimum value of the time step, which is less than ¼ second that is required for the numerical stability and convergence as shown in the inequality (4-18) when we use the explicit finite difference method to solve the heat conduction problem of equation (4-16). With above method (ED method), we can solve our objective differential equation (4-8) using the explicit difference method shown in the equation (4-20) that meets the stability requirement.

In order to guarantee the above explicit method convergent and stable, we tried to validate the explicit difference method meets the following theorem [64]:

"If the explicit method $y_{n+1} = y_n + hf(x_n, y_n)$ is used to solve the differential equation $\frac{dy}{dx} = f(x, y)$, and the function f meet the Lipschitz relationship of y for a positive constant L>0 as: $|f(x, y_1) - f(x, y_2)| \le L|y_1 - y_2|$, $\forall y_1, y_2$, this explicit method is convergent. Here, h is the change step of variable x, thus $x_{n+1} = x_n + h$."

With this theorem, we will discuss the convergence of the explicit method (equation (4-20)). We will start at equation (4-8) and let:

$$f(T_i) = \frac{1}{m_i}[\sum_{j,F_{j,i}>0} F_{j,i} \cdot T_j + \sum_{j,F_{j,i}<0} F_{j,i} \cdot T_i + S_Q / C_p] \tag{4-23}$$

where, m_i is the mass of the indoor air in the zone i.

For any two different indoor air temperatures T_i^1 and T_i^2 of zone i, we have:

$$f(T_i^1) - f(T_i^2) = \frac{1}{m_i}[\sum_{j,F_{j,i}>0} F_{j,i}^1 \cdot T_j + \sum_{j,F_{j,i}<0} F_{j,i}^1 \cdot T_i^1 + S_Q / C_p - \sum_{j,F_{j,i}>0} F_{j,i}^2 \cdot T_j - \sum_{j,F_{j,i}<0} F_{j,i}^2 \cdot T_i^2 - S_Q / C_p]$$

$$f(T_j^1) - f(T_i^2) = \frac{1}{m_i}[\sum_{j,F_{j,i}>0} F_{j,i}^1 \cdot T_j - \sum_{j,F_{j,i}>0} F_{j,i}^2 \cdot T_j + \sum_{j,F_{j,i}<0} F_{j,i}^1 \cdot T_i^1 - \sum_{j,F_{j,i}<0} F_{j,i}^2 \cdot T_i^2]$$

$$|f(T_i^1) - f(T_i^2)| = |\frac{1}{m_i}[\sum_{j,F_{j,i}>0} F_{j,i}^1 \cdot T_j - \sum_{j,F_{j,i}>0} F_{j,i}^2 \cdot T_j + \sum_{j,F_{j,i}<0} F_{j,i}^1 \cdot T_i^1 - \sum_{j,F_{j,i}<0} F_{j,i}^2 \cdot T_i^2]|$$

$$|f(T_i^1) - f(T_i^2)| \le \frac{1}{m_i}|\sum_{j,F_{j,i}>0} (F_{j,i}^1 - F_{j,i}^2) \cdot T_j| + \frac{1}{m_i}|\sum_{j,F_{j,i}<0} F_{j,i}^1 \cdot T_i^1 - \sum_{j,F_{j,i}<0} F_{j,i}^2 \cdot T_i^2| \tag{4-24}$$

Without loss of generalization, we can assume $T_i^2 = T_i^1 + \Delta T_i$, with $\Delta T_i > 0$. If we combine the equation (4-12) with the Boussinesq assumption, we have:

$$|F_{j,i}^1 - F_{j,i}^2| = C_d \cdot A \cdot |\sqrt{m} - \sqrt{m + \Delta m}| \le C_d \cdot A \cdot \sqrt{\Delta m} \tag{4-25}$$

where, $m = P_j - \rho_j gh(T_j - T_i^1) + P_w$, and $\Delta m = \rho_j gh\Delta T_i$.

Thus, we can get the following inequality:

$$\frac{1}{m_i}|\sum_{j,F_{j,i}>0} (F_{j,i}^1 - F_{j,i}^2) \cdot T_j| \le \frac{n}{m_i} C_d \cdot A \cdot \sqrt{\rho gh\Delta T_i} \tag{4-26}$$

where, n is the number of zones that connects with zone i and have positive airflow rate flowing into zone i; Cd is the discharge coefficient; A is the opening area; ρ is the air density; h is the relative height between the midpoint of zone j and zone i. Here we choose the corresponding values of Cd, A, ρ and h when their expression $C_d \cdot A \cdot \sqrt{\rho g h}$ is the maximum value among all the connected zone j.

After we derived the inequality (4-26), we only need to get a similar relationship for the second item in the right side of inequality (4-24). However, for the second item in equation (4-24), we can not guarantee there is a relationship like following inequality:

$$\frac{1}{m_i}\left|\sum_{j,F_{j,i}<0} F_{j,i}^1 \cdot T_i^1 - \sum_{j,F_{j,i}<0} F_{j,i}^2 \cdot T_i^2\right| \le \frac{1}{m_i} f(|\Delta T_i|) \tag{4-27}$$

where, $f(|\Delta T_i|)$ is a function of the absolute value of the temperature difference $\Delta T_i = T_i^2 - T_i^1$.

We can verify this conclusion through an example case. For instance, if $|\sum_{j,F_{j,i}<0} F_{j,i}^1| < |\sum_{j,F_{j,i}<0} F_{j,i}^2|$), then we have:

$$\begin{aligned}
&\frac{1}{m_i}\left|\sum_{j,F_{j,i}<0} F_{j,i}^1 \cdot T_i^1 - \sum_{j,F_{j,i}<0} F_{j,i}^2 \cdot T_i^2\right| = \frac{1}{m_i}\left|\sum_{j,F_{j,i}<0} F_{j,i}^1 \cdot T_i^1 - \sum_{j,F_{j,i}<0} F_{j,i}^1 \cdot T_i^2 - \Delta F \cdot T_i^2\right| \\
&= \frac{1}{m_i}\left|\sum_{j,F_{j,i}<0} F_{j,i}^1\right| \cdot \left|(T_i^2 - T_i^1)\right| + \frac{1}{m_i}\left|\Delta F \cdot T_i^2\right| = \frac{1}{m_i}\left|\sum_{j,F_{j,i}<0} F_{j,i}^1\right| \cdot \Delta T_i + \frac{1}{m_i}\left|\Delta F \cdot T_i^2\right|
\end{aligned} \tag{4-28}$$

where, ΔF (>0) is the difference of $|\sum_{j,F_{j,i}<0} F_{j,i}^2|$ and $|\sum_{j,F_{j,i}<0} F_{j,i}^1|$.

From the example condition described as equation (4-28), we can see that it is impossible to derive a Lipschitz relationship for the explicit finite difference energy equation (4-20) since there is an additional item in equation (4-28) besides the item including ΔT_i. The additional item cannot be expressed as a function of ΔT_i. That is to say, we cannot theoretically verify the convergence of this explicit difference method. Thus we recommend implicit method for the MultiVent program, although the above method (ED method) can provide stable and convergent way to solve the differential energy equation and generate good results for typical natural ventilation. For example, in the following case studies, the full scale building case in section 4.3.1.2 can be calculated using the ED method. The ED method has advantages of easy programming and fast calculation if the simulation can converge.

- Implicit difference method

As discussed above, the explicit (forward) difference method (ED) cannot theoretically guarantee stable and convergent during numerical simulation in the MultiVent program. Therefore, we may use the implicit difference method to solve the thermal model equation as:

$$T_i^{k+1} = T_i^k + \frac{1}{2}\left(\frac{\Delta t^{k+1}}{m_i}\left[\sum_{j,F_{j,i}^{k+1}>0} F_{j,i}^{k+1}\cdot T_j^{k+1} + \sum_{j,F_{j,i}^{k+1}<0} F_{j,i}^{k+1}\cdot T_i^{k+1} + S_Q/C_p\right]\right.$$
$$\left. + \frac{\Delta t^k}{m_i}\left[\sum_{j,F_{j,i}^{k}>0} F_{j,i}^{k}\cdot T_j^{k} + \sum_{j,F_{j,i}^{k}<0} F_{j,i}^{k}\cdot T_i^{k} + S_Q/C_p\right]\right) \qquad (4\text{-}29)$$

Unfortunately, the equation (4-29) is not a linear equation but a nonlinear equation because the airflow rates ($F_{j,i}$) are functions of indoor air temperatures. Thus, the equation (4-29) and equation (4-12) are made up of a complicated nonlinear equation system. Thus the simple iteration method applied to solve equation (4-19) is not suitable here.

Alternatively, we may use a quasi-implicit difference method described as following method (called ID method thereafter):

a). Choose a constant time step Δt equal to 10s.

b). At time step k, we do following calculations (see Figure 4.3):

(1) Solve the linear equations:

$$T_i^{k+1} = T_i^k + \frac{1}{2}\left(\frac{\Delta t}{m_i}\left[\sum_{j,F_{j,i}^{k}>0} F_{j,i}^{k}\cdot T_j^{k+1} + \sum_{j,F_{j,i}^{1}<0} F_{j,i}^{k}\cdot T_i^{k+1} + S_Q/C_p\right]\right.$$
$$\left. + \frac{\Delta t}{m_i}\left[\sum_{j,F_{j,i}^{k}>0} F_{j,i}^{k}\cdot T_j^{k} + \sum_{j,F_{j,i}^{k}<0} F_{j,i}^{k}\cdot T_i^{k} + S_Q/C_p\right]\right)$$

and get a temporary temperature for time step k+1 as T^{k+1*}.

(2) Calculate the mid-point temperature of T^k and T^{k+1*} as $T^{k+1/2} = (T^k + T^{k+1*})/2.0$. Then calculate the flow rates under the mid-point temperature $T^{k+1/2}$ as $F^{k+1/2}$.

(3) Solve the linear equations:

$$T_i^{k+1} = T_i^{k+1/2} + \frac{1}{2}\left(\frac{\Delta t/2}{m_i}\left[\sum_{j,F_{j,i}^{k}>0} F_{j,i}^{k+1/2}\cdot T_j^{k+1} + \sum_{j,F_{j,i}^{1}<0} F_{j,i}^{k+1/2}\cdot T_i^{k+1} + S_Q/C_p\right]\right.$$
$$\left. + \frac{\Delta t/2}{m_i}\left[\sum_{j,F_{j,i}^{k}>0} F_{j,i}^{k+1/2}\cdot T_j^{k+1/2} + \sum_{j,F_{j,i}^{k}<0} F_{j,i}^{k+1/2}\cdot T_i^{k+1/2} + S_Q/C_p\right]\right)$$

and get a new temporary temperature for time step k+1 as T^{k+1*}.

(4) Repeat step (2) and (3) for until the difference of between the new T^{k+1*} and the previous T^{k+1*} is relatively small (e.g. <0.005°C).

c). Check whether the temperature has converged using the inequality (4-30). If not, repeat step b) until temperature reaches convergence.

Generally, the implicit method can provide stable and fast convergent solution for the differential equations, such as equation (4-8). From the physical analysis in the explicit method (ED method) in the time step range (0.1s, 30s), we understand that the constant time step (Δt) equal to 10s should be reasonable for typical natural ventilation.

The temperature convergence is examined by following inequality in the MultiVent program:

$$\max | T^{k+1} - T^{k} | \leq \varepsilon^{T} = 0.01^{o}C \qquad (4\text{-}30)$$

Because we adopt a constant time step 10s in the implicit difference method (ID method), we don't need to worry that a too small time step may introduce fake convergence when using equation (4-3) to examine the temperature convergence.

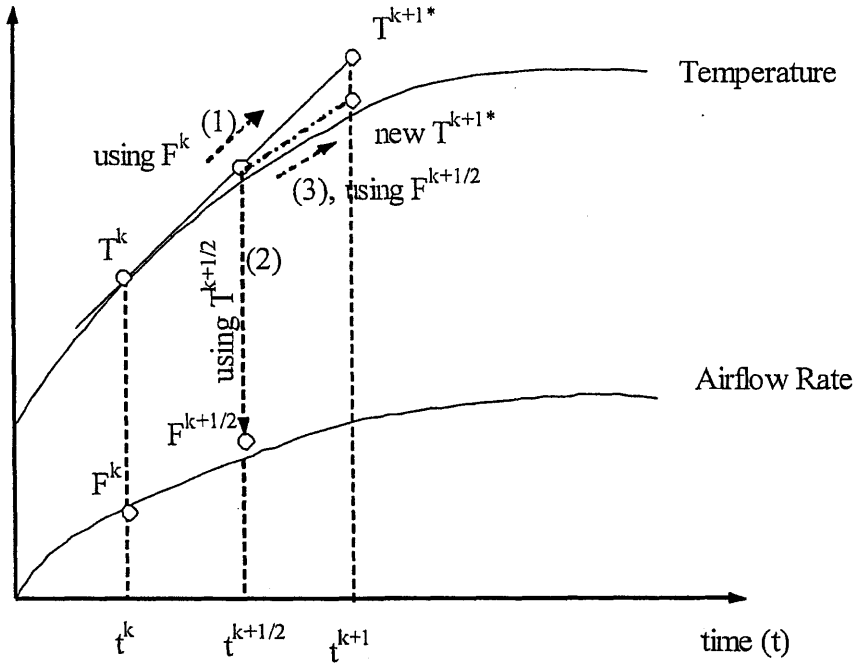

Figure 4.3 The calculation process of the quasi-implicit difference method

4.2.3.4 Solution process summaries

The following steps are the complete solution process of MultiVent:

Step 0. Get initial conditions

- Get the initial indoor zone air temperatures from user input
- Get outside air temperature from user input

Step 1. Calculate the initial pressures and flows

- Calculate the initial pressure of each zone $P_i = -\rho_i g h_i$, with assumption of zero reference pressure at height zero.
- Calculate the initial flow of each opening $F_{j,i} = C_d A(\frac{2(P_j - P_i + P_S + P_W)}{\rho_j})^n$.

Step 2. Calculate temperature T^{k+1}

- Choose a time step Δt equals to 10s.
- Use step (b) in the implicit difference method (ID method) to calculate the new temperatures T^{k+1}

Step 3. Calculate the new pressures that make flow balanced under temperature T^{k+1}

- Use equations (4-13) and (4-14) to get the flow balanced pressures when temperature T^{k+1} doesn't change.
- Get the balanced flows $F_{j,i}$ at same time

Step 4. Temperature converged or not

- Examine the temperatures' convergence by using equation (4-30).
- If the temperature converges, then stop calculation and output.
- Otherwise, go back to step 2.

The following diagram (Figure 4.4) shows the calculation process of MultiVent:

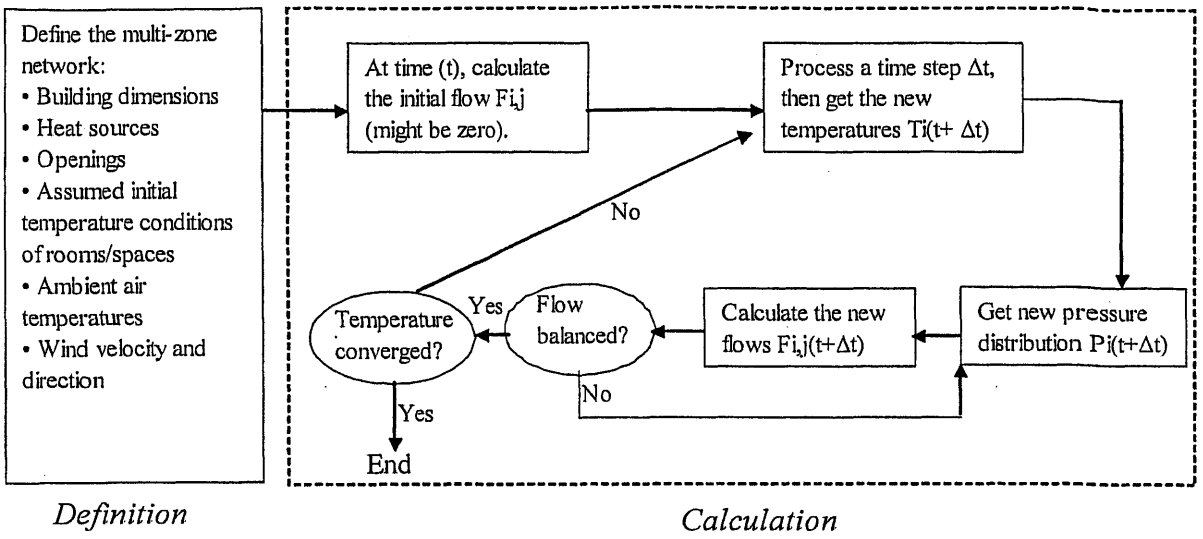

Figure 4.4 Diagram of the calculation process in MultiVent

4.3 Validation of the MultiVent program

The applications of the MultiVent for buoyancy ventilation and wind-buoyancy combined ventilation have been studied separately. Several typical natural ventilation cases are used to investigate the multi-zone model for natural ventilation prediction by applying the MultiVent program.

4.3.1 Buoyancy ventilation

4.3.1.1 Luton model building case

1. Case description

MIT Building Technology group and BP Institute and Martin Center of Cambridge University are monitoring the indoor environment for a naturally ventilated building at Luton, UK [65]. A 1/12 scale air-filled model building was built at MIT to simulate its performance.

This model building has overall dimensions of 2.75m×1.76m×1.32m (see Fig. 4.4). There is an atrium, 0.35m×1.76m×1.32m, in the middle of the model building. At the top there are three 0.1m×0.1m openings for stack vents. Two openly planed rooms are located on each side of the atrium. Each of the room has a heat source of 300W, which models the internal heat load in the real building and creates the buoyancy flow. Seven windows, 0.02m×0.12m, and seven top vents, 0.02m×0.12m, are uniformly distributed on each room's exterior wall (e.g. see Figure 4.5). This model building is placed in a test chamber, which can model the ambient air temperature controlled by an air conditioning system. In order to study the pure buoyancy ventilation, the air supplying velocity from diffuser in the test chamber wall is very low (around 0.09m/s). Figure 4.6 shows the locations of the heat plates in each floor. There is a large heat plate in the first floor with strength of 300W that can simulate the uniform heat source; while each of the other three rooms has two 'point' heat sources with strength of 150W/each to simulate the non-uniform heat sources.

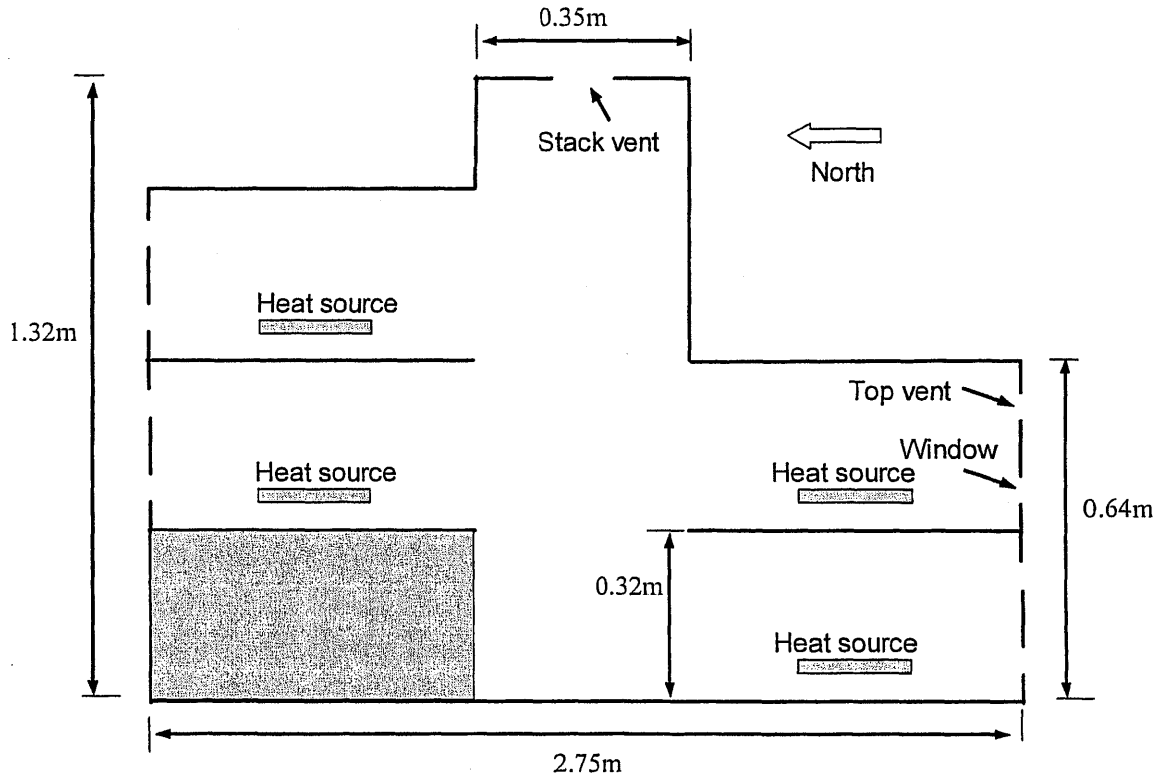

Figure 4.4 Sketch of the model building (vertical view)

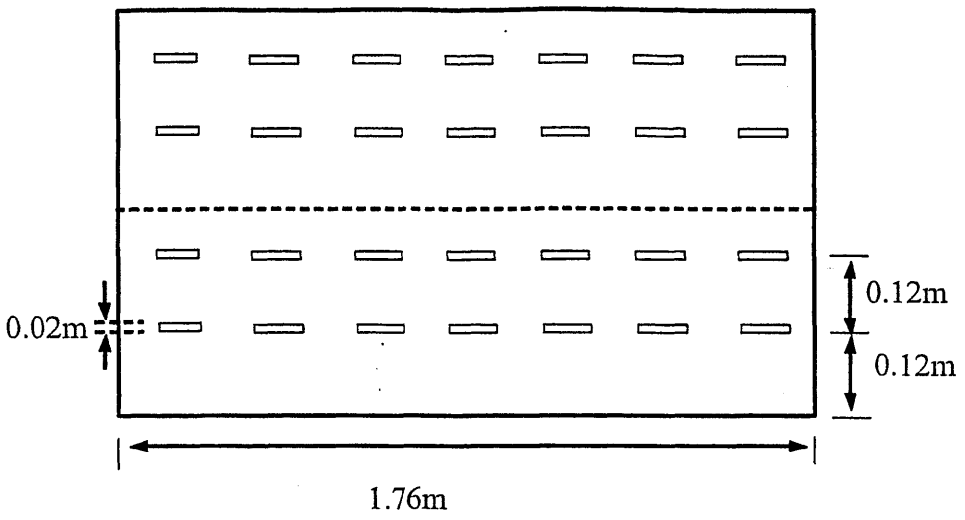

Figure 4.5 Side (vertical) view of the south wall

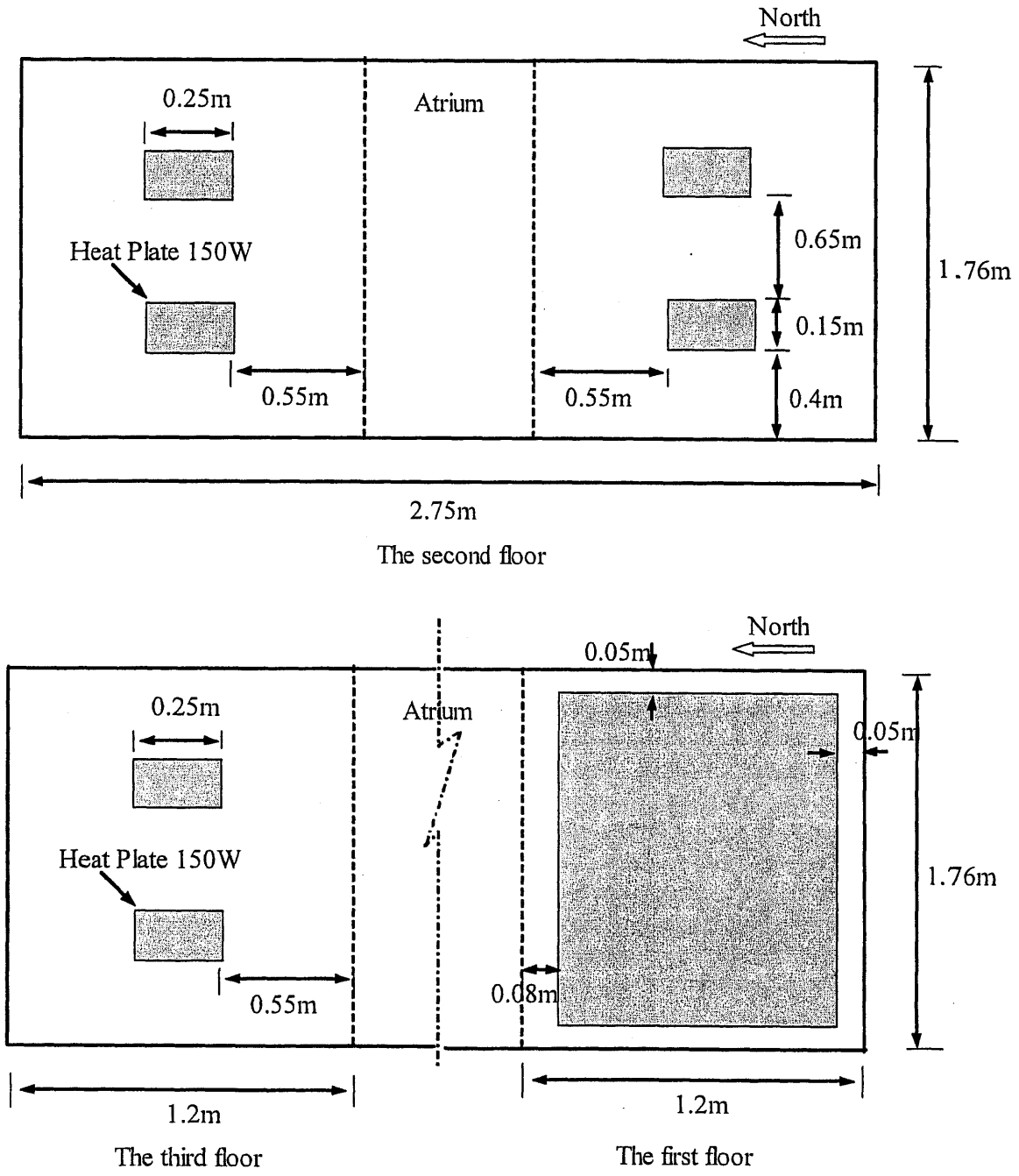

Figure 4.6 Plan view of each floor in the model building

2. Define multi-zone model networks

In order to use MultiVent to predict the buoyancy ventilation of the model building, we need to create the multi-zone model network at first step. Due to the large openings and atrium in this model building, different methods for dividing the zones may generate different results when applying the multi-zone model to calculate natural ventilation.

Figure 4.7 shows two methods to define the zones. To compare the multi-zone model calculation, the full CFD simulation of the entire building (see Figure 4.8) has been carried out and its result was considered as the reference values to evaluate the MultiVent calculation. As above discussion, the multi-zone model is a simple model that can provide the bulk parameters of the indoor air with fast convergence. In contrast, CFD uses turbulence models to solve the Navier-Stokes equations to predict detailed information on the indoor environment.

The opening between the zone 4 and the room (zone 0, 1, 2, or 3) has been uniformly divided into eight vertical sub-openings, although the atrium is considered as a single zone (zone 4) in case 1. In other word, the so called Multiple Opening Model developed in the CONTAM has been applied into case 1 (see Figure 4.7).

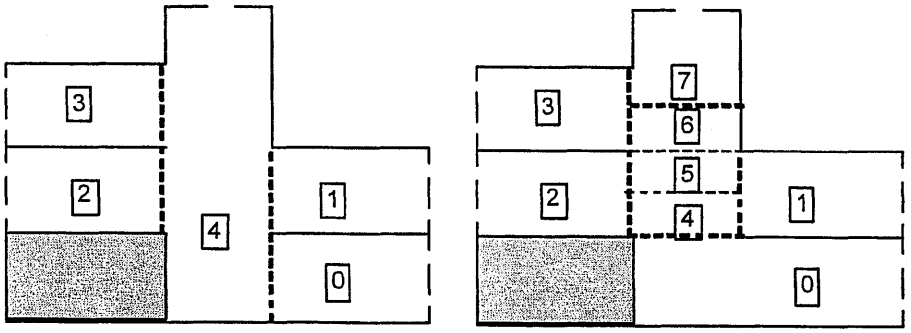

Figure 4.7 Two different methods for dividing the zones (Multiple Opening Model applied to case 1)

The RNG $k-\varepsilon$ model was used in the CFD simulation because this model has steady and easily convergent advantages. The CFD program, PHOENICS [8], is adopted to do the detailed simulation for the whole building.

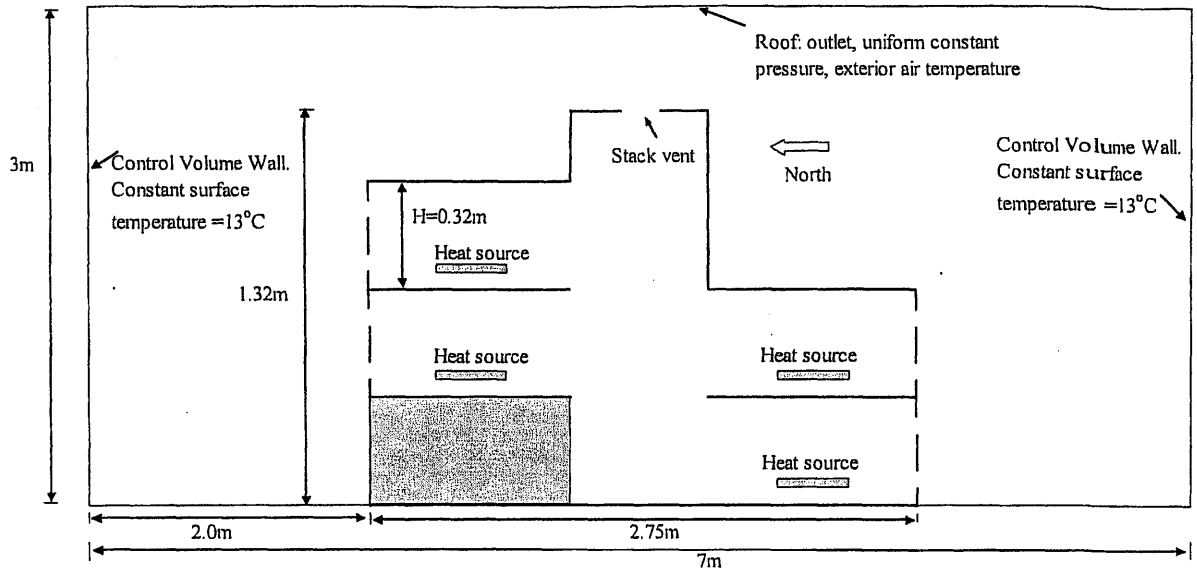

Figure 4.8 Full CFD simulation of the buoyancy ventilation for the model building

3. Simulation and comparison

In this case, buoyancy ventilation has been initially considered without any wind over the building exterior. In this model experiment, the outside (ambient) air was controlled at a constant temperature of 13°C.

The results of the two cases' MultiVent calculation and full CFD simulation for buoyancy ventilation are compared in Table 4.2 and 4.3. It is clear that case 2 provided a better solution for this buoyancy ventilation. Thus, properly divided atrium and large openings can improve the accuracy of the multi-zone model simulation.

The full CFD simulation result in Table 4.2 is a rough average temperature for each zone. When calculating the average zone air temperature from the full CFD simulation, the same zone divisions as case 2 of MultiVent simulation were used (see Figure 4.4, case 2). Air temperatures at twelve typical points in each space were counted. To validate the MultiVent program, airflow rates from MultiVent case 2 through windows and top vents of each room, and through the stack vent are also compared with the full CFD simulation results, shown in Table 4.3. In Table 4.3, the airflow velocity is the average of air

movements through all windows (or top vents) at each room. For this example of buoyancy ventilation, the MultiVent yields accurate results.

Table 4.2 Comparison of zone air average temperatures for MultiVent different strategies and full CFD simulation (°C)

Zone	Full CFD	MultiVent calculation	
		Case 1	Case 2
0	23.48	24.84	25.29
1	29.43	42.69	32.28
2	29.38	42.69	32.28
3	37.19	45.16	39.77
4	25.67	31.63	28.32
5	27.74	-	32.29
6	30.20	-	32.35
7	35.21	-	38.05

Table 4.3 Comparison of the average airflow velocity at openings between MultiVent and full CFD simulation (m/s)

Opening		MultiVent case 2	Full CFD
1st floor south	Windows	0.57	0.58
	Top vents	0.51	0.52
2nd floor south	Windows	0.36	0.32
	Top vents	0.19	0.16
2nd floor north	Windows	0.36	0.32
	Top vents	0.19	0.17
3rd floor north	Windows	-0.28	-0.26
	Top vents	-0.52	-0.49
Stack vents		-0.64	-0.66

Note: The negative sign means air leaving building.

4. Comparison between the uniform heat source and non-uniform heat source

The multi-zone model assumes well-mixed condition in the zones. Pervious study of the Luton model building showed that the MultiVent program can correctly predict buoyancy

ventilation if we properly deal with the large openings and the atrium. As we compared the MultiVent calculation with the full CFD simulation, the heat sources in the Luton model building is shown in Figure 4.6. It is necessary to compare the CFD simulation results of different heat source distributions, for instance, uniform and un-uniform ('point') distributions.

We have run the full CFD simulation for this Luton model building with buoyancy ventilation for non-uniform heat distributions. The building scale and heat source distribution are the same as shown on Figures 4.5 and 4.6, except that the heat source distribution of the first floor has been changed into the same distribution as the other three rooms. Therefore, the first floor has two 'point' heat sources and each of them has strength of 150W.

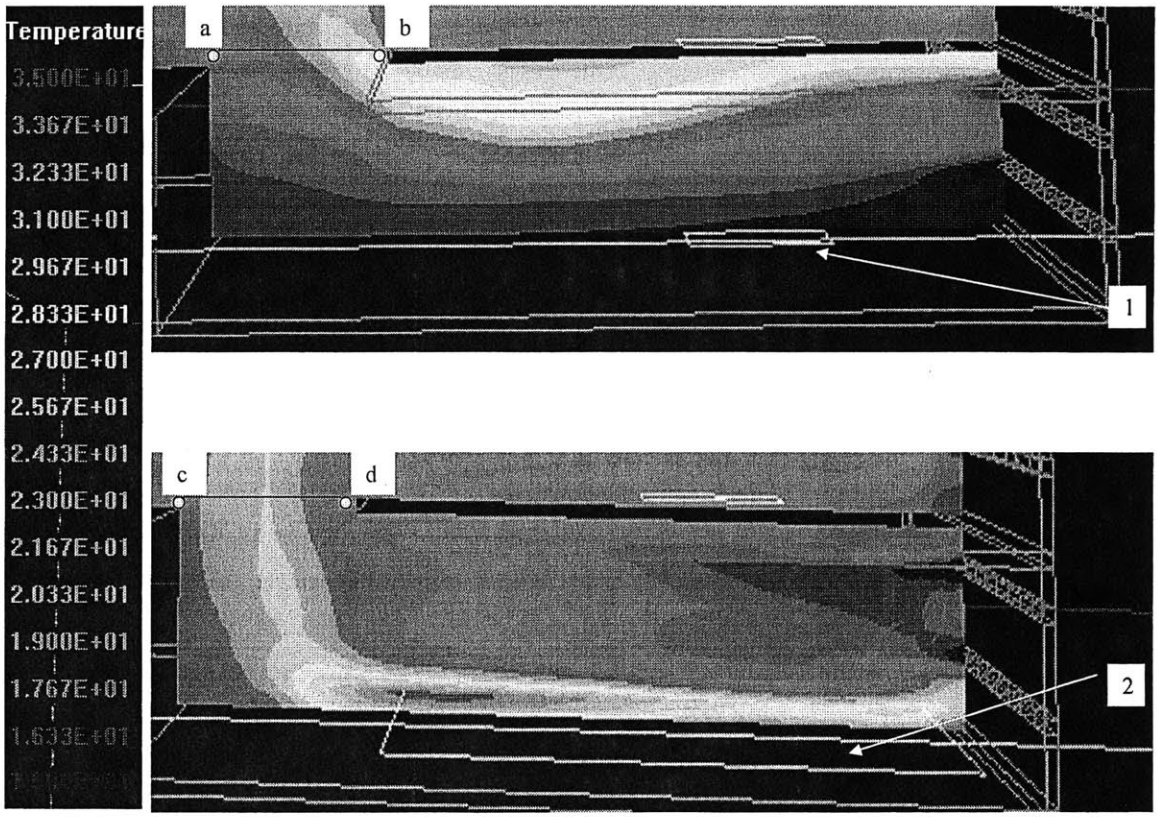

Figure 4.9 Comparison of the temperature distributions of non-uniform heat source (top one) case and uniform heat source case (bottom one). 1 is one of two heat sources in the non-uniform heat source case; and 2 is the heat source of the uniform heat source case.

Figure 4.9 shows the temperature distribution at the middle section of the first floor room. There is a significant difference between the temperature distribution in the first floor room under different heat source types (uniform or non-uniform). Due to the plumes of the non-uniform heat sources, the high temperature air is gathered in the top part of the room. In contrast, the uniform heat source generates higher temperature air at the lower part of the room. Here we assume all the heat sources are located in the lower part of the room.

Although the air temperature distributions of these two cases are different, there are three similar factors between the two cases that are important to validate the MultiVent program:

- Average temperature of indoor air
  The average indoor air temperature is almost same although the temperature distribution is different. The average indoor air temperature in the uniform heat source case is 23.48°C and the non-uniform heat source case has a 23.40°C of average indoor air temperature.
- Average exhaust air temperature
  The air leaving the first floor room has similar average temperature (see the line 'ab' and 'cd' in Figure 4.9). The non-uniform heat source case has a average leaving air temperature is 24.88°C, while the uniform heat source case has an average leaving air temperature of 25.06°C.
- Airflow rates
  The average velocities at the windows and top vents of the first floor room are respectively 0.58m/s and 0.51m/s for the un-uniform heat source case. In contrast, the average velocities at the windows and top vents for the uniform heat source case are respectively 0.58m/s and 0.52m/s.

If two cases have similar values for these three factors, we can see that both cases ca be used to evaluate the multi-zone model calculation because these three factors can fully decide the performance of a zone in the multi-zone model calculation. With the well-mixed zone assumption, the multi-zone model can not tell the difference between two cases although their detailed parameter distributions are different, if their average indoor air temperature, average exhaust air temperature and airflow rate are the same. Also, any two of the above three factors can determine the other factor for the multi-zone case according to energy conservation law.

In above CFD simulations, the heat source type is the fixed heat flux. The radiation, for example to the ceiling, is not considered. Thus, the facades and floor of the model building are adiabatic. Therefore, there is no the tight circulation air cells that are seen experimentally between a warm lower plate and a cool higher plate.

To investigate the detailed distribution in a particular zone, it is necessary to couple the CFD simulation with the MultiVent calculation. That is to say, MultiVent calculation results will provide boundary condition to the CFD simulation for a particular zone, which will be discussed in Chapter 6.

5. Generalizing strategy for applying the MultiVent program

From above simulation and comparison between the MultiVent and full CFD calculation results, we can see that the MultiVent program can provide accurate prediction for natural ventilation, at least here for buoyancy ventilation. However, in order to properly apply the MultiVent program, we may need to carefully deal with two factors in building configurations: large openings and atrium. For the Luton model building, we must divide the large opening into two sub-openings and correspondingly divide the connected atrium space into two zones. In Chapter 7, we will examine the general conditions under which the user may have to divide the large opening and atrium into two sub-parts.

4.3.1.2 A full scale building case with plume impacts

In this case, a full scale building is examined through MultiVent. From the above study, we know that the MultiVent could predict buoyancy ventilation correctly in the Luton model building. In order to implement the methods to full scale buildings, the detailed study on a typical full scale building case is required. This case is an example of the application of the MultiVent program to an extreme condition (or sometimes bad natural ventilation design).

As we know, in some natural ventilation designs, the plume from lower floor may impact the upper floor's natural ventilation by air reentering into the upper floor's window and increase the indoor air temperature of the upper floor. However, it may not be able to significantly change the design because of the exterior façade's visual requirements, although this natural ventilation design is not good. Therefore, how to quantitatively

assess this design is very important for architects before they implement the design into construction. This case study has provided a method to deal with the plume impacts and investigated the methods applied in above Luton model building case.

1. Case description

A three-floor building with a stairwell is designed here to investigate the application of MultiVent to buoyancy ventilation in the full scale building.

Figure 4.10 shows the sketch of this three-floor building. The three openings between the three rooms and ambient environment have same size and same relative location to each floor. All the openings, except the stack vent between the stairwell and ambient environment, have same width of 2m, and all of them are symmetric in the width direction. Thus, the second floor's window is located vertically below the third floor's window. The width of the stack vent is 1 meter. The full width of the building is four meters (vertical to the paper).

In each room, there has a different heat source: 2000W, 3000W and 1500W respectively distribute from the first floor the third floor. The heat source is located at one meter above the floor in the middle of each room.

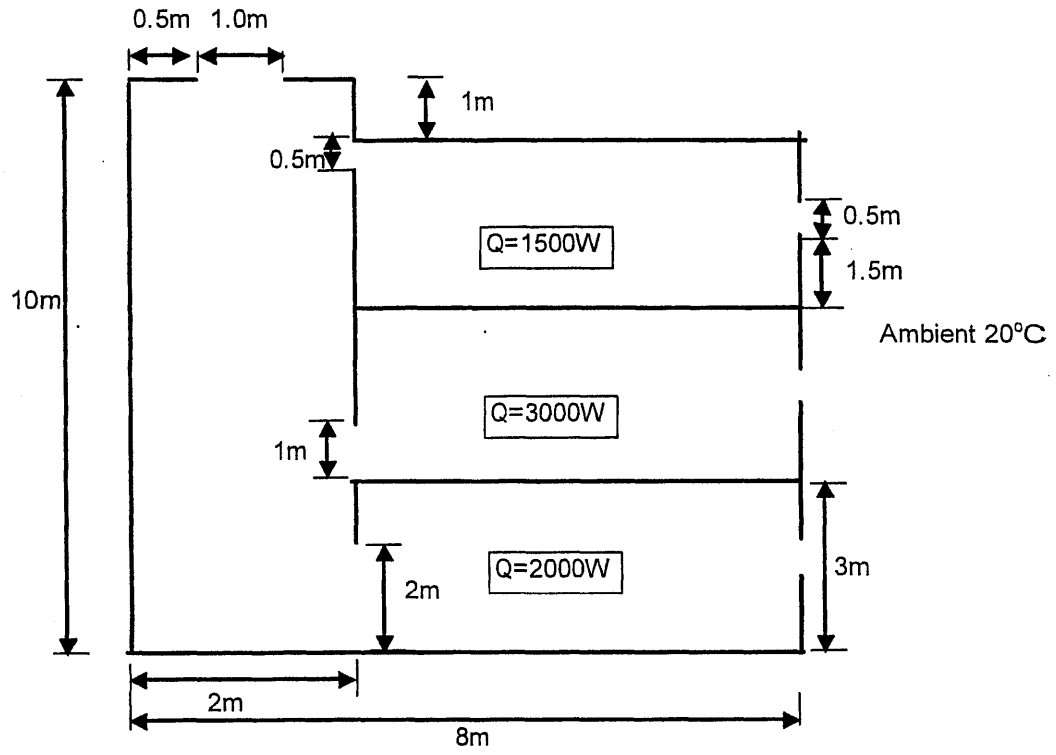

Figure 4.10 Sketch of the 3-floor naturally ventilated building with a stairwell

This naturally ventilated building might be not a good design because the window of the second floor may generate a plume that will reenter the third floor through the third floor room's window.

2. Application of the MultiVent

A two-step method will be used to study the application of MultiVent to buoyancy ventilation. The first step finds that there may have plume problem and the second step gives an estimation of the plume thickness and counts in the plume's impacts.

Step 1

According to the strategy of applying MultiVent investigated by the Luton model building case, this full scale building is divided into five zones as shown in Figure 4.11. In this case, the discharge coefficients (C_d) of opening 7 and 8 are set equal to 0.95, while C_ds of other openings are set as 0.7. All these discharge coefficients may just use the default values of MultiVent program, which are similar as above setting values.

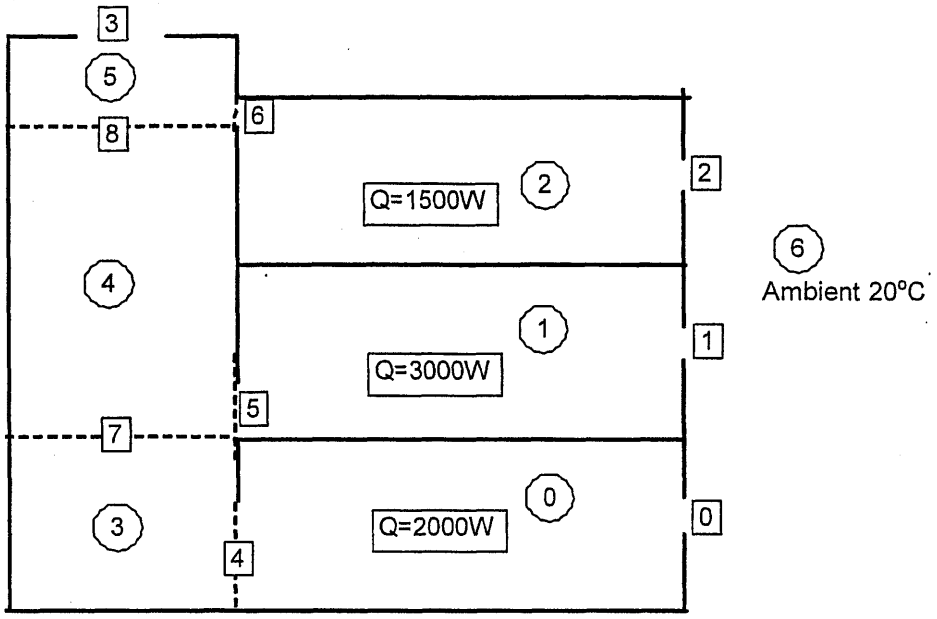

Figure 4.11 Zone divisions of step 1

After the MultiVent calculated this case, we can get the air flow pattern shown as Figure 4.12. MultiVent correctly predicts the two neutral pressure levels in this buoyancy ventilation case.

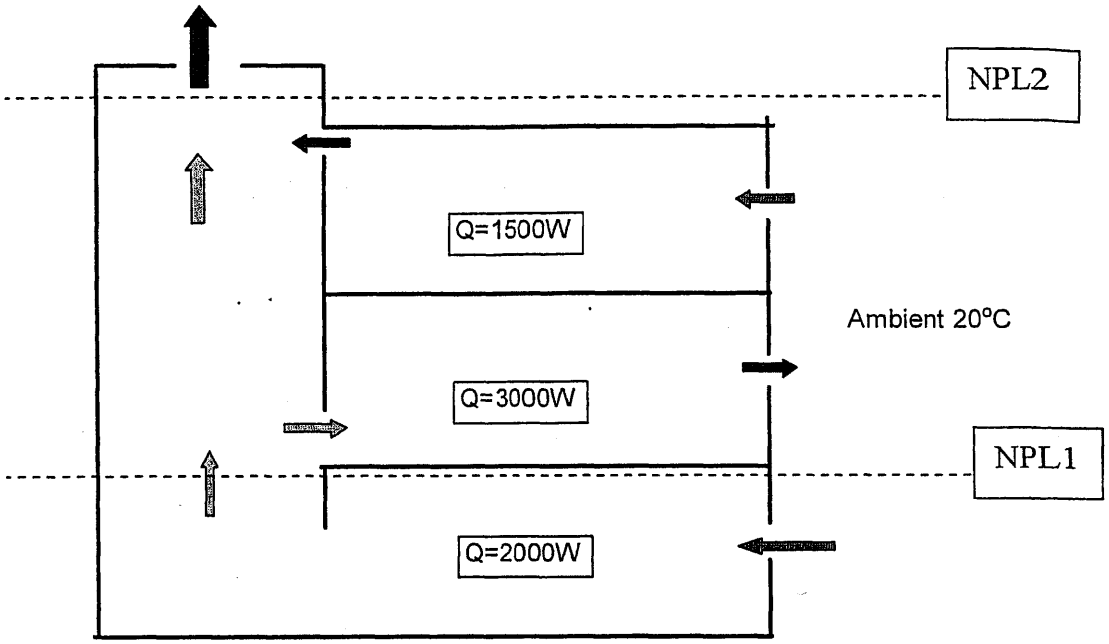

Figure 4.12 Air flow pattern results of step 1

Step 2

With the results of the step 1, the plume of the leaving air from the second floor (see Figure 4.11, opening 1), which may reenter the third floor through opening 2 (see Figure 4.11) and worse the third floor's indoor thermal environment, we need to consider the impacts of the plume. In order to study the plume, two ambient artificial zones are added into the MultiVent network. Figure 4.13 shows the zone divisions for step 2.

Similarly, in this step, the discharge coefficients (C_d) of opening 7, 8, 9,10 and 11 are set as 0.95, while C_ds of other openings are set as 0.7. The affected distance of the plume attached to the exterior wall is around 0.4m. Therefore, we set the width of the zone 6 and 7 equal to 0.4m (see Figure 4.13).

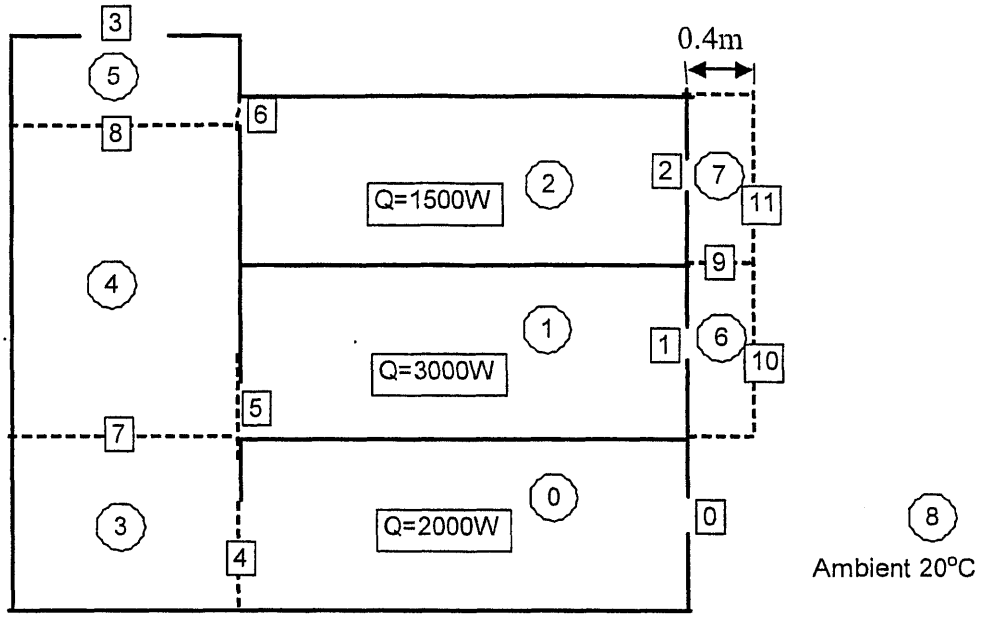

Figure 4.13 Zone divisions of step 2

The airflow pattern of step 2 calculation is shown in Figure 4.14. The MultiVent predicts that the plume from the second floor's window mixes with ambient air and re-enters into the third floor. Therefore, the simulation results of step 1 seem not correctly predicting the thermal environment of the third floor.

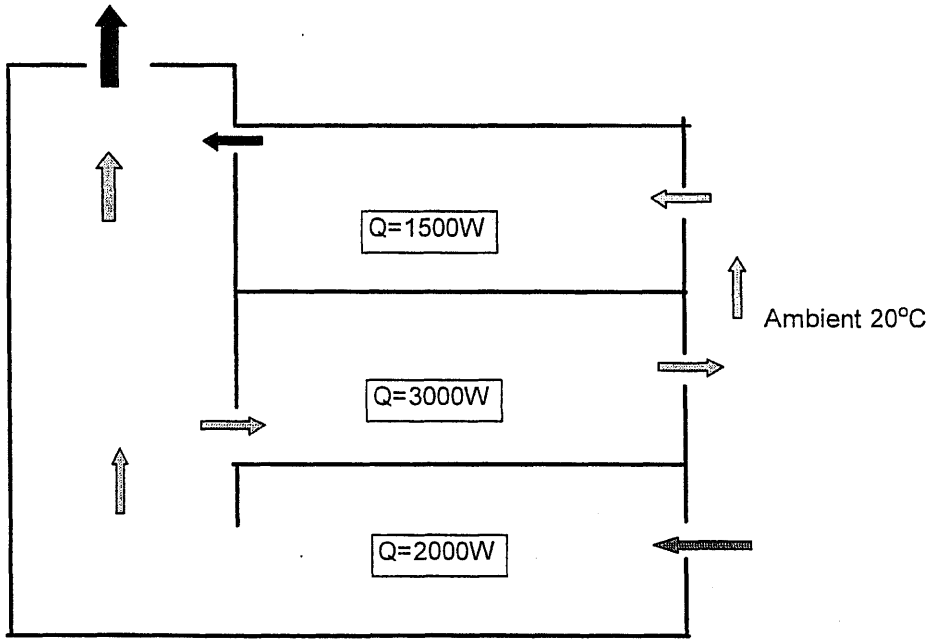

Figure 4.14 Flow pattern of step 2

Because the warm air from the second floor will reenter the third floor room, this building seems not a good natural ventilation design, which could be avoided. For instance, we can reduce the impacts of the lower floor's plume by adding some structures underneath the upper floor's window. Of course, if there has any wind (e.g. the wind velocity is higher than 0.1~0.2m/s), the plume will be disturbed and may not reenter the window of the third floor. Therefore, this extreme condition of the plume impacts in natural ventilation may not often happen in real buildings.

3. Comparison of MultiVent results and full CFD simulation

The full CFD simulation for this full scale buoyancy ventilation building has been carried out. In generally, the average indoor air temperature should be similar between MultiVent calculation and CFD simulation if the airflow through openings is same and airflow pattern is same (see Figure 4.11). Thus, we only need to compare the airflow rates between the full CFD simulation and MultiVent calculation.

Table 4.4 The comparison of the average velocity between the full CFD simulation and MultiVent calculation (m/s)

Opening #	Full CFD simulation	Step 1 of MultiVent	Step 2 of MultiVent
0	0.68	0.70	0.67
1	0.29	0.29	0.30
2	0.32	0.17	0.25
3	0.79	0.60	0.65

From Table 4.4, it is obvious that the plume strongly impacts the airflow rate of the third floor (opening # 2). If we compare the temperatures of the full CFD and the MultiVent, the plume affects not only the temperature of the third floor (zone 2) but also the temperature of the second floor (zone 1), as shown in Table 4.5. Therefore, using two outside zones in step 2 to deal with the plume, the MultiVent calculation results will be improved significantly. Figure 4.15 shows the airflow pattern in the full CFD simulation, which is very similar to the airflow pattern of step 2. It is obvious that the plume from the second floor does reenter the third floor.

Table 4.5 The temperature comparison between the full CFD simulation and the MultiVent calculation (°C)

Zone #	Full CFD simulation	Step 1 of MultiVent	Step 2 of MultiVent
0	22.60	22.38	22.49
1	29.59	28.68	29.49
2	27.32	25.66	26.96

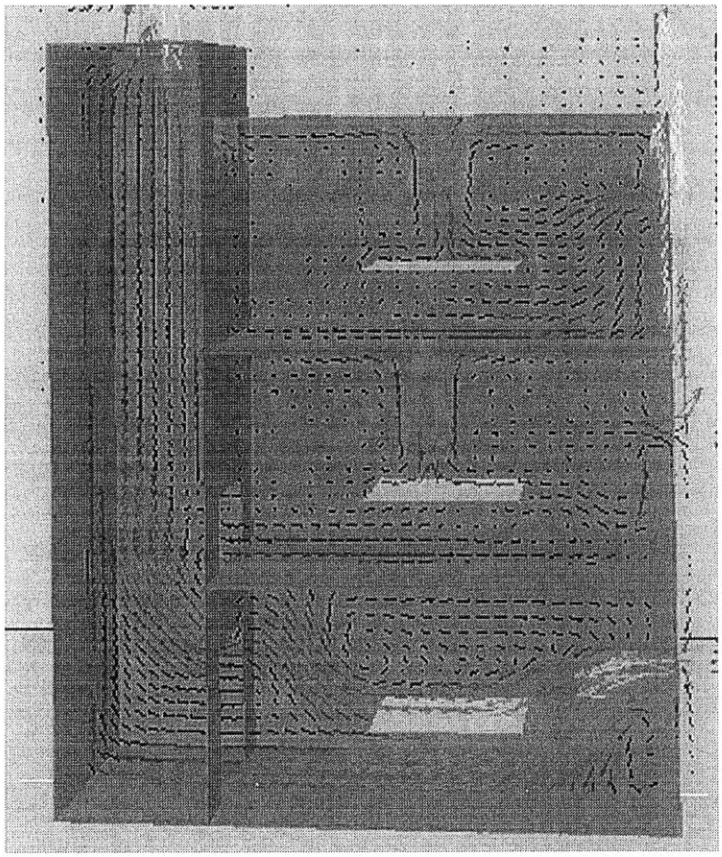

Figure 4.15 Flow pattern of full CFD simulation

4.3.2 Wind-buoyancy combined ventilation of Luton model building

Under real conditions, the outside wind is very difficult to describe and simulate because of its fluctuation. To simplify this problem, the ambient wind was assumed constant. According to previous research [3], the wind varies with vertical distance as:

$$V_i = V_0 (\frac{H_i}{H_0})^{\alpha} \tag{4-31}$$

where, V_0 is the wind velocity at reference height H_0. In this Luton model building case study, V_0 is set as 1m/s and H_0 equals to 1.2m. The constant α, dependent on the roughness of the ground, is set as 0.2 in this example.

To simulate the wind-buoyancy combined natural ventilation, we need to correctly set the wind pressure coefficients for MultiVent calculation. Some previous studies have shown good estimations for calculating the wind pressure coefficients [66]. Table 4.6 shows the wind pressure coefficient at each floor's opening in the MultiVent calculation.

Table 4.6 Wind pressure coefficients in MultiVent calculation for Luton model building

Openings	Ground Floor south & First Floor south	First Floor north & Second Floor north	Stack vents
Cw	0.85	-0.4	-0.4

When the wind velocity is 1m/s and internal heat source in each room is 300W, the ratio of total wind-driven pressure to the total buoyancy pressure is around 0.9, which is estimated in following calculation.

$$\frac{\Delta P_S}{\Delta P_W} \approx \frac{\rho g h \Delta T/(T+273)}{0.5\rho v^2 (C_{W,\max} - C_{W,\min})} = \frac{9.8\times 1.1\times 20/300}{0.5\times 1\times (0.85+0.4)} = 1.1$$

Therefore, the buoyancy and wind-induced pressures have similar magnitude. Here, the zone divisions in MultiVent calculation are same as the case 2 of Figure 4.7, which divides the atrium and large openings into sub-spaces and sub-openings. The control volume and the wind profile of the full CFD simulation for this wind-buoyancy combined ventilation are sketched in Figure 4.16. In CFD simulation, the left vertical surface of the control volume is set as an outlet that has zero pressure boundary condition, while the right vertical surface of the control volume is set as an inlet that has a velocity distribution as the wind-velocity profile described as equation (4-31). The other exterior surfaces of the control volume are set as solid walls with adiabatic boundary conditions.

Same as previous CFD simulation study, the RNG k-ε model is applied to CFD simulation.

Table 4.7 shows the comparison of the average air movement velocities at 14 openings of each room in the model building between the MultiVent calculation and the full CFD simulation. From this comparison, we can see that the airflow rates between MultiVent calculation and the full CFD simulation have a good agreement. It seems that the MultiVent can accurately predict the airflow rates when compared with the full CFD simulation for wind-buoyancy combined ventilation.

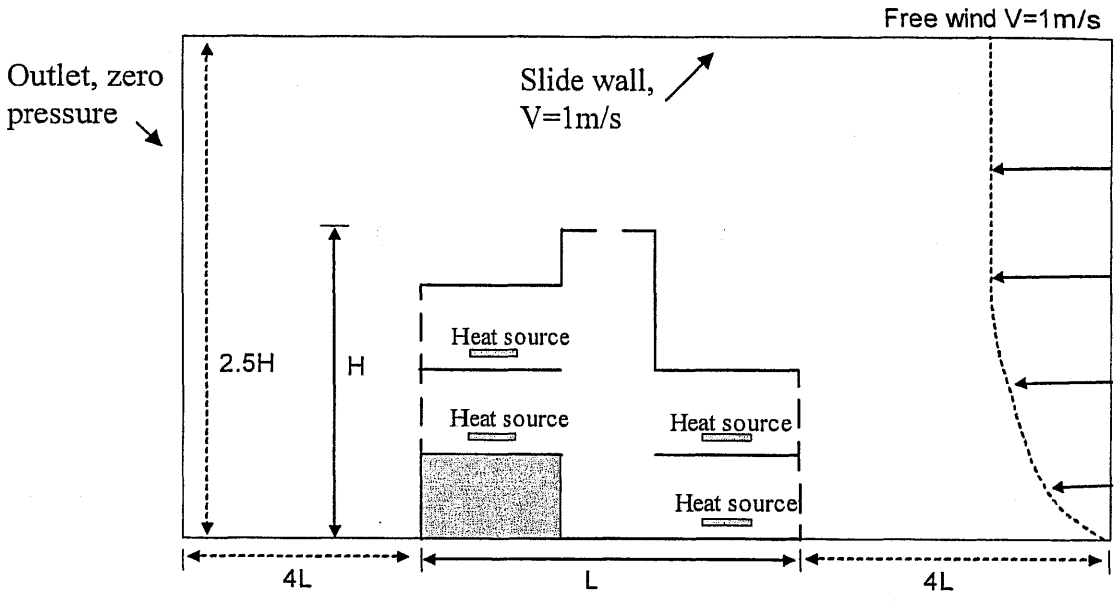

Figure 4.16 Diagram of the full CFD simulation for wind-buoyancy combined ventilation

Table 4.7 Comparison of the average airflow velocities at openings of each room between the MultiVent calculation and full CFD simulation (m/s)

(Average velocity m/s)	MultiVent calculation	Full CFD simulation
Ground floor south room	0.90	0.94
First floor south room	0.82	0.85
First floor north room	-0.46	-0.44
Second floor north room	-0.63	-0.65
Stack vents	-0.72	-0.69

Note: The negative velocity means the air leaving the building.

4.4 Analysis of the calculation error in MultiVent

4.4.1 Source of the error in MultiVent

Besides the system error that is generated from the assumptions in the MultiVent, there are two other calculation error sources:

1. Discharge coefficient Cd

In the program of MultiVent, we used the empirical formula to calculate the discharge coefficient according to the size of the opening. Flourentzou et al [15] have studied the discharge coefficients of general size openings in natural ventilation and found that the velocity coefficients $\varphi=0.7\pm0.1$ and jet contraction coefficients $\varepsilon=0.85\pm0.1$. As a result, the experimental measurements have shown a good agreement with the generally accepted value of discharge coefficient $Cd=\varphi\cdot\varepsilon=0.6\pm0.1$.

However, there may be some differences between the estimated discharge coefficients for different size of openings with the empirical formula and the real discharge coefficients of the naturally ventilated building's openings. Even for the general size openings that have been validated by Flourentzou's experiments, the estimation of discharge coefficients still have slight error because the precision of the experiments were of the order of 20%. It is obvious that these inaccuracies of the discharge coefficients may generate calculation errors in the MultiVent program.

2. Wind pressure coefficient Cw

The MultiVent program used the calibrated formula by Wang et al [61] to estimate the wind pressure coefficients around the facade of the building. In Wang's work, the k-ε turbulence model has been applied into CFD simulation. As we know, the k-ε model cannot correctly simulate the wind-driven flow at the leeward side of the building. Jiang[23] found that there may be a maximum difference of 40% between the wind pressure coefficients at the leeward side of the building calculated by k-ε model and predicted by the LES simulation. Therefore, the estimated wind pressure coefficients also will generate errors in the MultiVent program.

4.4.2 Sensitivity analysis of the error sources

Both the estimations of the discharge coefficients and the wind pressure coefficients will generate errors when we use the MultiVent program to predict natural ventilation. The effects of the precision of the estimations for both types of coefficients will be analyzed in follows.

1. Discharge coefficient Cd

We want to examine a single-zone room (see Figure 4.17) with buoyancy ventilation to understand the impact of the discharge coefficients.

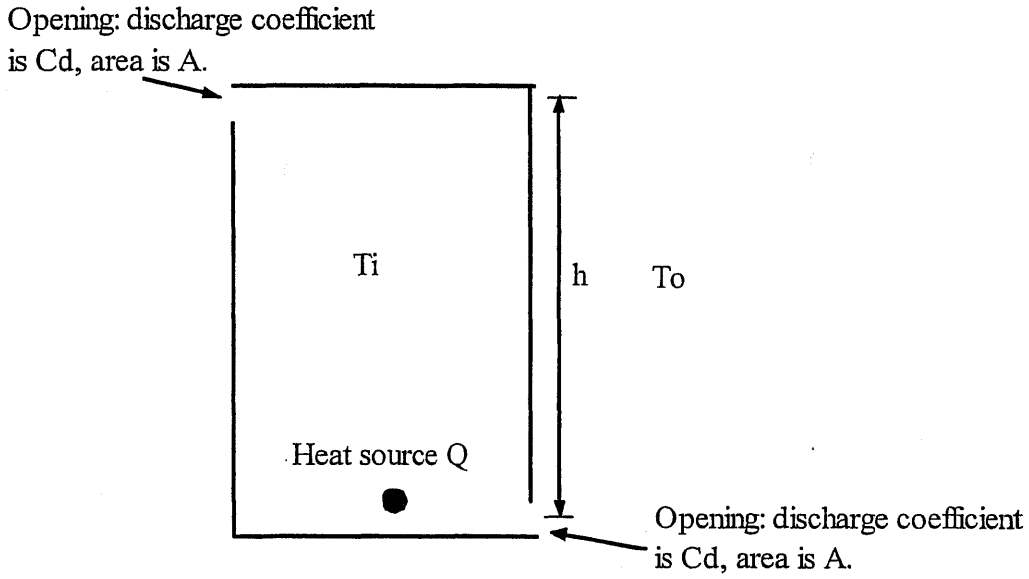

Figure 4.17 A buoyancy ventilated single-zone room (vertical view)

To simplify the problem, we assume the two openings of this single-zone room have the same parameters (discharge coefficient Cd and area A). In steady state, the indoor air temperature is assumed to be well mixed at Ti and the outside air temperature is To. There is a point heat source at bottom of the room that has heat strength of Q. The pressure drop at either of the openings can be calculated as:

$$\Delta P = \frac{\rho g h (T_i - T_o)}{2(T_o + 273)} \tag{4-32}$$

where, ρ is the air density and the g is the gravity constant.

In steady status, there is an energy balance equation as:

$$T_i - T_o = \frac{Q}{F \cdot C_p} \tag{4-33}$$

where, F is the mass airflow rate through the openings and Cp is the specific heat of air.

The mass airflow rates through the openings can be calculated as:

$$F = C_d A \sqrt{2\rho \Delta P} \tag{4-34}$$

Thus, combining above three equations can get:

$$F = \rho C_d A \sqrt{\frac{ghQ}{FC_p(T_o + 273)}} \tag{4-35}$$

From the equation (4-35), we can derive the relationship of the mass airflow rate and the discharge coefficient as:

$$F = \rho^{2/3} C_d^{\ 2/3} A^{2/3} \left(\frac{ghQ}{C_p(T_o + 273)}\right)^{1/3} \tag{4-36}$$

Therefore, the mass airflow rate F is proportional to $Cd^{2/3}$. We can check the flow rate differences corresponding to different discharge coefficients. If the discharge coefficient changes 10%, the mass airflow rate will change 6%. Similarly, if the discharge coefficient changes 20%, the mass airflow rate will change 11%.

From the equation (4-33), it is obvious that the temperature difference between the indoor air and the outside air will have a same rate of change as the mass airflow rate when the discharge coefficient changes, although the temperature difference will increase as the mass airflow rate decreases.

After examined the theoretical analysis of the discharge coefficient impact in a single-zone room, an example case of a full scale building with three rooms and an atrium is designed here to investigate the impact of the discharge coefficient in the MultiVent program. This building has three floors and there is one room in each floor. The main configuration of the building is shown as the left sketch in Figure 4.18. All the three rooms have same size of 5m×4m×3m (Length×Width×Height). There is an atrium in the building with a size of 2m×4m×10m (Length×Width×Height). Three heat sources, 2500W, 2800W and 3000W, are respectively located in the three rooms from first floor to the third floor. Each room has a same size window, 0.4m×1m (Height×Width), which connects the ambient environment. The distance of the window to the room's floor is

same and equal to 1 meter. There is a stack vent at the top of the atrium to exhaust air to ambient with an area of $0.4m^2$.

The right sketch in Figure 4.18 shows the zone division in the MultiVent calculation. In following simulation, we will change the discharge coefficient values of the four exterior openings (three windows and one stack vent) to examine the four air temperatures (three rooms' indoor air temperature and the stack vent's exhaust air temperature) and the four airflow rates (airflow rates though the three windows and the stack vent).

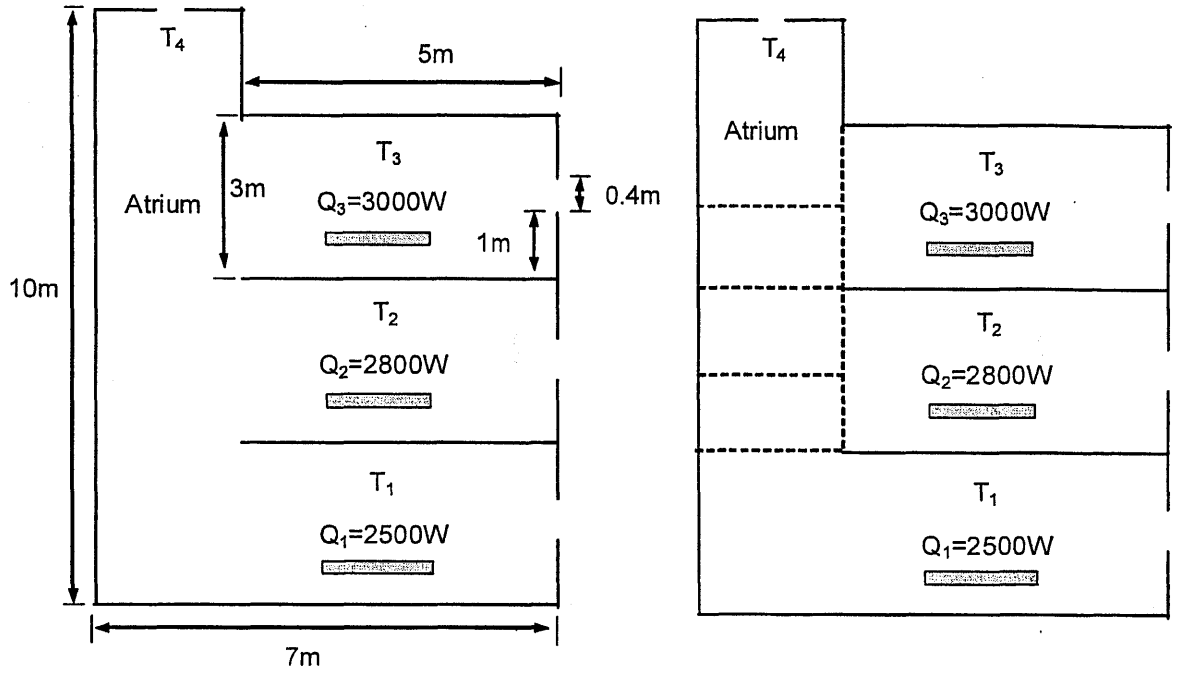

Sketch of the example building (vertical view)

Zone division of the example building (vertical view)

Figure 4.18 An example building to investigate the impact of discharge coefficient

The simulation results of the MultiVent for this example building are shown in Table 4.8 and Table 4.9. The temperature variation and airflow rate variation follow a consistent rule as above theoretical analysis. When the discharge coefficient changes around 20%, the temperature and airflow rate will change ~10%. Similarly, as the discharge coefficient changes 33%, the temperature and airflow rate will change around 20%.

Table 4.8 Temperature variation with the discharge coefficients

Temperature	Cd value of the four exterior openings			Relative error ($\lvert \Delta T \rvert / (\overline{T} - 20)$)		
	0.5	0.6	0.7	Cd=0.5 to Cd=0.6	Cd=0.6 to Cd=0.7	Cd=0.5 to Cd=0.7
T_1	26.52	25.78	25.22	12%	10%	22%
T_2	28.08	27.16	26.47	12%	10%	22%
T_3	31.49	30.21	29.34	11%	8.9%	20.6%
T_4	31.33	30.04	29.07	12%	10%	22%

Table 4.9 Airflow rate variation with the discharge coefficients (kg/s)

Air flow rate	Cd value of the four exterior openings			Relative error ($\lvert \Delta V \rvert / \overline{V}$)		
	0.5	0.6	0.7	Cd=0.5 to Cd=0.6	Cd=0.6 to Cd=0.7	Cd=0.5 to Cd=0.7
V_1	0.38	0.42	0.47	10%	11%	21%
V_2	0.25	0.28	0.31	11%	11%	21%
V_3	-0.19	-0.21	-0.23	10%	10%	19%
V_4	-0.44	-0.5	-0.55	12%	10%	21%

For more complex buildings, the interaction effects of the multiple zones, openings and ventilation forces will generally decrease the impact of the inaccuracy of some discharge coefficients. Consequently, the MultiVent program can provide simulation with the calculation accuracy in the order of 10% if the estimation of the discharge coefficients has precision of 20%.

2. Wind pressure coefficient Cw

The cross-ventilation is most sensitive to the wind pressure coefficient Cw. We will investigate a single-zone with two identical openings in the opposite walls (see Figure 4.19). Assume the ambient free wind velocity is V. The wind pressure coefficient of the opening at windward side is $C_{w1}(>0)$ and the wind pressure coefficient of the opening at leeward side is $C_{w2}(<0)$.

Let Pi be the air pressure of the mid-point inside the room and Po the ambient air pressure at same height of the mid-point of the room space. The pressure drop at the windward side opening can be calculated as:

$$\Delta P_1 = P_o - P_i + 0.5C_{w1}\rho V^2 \tag{4-37}$$

Similarly, the pressure drop at the leeward side opening also can be calculated as:

$$\Delta P_2 = P_i - P_o + 0.5C_{w2}\rho V^2 \tag{4-38}$$

If we assume the two openings have same configuration, the pressure drop at the two openings should be same because of mass conservation in steady state if the density is the same:

$$P_o - P_i + 0.5C_{w1}\rho V^2 = P_i - P_o + 0.5C_{w2}\rho V^2$$

Then we can get:

$$P_i = P_o + \frac{1}{4}(C_{w1} + C_{w2})\rho V^2 \tag{4-39}$$

From the equation (4-37) and equation (4-39), the pressure drop at each opening can be written as:

$$\Delta P = \frac{1}{4}(C_{w1} - C_{w2})\rho V^2 \tag{4-40}$$

Therefore, the mass airflow rate F is proportional to the difference of the two wind pressure coefficients as: $F \propto \sqrt{C_{w1} - C_{w2}}$.

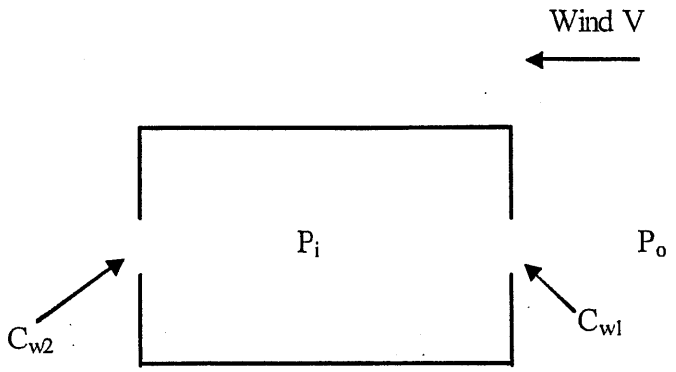

Figure 4.19 A single-zone room with cross-ventilation (plan view, no heat source)

Here we will examine the mass airflow rate changing with the wind pressure coefficients. Assume the C_{w1} equal to 0.7, and the C_{w2} equal to -0.4 under general conditions. We will calculate how much the airflow rate will vary with the wind pressure coefficients.

Table 4.10 The mass airflow rate variation with the wind pressure coefficients

Case	1	2	3	4
Cw1	Change 10%	Change 20%	Not change	Not change
Cw2	Not change	Not change	Change 20%	Change 40%
Airflow rate F	Change 3%	Change 6%	Change 3%	Change 6.5%

From Table 4.10, it seems that the pressure coefficient difference will change the airflow rate by a relatively small fraction of the discharge coefficient variation. This case considers the extreme conditions when the wind pressure coefficients change for a single zone with negligible buoyancy effect and two openings. Under general conditions, the interactions of the buoyancy effects, the multiple zones and openings should decrease the impacts of the wind pressure coefficients.

4.4.3 Comparison of MultiVent results with CFD simulation

In order to validate the MultiVent program, the calculations for several cases have been carried out in pervious sessions. The results of the Luton model building case in this section (Chapter 4) with buoyancy ventilation showed the biggest temperature difference between the MultiVent calculation and the full CFD simulation. To evaluate the relative error of temperature prediction, we define a parameter as follows:

$$\eta = \frac{|T_m - T_c|}{|T_e - T_o|} \tag{4-41}$$

where, T_m is the zone air temperature predicted by the MultiVent program;

T_c is the zone air temperature calculated by the full CFD simulation;

T_e is the exhaust air temperature calculated by the MultiVent program;

T_o is the outside/ambient air temperature.

With the data of Table 4.2, we can calculate the relative temperature errors (η) and get the following Table 4.11. In this Luton model building's buoyancy ventilation, the ambient air temperature is 13°C. The results of case 2 (see Figure 4.7) are compared with the full CFD simulation in Table 4.11 because case 2 provides the most accurate MultiVent calculation for the buoyancy ventilation.

Table 4.11 The relative temperature errors (η) between the MultiVent calculation and the full CFD simulation

Zone	Full CFD simulation (T_c)	MultiVent calculation of case 2 (T_m)	Relative errors (η)
0	23.48	25.3	7.56%
1	29.43	32.28	11.00%
2	29.38	32.28	11.20%
3	37.19	39.77	9.96%
4	25.67	28.32	10.23%
5	27.74	32.29	17.57%
6	30.20	32.35	8.30%
7	35.21	38.05	10.97%

From Table 4.11, we can see that the relative errors lie in the range of 8% to 18%. Except the zone 5, the MultiVent program can provide a good temperature prediction for other zones in the Luton model building with ~10% precision. The maximum error 17.57% happens in the zone 5, which is mainly generated by the well-mixed assumption of the multi-zone model. In this Luton model building case, comparing with zone 5, the other zones are much closer to the well-mixed condition. The working rooms, including zone 0, 1, 2, and 3, are important for the prediction of the indoor thermal environment, while

other zones (including zone 4, 5, 6 and 7) are not very important for the thermal environment prediction.

Therefore, if based on the assumptions of the MultiVent program, with the analysis of the discharge coefficient and wind pressure coefficient, we can conclude that the MultiVent program should provide simulation with accuracy in the order of 10% in general natural ventilation, which is validated by previous case studies. Even counting in the errors generated by the assumptions of the multi-zone model, the MultiVent program could provide prediction for natural ventilation with accuracy of 20%.

4.5 Conclusions

The multi-zone model is a useful tool to predict natural ventilation, both buoyancy and combined wind-buoyancy ventilation if we properly apply the multi-zone model to natural ventilation. For instance, properly divide the zones in the naturally ventilated buildings.

Two special factors should be carefully considered when using the multi-zone model to predicting natural ventilation: large openings and atrium, which are often designed in natural ventilation to promote ventilation rate. The division of the atrium, or other large vertical connection spaces, has a strong impact on the result of the multi-zone model calculation. Therefore, it is recommended that we divide the atrium into at least two smaller zones for each floor. To generalize the zone dividing method for the atrium, it would be better to divide the atrium space into two smaller zones for each floor even if there is only one room in each floor to capture the reverse flows between the room and the atrium (see Figure 4.20). There is an example for this condition with buoyancy ventilation shown in Figure 4.20. In Figure 4.20, the right side graph shows the recommended zone divisions for the atrium space and the room in the second floor. If we divided the atrium space of the second floor into a uniform zone, the uniform air temperature of this atrium space will impact the buoyancy effect between the atrium and the room although we may apply the multiple-opening model to the surface (opening) between them. It is obvious that the two zones of the atrium space at the second floor should have different temperatures that should generate different buoyancy forces. However, for the atrium space at the first floor, it doesn't need to be divided into two

zones because there are not reverse flows between the atrium space and the first floor space. This first floor atrium space can be combined with the first floor room into a single zone.

Even in some extreme cases, such as the above case of a real scale building with plume impacts on the other rooms, MultiVent still can predict natural ventilation with acceptable accuracy. In this case, the calculation should be completed in two steps: first step is to calculate the building in general conditions and find the existence of the plume; second step is to define a new zone system that includes the outside zones connected the plume openings and then reach a better prediction for the natural ventilation under this extreme conditions. However, these extreme cases should be prevented from happening because they bring bad natural ventilation and indoor thermal conditions. MultiVent is validated; it can help us predict this condition and improve the design.

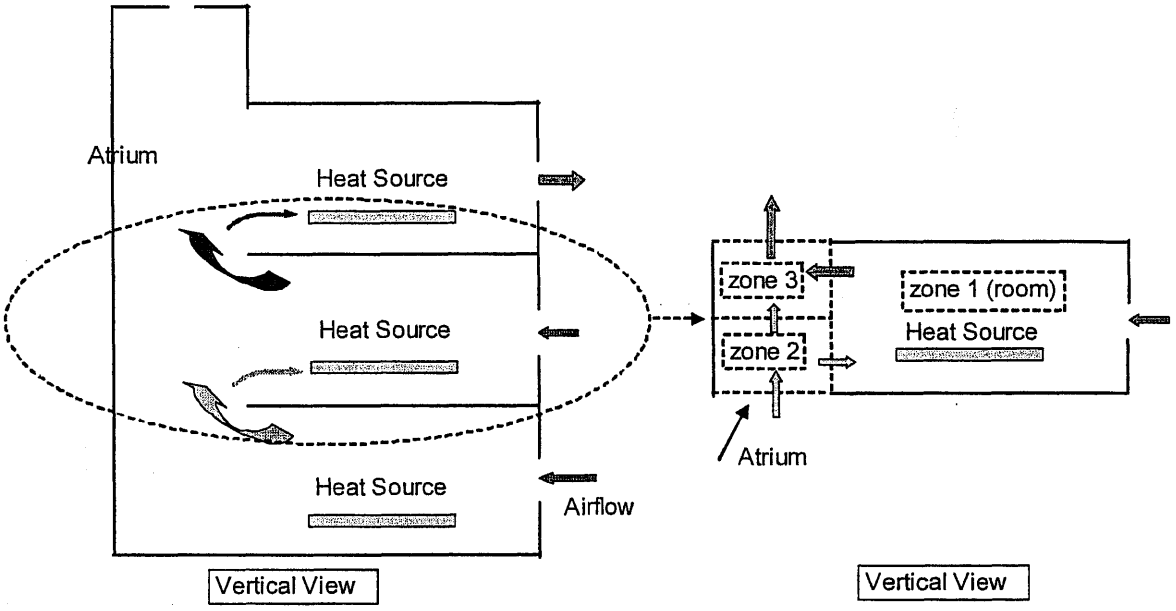

Figure 4.20 An atrium aided naturally ventilated building with one room in each floor

Through the implementation of MultiVent to buoyancy and combined wind-buoyancy ventilation, we found that MultiVent could correctly predict natural ventilation quickly. For example, only a couple of minutes are needed to simulate these multiple space buildings. Thus, it is obvious that integration of the multi-zone model with CFD can save a significant amount of computation time. The integration needs to transfer the MultiVent calculation results to the CFD simulation as boundary condition in order to provide more detailed information on some particular zones that the user is interested in.

With the analysis of the discharge coefficient and wind pressure coefficient, we can conclude that the MultiVent program should provide simulation with accuracy in the order of 10% in general natural ventilation when the discharge coefficients and windward wind pressure coefficients have a precision of 20% and the leeward wind pressure coefficients have a precision of 40%.

In Chapter 6, the integration of MultiVent with CFD simulation for applications in natural ventilation will be investigated.

Chapter 5

On-line Calculation Service of MultiVent

5.1 Introduction

MultiVent is a multi-zone model program designed for evaluating natural ventilation using Sun Java language. In order to provide on-line calculation for architects and engineers, we have built a web-server for the MultiVent. Apache Tomcat 4.1 is applied to build the server. XML and Servlet are adopted to connect the MultiVent java codes with the server. As we focus on the potential users as primarily made up of architects in the design phase, the web-server is constructed to be simple and easy use.

Apache Tomcat is the servlet container that is used in the official reference implementation for the Java Servlet and JavaServer Pages technologies. Java Servlet technology provides web developers a simple, consistent mechanism for extending the functionality of a web server and for accessing existing systems. Tomcat is developed in an open and participatory environment. Tomcat 4.1 can be downloaded and updated via website: http://jakarta.apache.org/tomcat/.

In order to use the MultiVent on-line calculation service, the user needs to input the definition data for the case to be evaluated. After finishing the case definition, the user may review the definition data. If the definition is correct and complete, the user may carry out the on-line calculation and view the graphs of the calculation results.

The following section will begin by introducing the structure of the web-server. To illustrate how to properly use the MultiVent to evaluate natural ventilation design, the server provides two choices for on-line calculation: choosing pre-existing building scenarios or user self-designed cases.

5.2 Structure of MultiVent web-server

5.2.1 Function structure of MultiVent web-server

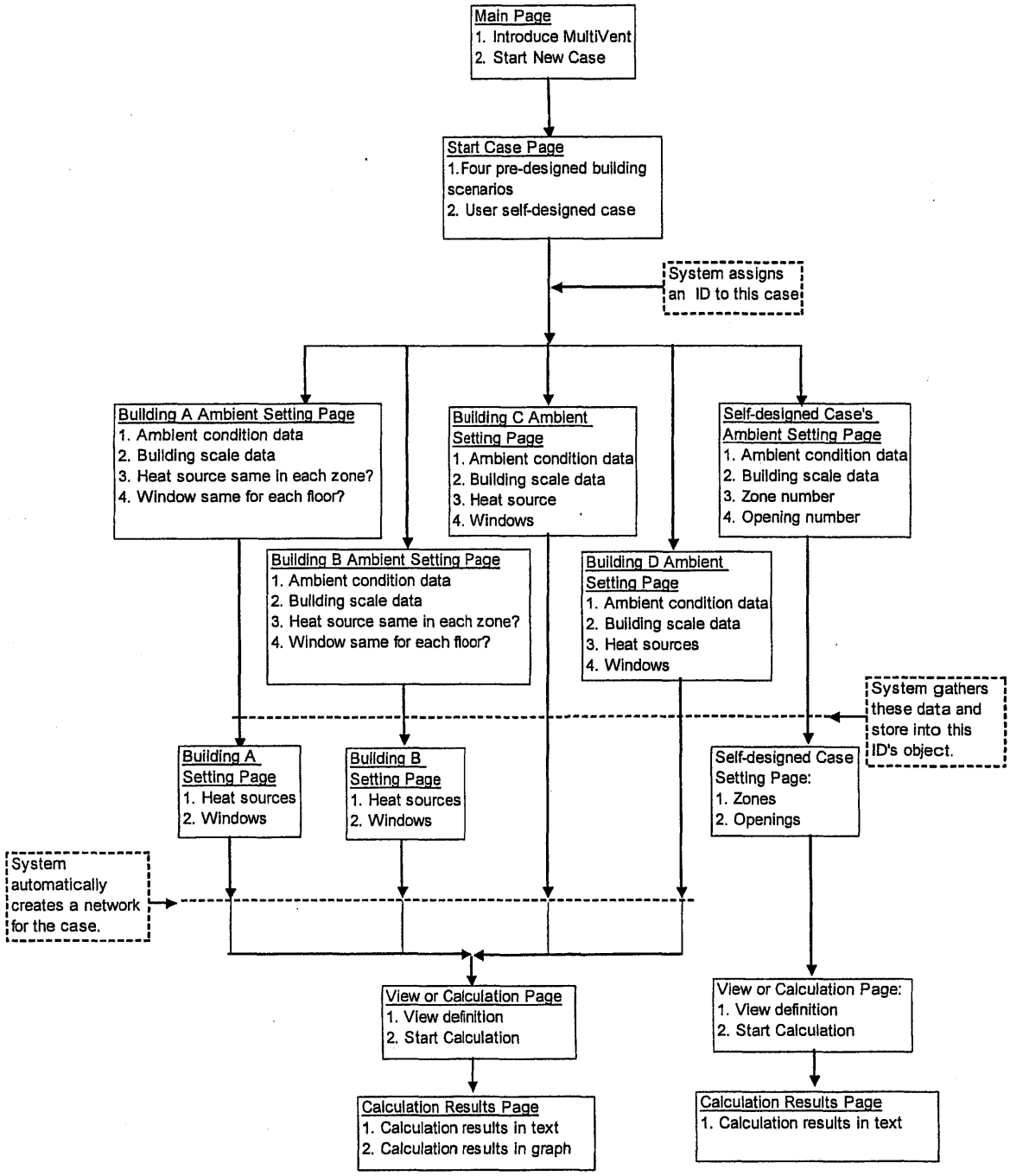

Figure 5.1 Structure of the MultiVent web-server

To complete the typical applications of the MultiVent to natural ventilation design, we construct the functions that are implemented in the web server, shown in Figure 5.1. The building A, B, and D can be respectively referred to Figure 5.3, 5.4, and 5.5. The building C is the single-sided natural ventilation building with a lower opening and a upper opening in the same side wall.

The web service functions can be divided into two main parts: building scenarios and self-designed case.. All of the calculations are carried out on the server, not on client side. This model is generally called server side (SS) model that doesn't need the user to install any software. In addition, this method controls the security of data and source codes. However, it slows the processing speed.

In the MultiVent web server, system (server) assigns a user ID for each case. The user ID is identified by the current time with milliseconds when the case is created. Through this method, the server can manage all of the cases' data, without conflicting between different users who use the MultiVent server at same time. Besides, the user ID provides a way for tracking and managing the previous cases in the MultiVent server's future development.

After the user defines the ambient conditions for a case, the server will gather all of the input data into an object of class 'DataPool' created by this case's ID. Therefore, there is no limitation for the number of simultaneous users, as long as the server has enough memory and CPU capacity.

5.2.2 Directory structure of MultiVent web-server

To create a directory in Tomcat for the web server, it needs to be placed into a directory named webapps under the directory where you installed your Tomcat. For example, if we created a directory, MultiVent, for all the files for MultiVent web server, its complete path would be: C:\Program Files\Apache Group\Tomcat 4.1\webapps\MultiVent\.

Tomcat provides an Administration Tool for the server administrator. With this tool, the administrator can define the path of the server implemented. For the MultiVent web server, we created a new Context under the Host (localhost), and the document base is the same as the above complete path. However, the relative path is just '/MultiVent', which is very important and useful when we write the XML file. Another useful tip to be

mentioned here is that the parameter is 'reloadable' in the context. It is necessary to have the setting as 'true' when you change your XML or Java class. Otherwise, you have to restart your server computer to load the new revised edition.

Under the MultiVent directory, Tomcat needs specific locations for the various files required for the web server. Figure 5.2 shows the management directory tree of the files for the MultiVent web server. If the administrator wants to relocate the MultiVent web server, he/she only needs to move the total directory 'MultiVent', and won't bother to interrupt the relative locations of the files under this 'root' directory. Otherwise, the contents of 'web.xml' and class files may need to be changed and complied.

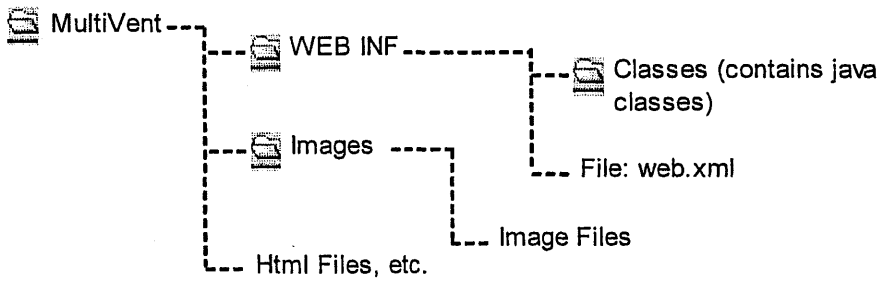

Figure 5.2 Directory structure of the MultiVent web server

When the user transfers data from the client side to the web server, there is a limitation for the amount of data set by Apache Tomcat. The default value of the data transfer is 1024 bytes. The web server manager can change this volume limit via Tomcat Server Administrator. In Tomcat Server Administration Tool, enter the "Service (Tomcat-Standalone)" option and choose the "Connector (8080)", then we can find the "Default Buffer Size" where the server manager can change the data volume limit. For MultiVent, we set it as 2048 bytes, which can permit the user to transfer the amount of data equivalent to 30 zones and 40 openings in a simulation.

5.3 Calculation Process in MultiVent Web Server

5.3.1 Building Scenarios On-line Calculation

The MultiVent web server provides four types of typical natural ventilated building scenarios for the user choice:

A. Atrium aided natural ventilation
B. Wind scoop aided natural ventilation
C. Single-sided natural ventilation
D. Cross ventilation

Except the building scenario D, cross ventilation case, all the other three building scenarios include the buoyancy effects. A user can define the heat source in each room of the building D although the building D does not have real buoyancy effect calculation because all the rooms locate in a same height (same floor).

Generally, these building scenario functions are designed for the users who are not familiar with multi-zone modeling or thermal calculations. This function can provide a training process for the beginning user, because it covers most common natural ventilation cases.

We mainly need to clarify how the MultiVent server deals with the zone definitions in its internal Java codes. The four types of building scenario will be illustrated one by one as:

1. Atrium aided natural ventilation

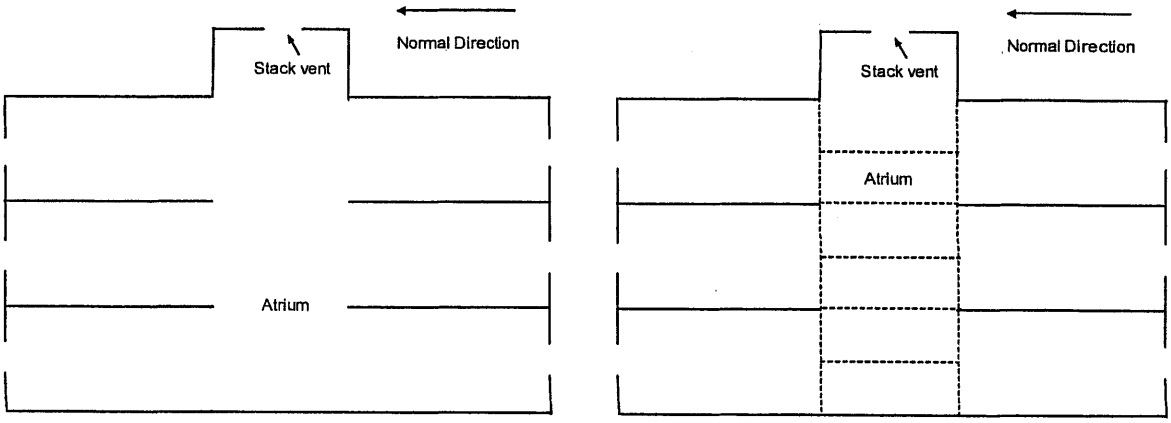

Figure 5.3 Building sketch and zone division of building A

Building type A is designed to calculate the natural ventilation in the buildings with a central atrium. This type of building is the same as the Luton model building we discussed in previous chapters. The normal direction defines a coordinate that is used to locate the outside wind direction, which is useful when we calculate the wind pressure

coefficients at the openings on the exterior walls. To standardize the simulation case, several assumptions are made for this type of building:

- The building is symmetric to the atrium.
- The connection between the working room and the atrium is fully opened. The opening located between the working room and the atrium has the same height as the working room. Here, the working rooms are the room spaces that locate on the two sides of the atria.
- Exterior windows only locate on the walls that are vertical to the normal direction. The exterior windows of the working rooms in the same floor have same elevation because symmetric to the atrium.
- The rooms of each floor have the same height.

The wind pressure coefficient at the stack vent is calculated through the equation (4-6). Assumptions are made here in order to apply equation (4-6) as follows:

- The section configuration of the atrium's attic part is rectangular.
- The atrium is higher around (or less) than 20% of the main building's height.
- The stack vent area is not too large compared with the atrium floor area.

Users can specify their case in building type A using the following features:

- Heat source loads in each working space.
- Area, height and/or elevation of each exterior window at each half floor
- Stack vent area and location
- The height of atrium
- Floor area of working space
- Floor area of atrium
- Number of the floors in building

After the user defines the information for building type A, the system will automatically generate a zone division as Figure 5.3 shown, which is validated through the previous Luton model building case.

2. Scoop aided natural ventilation

The scoop aided natural ventilation case is similar to the atria aided natural ventilation. It could be viewed as half of the atrium aided natural ventilation case.

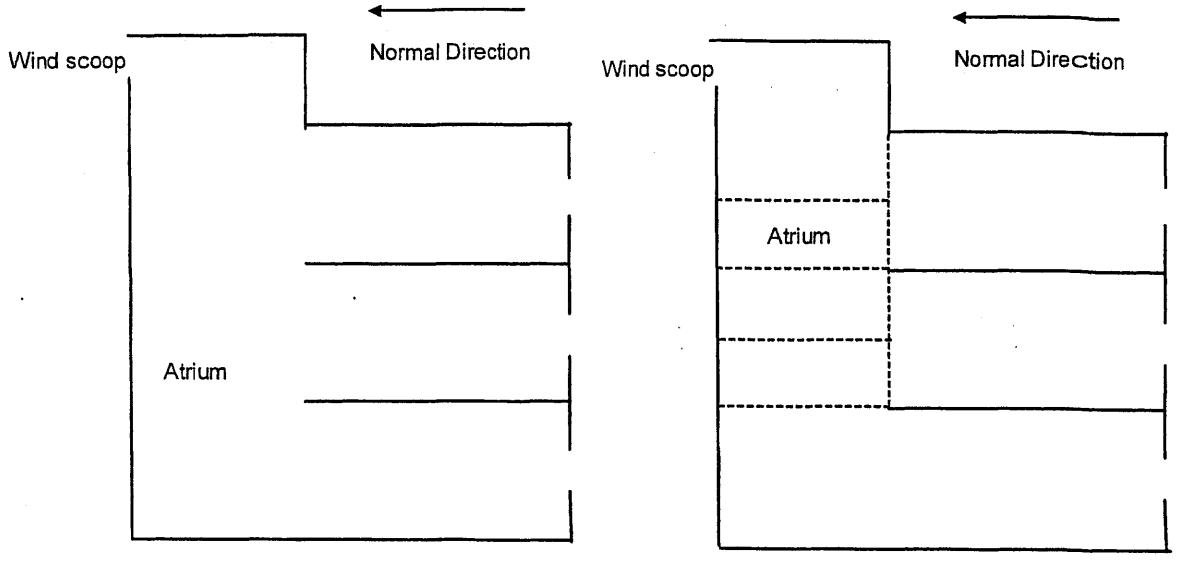

Figure 5.4 Building sketch and zone division of building B

Figure 5.4 shows the building sketch and the zone division for building type B. The assumptions and specified features of building type B are very similar as building type A.

3. Single-sided natural ventilation

When compared with other building types, the single-sided natural ventilation building is much simpler. It only has one room and two openings on the same side of the exterior wall. Thus, the user only needs to specify the room size, the heat source load in the room, and the two windows, plus the information about ambient environment. It provides a user an approach to understand the single-sided natural ventilation from the relationship of the heat source, the opening area and their locations.

4. Cross ventilation

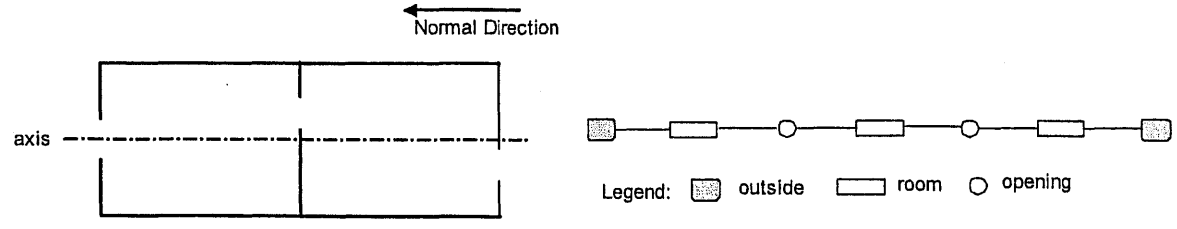

Figure 5.5 Plan view of building sketch and network illustration

The cross ventilation case is designed for a user to study cross ventilation under simple building plans. The normal direction shown in Figure 5.5 is used to locate the wind direction that is very important for cross ventilation. There is an axis in the middle of the building sketch in Figure 5.5, which is used to locate the relative locations of the openings. The flow resistance due to airflow changing directions between rooms will be neglected and not added to the local resistance of openings.

As with the first two types of buildings, the user can specify the length of each room, the openings, and the heat source loads. We also have following assumptions:

- All rooms are at the same floor level
- Same width for all rooms
- Only one opening between two rooms or room to ambient

Among these four building scenarios, the system automatically defines the initial indoor air temperature as 1°C above the ambient air temperature that a user inputs. The network system consisting of the zones, openings and ambient environment is also automatically created by the MultiVent server. After finishing the natural ventilation calculation, the MultiVent will visually show the results by graphing the airflow pattern and the temperature distribution in the building.

In order to visually show the results, we designed a strategy to graphically represent the results with lines, strings and arrows using different colors in Java codes. The Java codes then needs to decode the Java graph and then encode it into an image that finally can be shown in the web browser. The virtual result of an example on-line calculation for a scoop aided natural ventilation case, shown in Figure 5.6, is demonstrated in Figure 5.7. In this example, the width of the building is 5 meters. The window for each of the floor working spaces has a same area (0.2 m^2) and the relative location (1 meter above its floor).

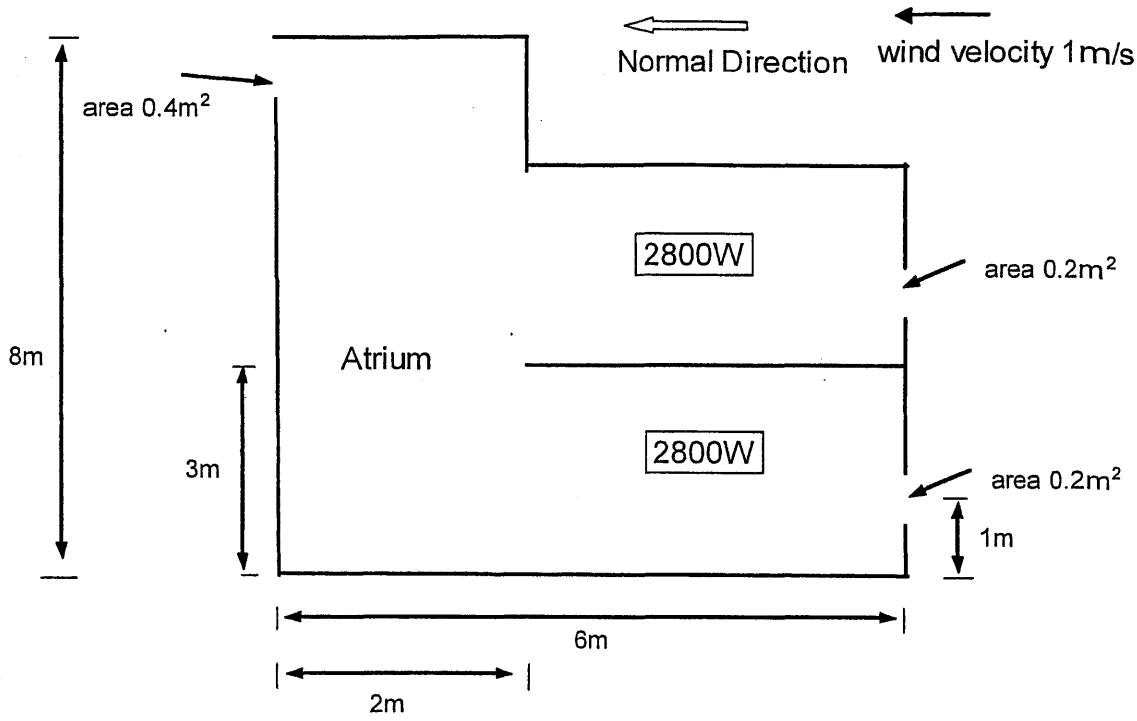

Figure 5.6 Example scoop aided natural ventilation case in vertical view

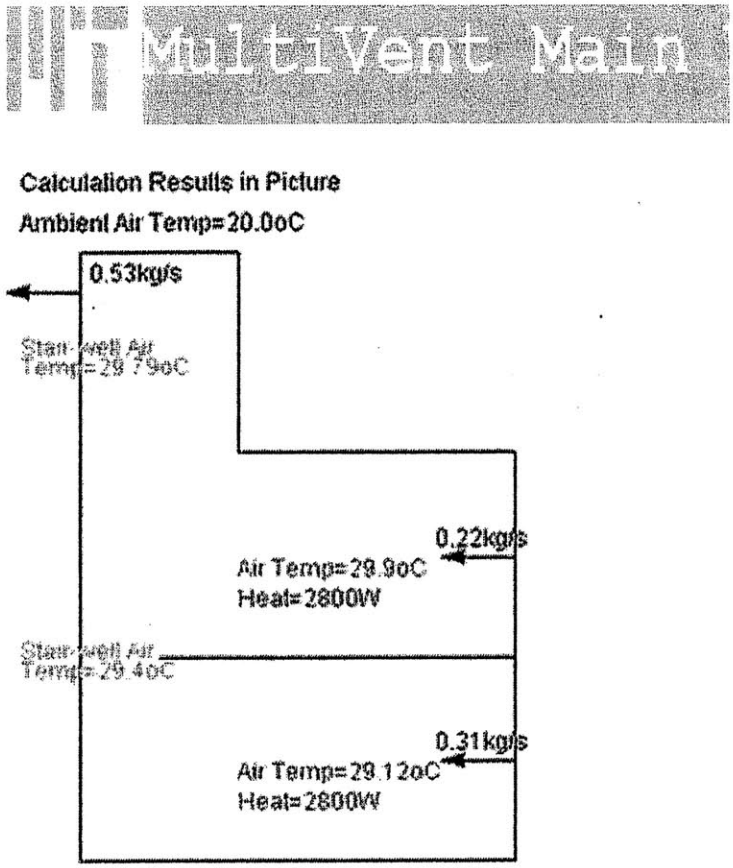

Figure 5.7 The visual graph of the example scoop aided natural ventilation case

5.3.2 User self-designed natural ventilation case

In addition to the four types of building scenarios, the MultiVent provides a tool to some professional or experienced users to access some special and more complicated natural ventilation cases. They can design a building that is not limited to the building scenarios.

As described in Figure 5.1, the user self-designed natural ventilation case also has two main steps: first, define the ambient environment and the scale information about the building; second, input the zone and opening information. Although this is the user self-designed natural ventilation case, some special parameters, such as wind pressure coefficient and discharge coefficient, are automatically predicted by the MultiVent program and do not need user inputs.

In the definition of opening information, the user needs to specify the location of the opening in the walls in order to calculate the wind pressure coefficient. Therefore, the four sides of walls relative to the north direction are defined as illustrated in Figure 5.8, which is also used to decide the wind direction.

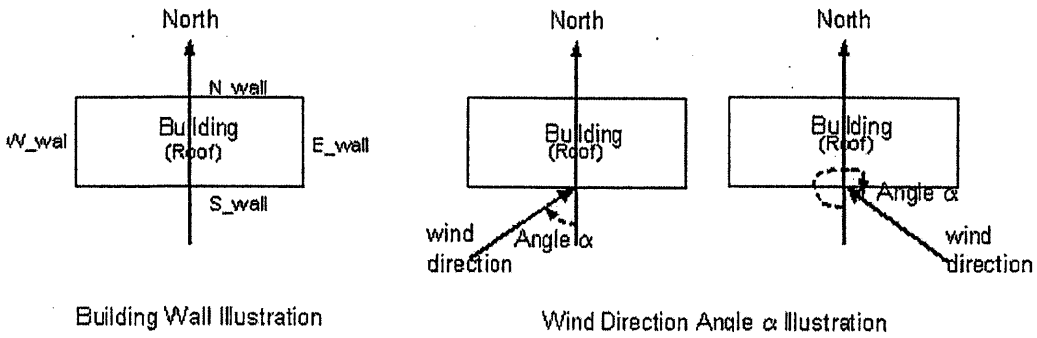

Figure 5.8 Building wall and wind direction illustration

5.4 Summary

Apache Tomcat is adopted to build the MultiVent web server with Java Servlet and XML. The function structure and management directory structure are demonstrated in this chapter.

Two choices are provided to users of the MultiVent web server:

- Four Common Building scenarios
- User self-designed case

In the building scenarios, four types of typical buildings are available for the user to study some simple natural ventilation cases. For each type of building, there are some assumptions and specified features. The user self-designed case provides more flexibility for a user to predict the natural ventilation in specified conditions. However, the self-designed case will require additional understanding of the multi-zone model and experience using the MultiVent.

This web server is a preliminary version of the MultiVent on-line service. It has many functions and visualization features to be improved upon in future. For example, the demonstration of the airflow pattern of the calculation results in the user self-designed case is a very interesting, but difficult task still to be solved.

The MultiVent on-line calculation service will provide a convenient method for users to simulate their natural ventilation design in future. However, we may still inspect some possible improvements for the MultiVent on-line calculation service. For example, the whole package of the MultiVent program can be re-written in C# and the on-line service package can be revised in .NET because the C# and .NET are integrated together. Thus C# and .NET can provide relatively simpler coding, web-managing and fast on-line processing compared with the combination of Java, Java Servlet and Tomcat.

Chapter 6

Integrating MultiVent with CFD (PHOENICS) for Natural Ventilation

6.1 Introduction

To design and control a large scale naturally ventilated building, the integration of the multi-zone model with computational fluid dynamics (CFD) may be required. The integration of the multi-zone model and CFD is a feasible quick means to deal with the overall building ventilation as well as to get some detailed information, such as the thermal comfort in a particular space.

There are at least two methods to integrate the multi-zone model with a CFD simulation. First is static integration, which simply transfers data once from the multi-zone model calculation results to the CFD simulation as boundary conditions. The second method is dynamic integration [2]. In dynamic integration, there are data transfers and feedbacks between the two models. Previous studies showed that the dynamic integration can improve the calculation of the multi-zone model in some simple mechanical ventilation cases. However, for natural ventilation the dynamic integration may not be able to improve the simulation if the user cannot properly apply the multi-zone model. For example, we may consider the well-known natural ventilation building, De Montfort Unversity (see Figure 6.1), which has multiple rooms and openings. To apply the multi-zone model program, such as MultiVent, we may get a network shown in Figure 6.2.

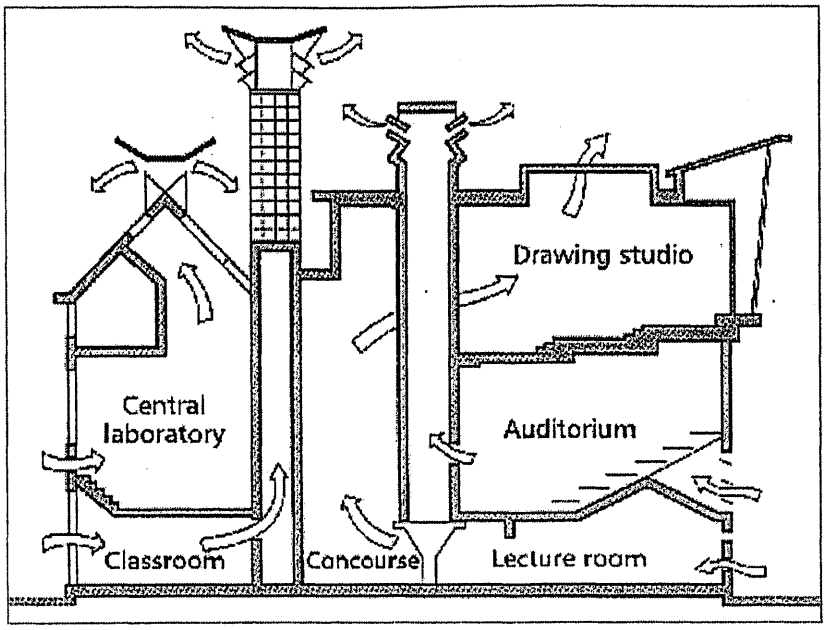

Figure 6.1 A naturally ventilated building in De Montfort University (by Y.G.Li)

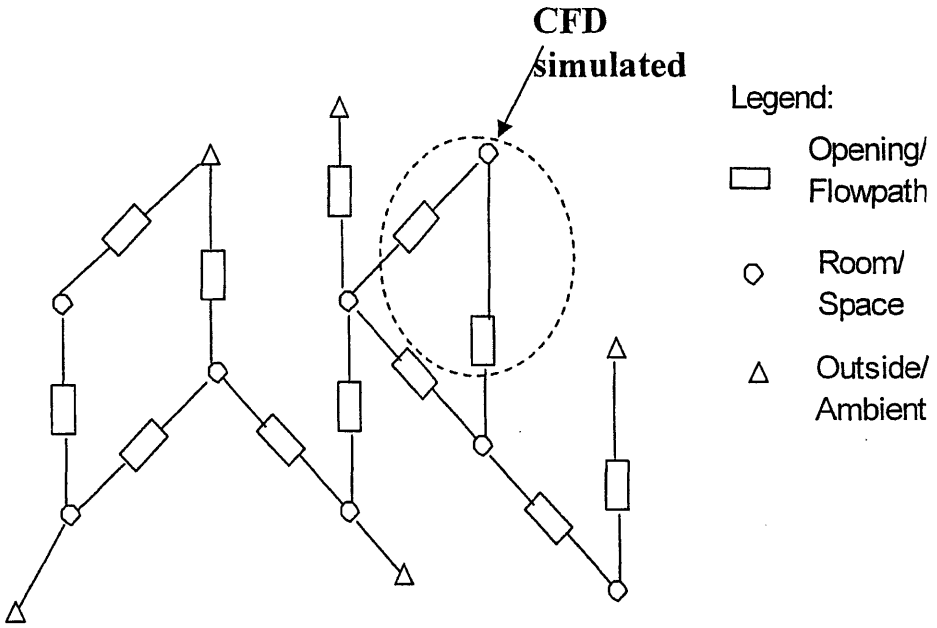

Figure 6.2 The network for multi-zone model calculation

As shown in Figure 6.2, the CFD simulation may only cover a very small part of the network, such as one or two rooms. It is obvious that the small CFD simulation part may not be able to improve the multi-zone model calculation for the whole building (network) if the multi-zone model cannot predict natural ventilation correctly by itself. If the user cannot properly deal with the special structure of naturally ventilated buildings, such as large openings and the atrium, the multi-zone model may not accurately predict the natural ventilation. As a result, if the multi-zone model provides wrong boundary conditions for CFD simulation, the dynamically integrated simulation may converge to a totally erroneous result.

Therefore, this work is trying to provide more accurate and reliable boundary conditions from the MultiVent program to the CFD simulation. In Chapter 4, several typical natural ventilation cases are investigated by applying the MultiVent. From these studies, we found that the MultiVent program can predict natural ventilation correctly in proper applications. The dynamic integration, which is used to improve the prediction of the multi-zone model, thus is not necessary for current work. To study the integration strategy, this research will focus on the static integration. In this chapter, we will examine the Luton model building [65] via statically integrating MultiVent with the CFD simulation.

6.2 Case description

The description of the Luton model building could be found in Chapter 4. Both the buoyancy ventilation and wind-buoyancy ventilation will be investigated in this chapter.

When integrating the multi-zone model with CFD, boundary conditions from the multi-zone model calculation results are provided to the CFD simulation for a particular space within the building. Here we assume that the third floor north side room in the Luton model building is the particular space of which the detailed information is wanted. In other word, only this room needs detailed simulation by CFD. The integration process could be summarized as following three steps:

1. MultiVent calculates the whole building.
2. Choose integrating boundary surfaces for CFD simulation.
3. CFD simulates the particular space with boundary conditions from the MultiVent calculation.

In Chapter 4, we have studied the methods to properly apply MultiVent to typical natural ventilation cases. After step 1, we need carefully consider step 2 to determine the integrating boundary surfaces, which may have strong impacts on the CFD simulation results.

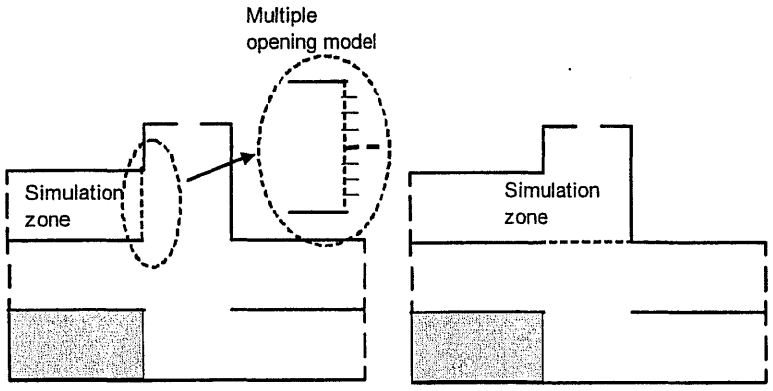

Strategy 1 Strategy 2

Figure 6.3 CFD simulation zones with different boundary surfaces

As we know, large openings and the atrium are usually designed in natural ventilation buildings to promote air flow rates. The existence of an atrium and large openings will affect the CFD simulation results if we do not properly select the integrating boundary surfaces. Two integrating boundary surface locations (see Figure 6.3), one at the vertical plane between the room and the atrium and the other including part of the atrium, are investigated by transferring boundary data from the MultiVent calculation results to the CFD simulation.

In step 3, we need to carry out the CFD simulation with the MultiVent supplied boundary conditions. There will be two choices to set the boundary conditions for CFD: either by using the velocity data or using the pressure data. To study these two integrating boundary conditions, we compare integrated simulation results of the velocity boundary condition method (see Figure 6.6 and 6.7) and the pressure boundary condition method (see Figure 6.8 and 6.9).

As shown in Figure 6.3, for strategy 1, the large opening is divided into eight small openings in the CFD simulation just as we did in the MultiVent calculation. The uniform velocity boundary condition from the MultiVent calculation results of case 2 (see Figure

4.7) is applied to each small opening in the CFD simulation. The airflow velocity at each small opening, in the MultiVent calculation, is derived as:

$$V_{0,(j,i)} = C_d[\frac{2\times(P_{0,j} - P_{0,i})}{\rho}]^{0.5} \tag{6-1}$$

where, the '0' subscript is labeled the small opening; the pressures of two sides of the small opening, $P_{0,j}, P_{0,i}$, can be calculated by following equations if we assume the small opening 0 located inside the building without wind pressure: $P_{0,i} = P_i + \rho_i g(h_i - h_0)$ and $P_{0,j} = P_j + \rho_j g(h_j - h_0)$ (see Figure 6.4).

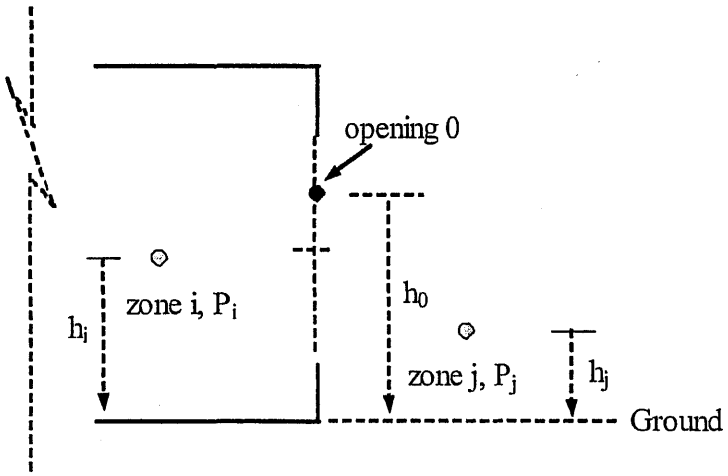

Figure 6.4 Illustration graph of the small opening 0

The uniform velocity can be calculated directly from MultiVent calculation results, which provide mass flow passing through each small opening.

$$V_{0,(j,i)} = \frac{F_{j,i}}{(\rho_{j,if.F_{j,i}>0}, or, \rho_{i,if.F_{j,i}<0}) \cdot A_0} \tag{6-2}$$

where, A_0 is the area of the small opening 0.

Small openings, such as the small opening 0 in equation (6-2), which sometimes may not touch the solid door frame, consist of a section through a stream tube. In a stream tube, the relationship between two points, such as the midpoints of zone j and zone i along a streamline, can be given by Bernoulli's equation. Therefore, the resistance power-law formula, such as equation (4-3), may not apply. However, to make the calculation in MultiVent consistent, we assume the power-law equation (4-3) still holds for the small

openings and use equation (6-1). Of course, the discharge coefficients (C_d) for the small openings are very close to unity (equal to 0.95 here), which means there is only a very small local resistance. This should be reasonable from the physical point of view. In contrast, the discharge coefficients of other vents and windows are set equal to 0.7 in the MultiVent calculation.

In the CFD simulation of strategy 2, a horizontal boundary surface that has the same height as the floor level of the third floor north room is adopted. A uniform velocity boundary condition, which is calculated by equation (6-2), is applied to this horizontal surface.

To examine the two integrating strategies in Figure 6.3, the integrated CFD simulation results are compared with the full CFD simulation. Parameters at four different elevations along six vertical lines are examined in the third floor north room. Figure 6.5 shows the six vertical line locations in the floor-plan.

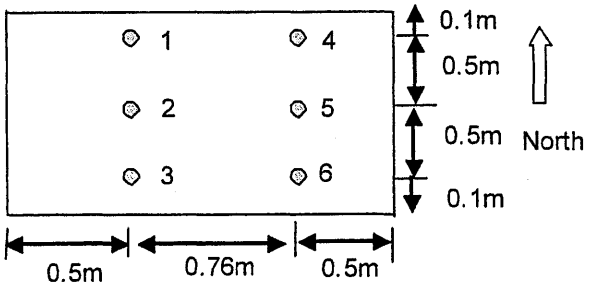

Figure 6.5 Plan view of the six locations examined in the 3rd floor north room

6.3 Integrated simulation results of buoyancy ventilation

6.3.1 Velocity integrated simulation results

Velocity and temperature parameters compared between the integrated CFD simulation results and the full CFD simulation results are shown in Figures 6.6 and 6.7. In these integration cases, the velocity integration method is applied to the CFD boundary condition. That is to say, the CFD simulation used velocity boundary conditions from the MultiVent calculation results that include airflow rates and air temperatures.

Figures 6.6 and 6.7 illustrate that both strategies can predict good temperature distribution, while strategy 1 cannot predict the velocity distribution as well as strategy 2, especially for the area close to the large opening. For strategy 2, the CFD simulation is applied to a portion of the atrium and the room space. Inaccuracies in the velocity distribution at the horizontal boundary surface will then be smoothed out before the flow enters the room. This is similar to the role of an entrance region in duct flow. In addition, in strategy 1 the atrium temperature is limited to either a single (case 1) or two (case 2) different values, whereas strategy 2 allows for a more detailed temperature distribution in the atrium space adjacent to the room. When using velocity data from the MultiVent as boundary conditions for the CFD model, setting one opening (e.g. the stack vents) as an outlet with a uniform pressure boundary condition may be helpful to easily meet the mass conservation of air in the CFD simulation.

6.3.2 Pressure integrated simulation results

An alternative method for setting boundary conditions in the CFD simulation uses the pressure data. Pressure data are transferred from the multi-zone model (MultiVent) calculation results to the CFD simulation as a boundary condition for an opening at height h_o can be calculated:

$$P_o = \frac{P_{o,j} + P_{o,i}}{2} \tag{6-3}$$

where, $P_{0,j}$ and $P_{0,i}$ are the two pressures at two sides of the opening at height h_0.

During pressure integration, all of the openings in the CFD simulation used pressure boundary conditions. In this pressure integration case, the CFD simulation zone is same as the strategy 2 of Figure 6.3, which shows a good simulation result in section 6.3.1. Figures 6.8 and 6.9 show the temperature and velocity comparisons between the pressure integration simulation results and the full CFD simulation results. These comparisons illustrate that the pressure integration yields a good agreement with full CFD simulation results. However, we may need to consider that the pressure in general CFD simulations indirectly affects mass and energy conservations. In addition, some CFD algorithms and turbulence models determine that the pressure simulation is not so accurate. As a general recommendation, we suggest using the velocity boundary integration method for coupling MultiVent with PHOENICS.

To clarify the integrated simulation cases, Table 6.1 summarizes the corresponding integrating strategy and boundary condition for each figure. In Figure 6.6 and 6.7, one integration case uses integration strategy 1 and the other uses strategy 2 (see Figure 6.3).

Table 6.1 The corresponding integrating strategy and coupling boundary condition for each integrated case (figure)

	Integrating strategy 1	Integrating strategy 2
Velocity boundary condition	Figure 6.6 and Figure 6.7	Figure 6.6 and Figure 6.7
Pressure boundary condition		Figure 6.8 and Figure 6.9

6.3.3 Discussion

Programs for the building simulation are often used within the planning process to improve the energy efficiency of the building. For the realization of such simulations, the applied building simulation tools (e.g. CFD simulation) have to be configured and parameterized for each building with complete information. Mostly this is a time-consuming and error-prone process because the necessary geometrical, topological and physical parameters are not completely available in the early design stage. However, the multi-zone model, such as MultiVent, can be adopted to simulate the whole building with little or preliminary design information.

With the calculation results of multi-zone model, CFD can then be used to simulate some particular spaces on which designers may have some detailed ideas. Applying CFD simulation to a single space will significantly reduce the computation time due to the much smaller grid number comparing with the CFD simulation to the whole building. Each of the above CFD simulations only cost approximately thirty minutes, which is significantly shorter than the ten hour cost of the full CFD simulation.

The above integration strategy studies show that we would better avoid taking the vertical surface as the integrating boundary surface. This problem is generated from the existence of the well-mixed assumption in the multi-zone model. Although the so-called Multiple Openings Model can divide the large vertical opening (surface) into several smaller sub-openings, it cannot solve the errors from the assumption of the uniform temperature in the connected space (i.e. atrium). In contrast, if we include part of the space connected with our interested space into the CFD simulation, it could smooth the airflow streamlines and improve the CFD simulation.

By studying the integration of MultiVent with PHOENICS in buoyancy ventilation cases, we can see that integration of the multi-zone model with the CFD simulation does accurately predict buoyancy natural ventilation and simulate the detailed thermal environment in the particular space. In following section, the integration strategy will be investigated under the wind and buoyancy combined ventilation.

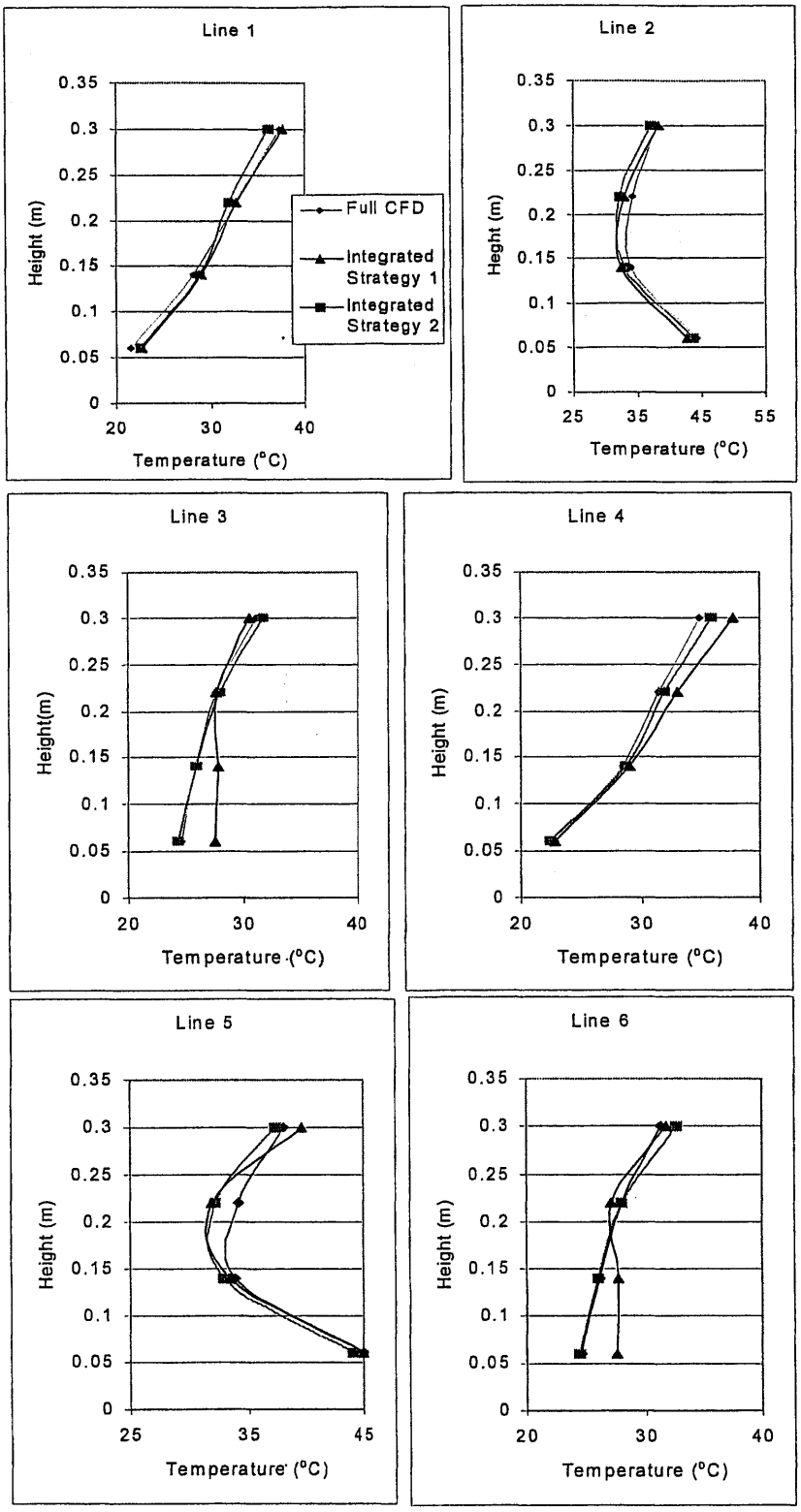

Figure 6.6 Temperature comparison of integrated strategy 1 and 2 (both using velocity boundary) results and CFD simulation results

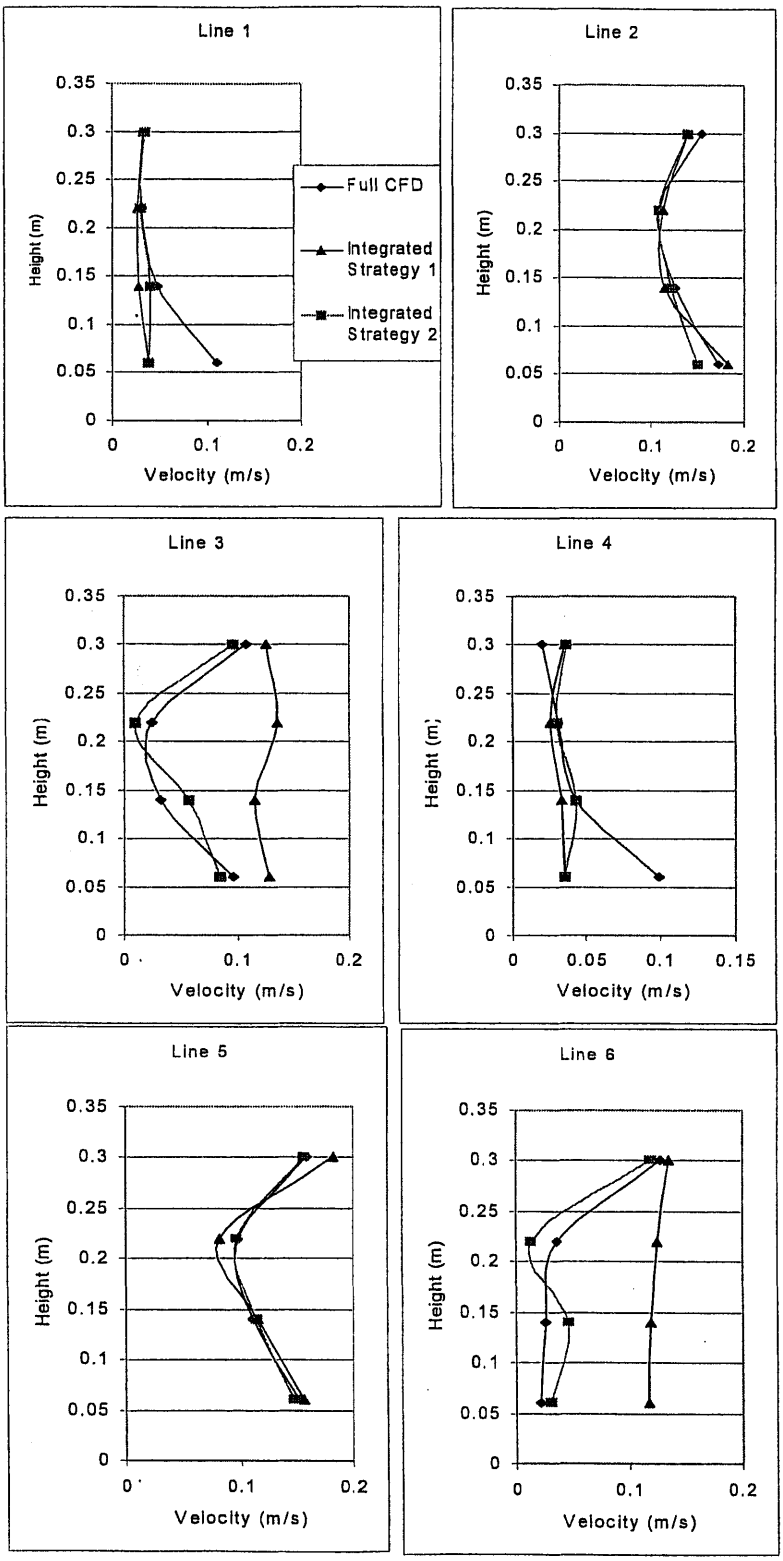

Figure 6.7 Velocity comparison of integrated strategy 1 and 2 (velocity boundary) results and CFD simulation results

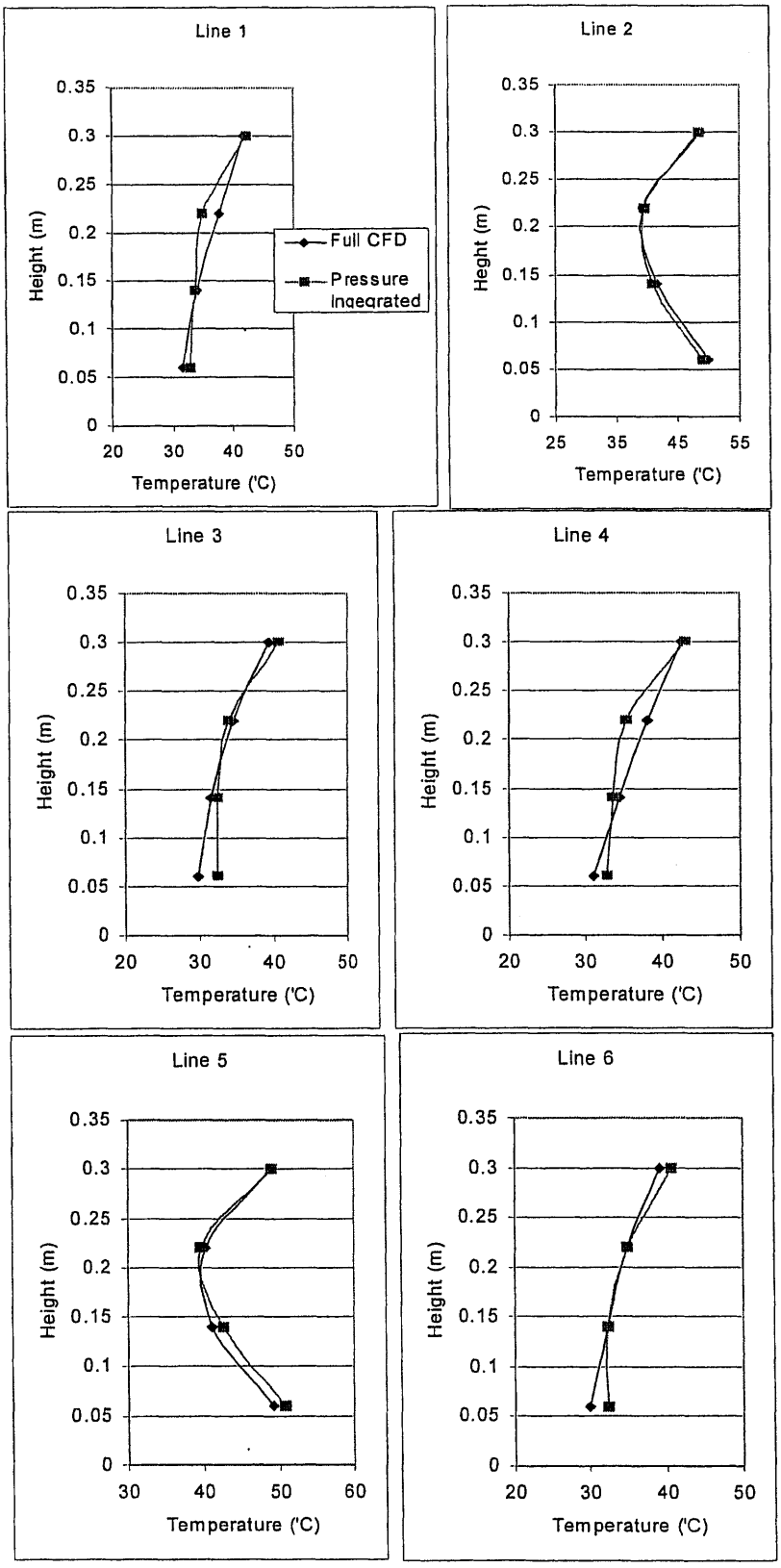

Figure 6.8 Temperature comparisons of pressure integration results and full CFD results

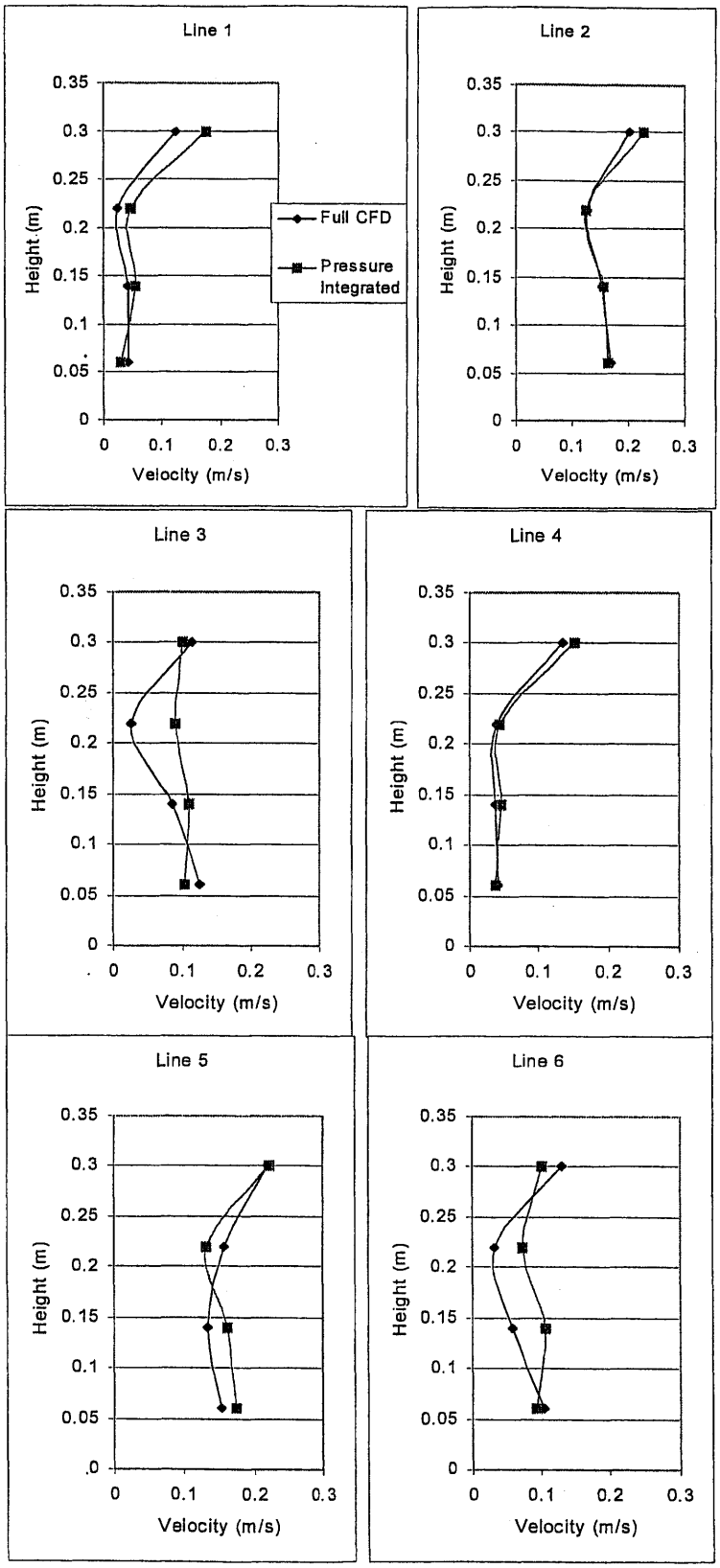

Figure 6.9 Velocity comparisons of pressure integration results and full CFD simulation results

6.4 Integrated simulation results of wind-buoyancy ventilation

With the simulation results of MultiVent calculation for the Luton model building case of wind-buoyancy ventilation in section 4.3.2, the CFD simulation of the third floor north room can be carried out. As discussed in previous sections, the integration strategy of including part of the atrium can provide more accurate CFD simulation results. Similarly, this integration method will be implemented in the wind-buoyancy ventilation (see Figure 6.10).

The velocity integration boundary condition is investigated in this section. Although we mainly use the mass flow rate from zone 5 to zone 6 as the velocity boundary condition for the inlet (see Figure 6.10), three outlets are also defined to easily keep mass conservation. In this case, we only simulate a simple cubic dome, which does not include the top part of the atrium. Under general condition, we may have to include this corresponding height of the atrium part space. For example, if the user is interested in the second floor north/south room space, the CFD detailed simulation dome should include the space zone 4 and 5. In the MultiVent calculation, the wind pressure coefficient of each exterior opening (windows and vents) is automatically generated by the MultiVent program with equation (4-6).

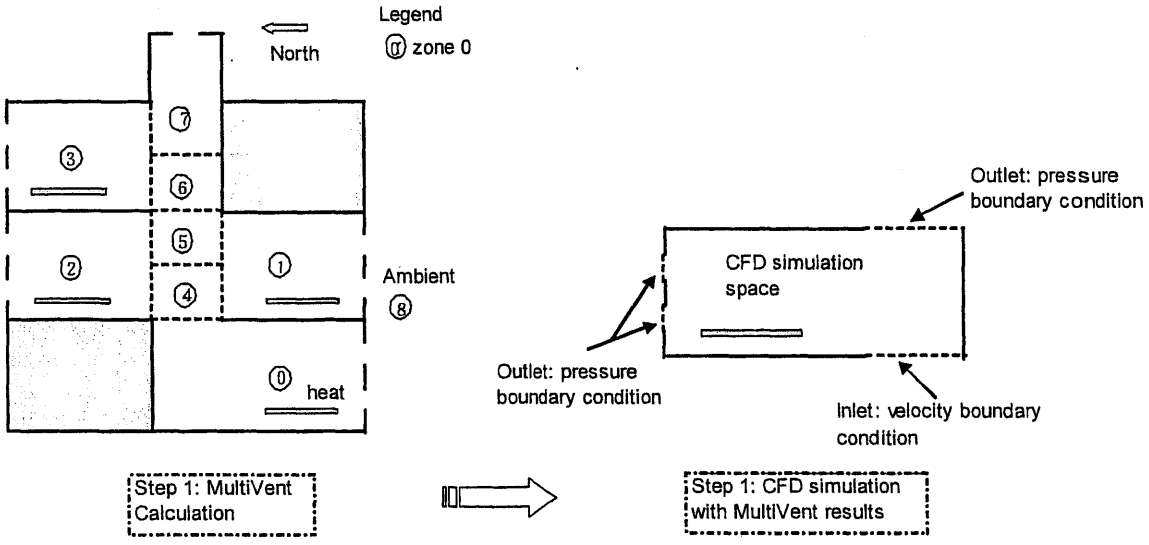

Figure 6.10 Integrated simulation process of wind-buoyancy ventilation case

The integrated simulation results for wind-buoyancy ventilation case are compared with the full CFD simulation results. Four points along six vertical lines in the third floor north

room are investigated through temperature and velocity comparison. The locations of the compared points are same as Figure 6.5. The full CFD simulation is that one shown in Figure 4.16.

Figure 6.11 shows the velocity comparison between the integrated simulation and the full CFD simulation. These two simulation results match very well, although there are small velocity differences in the locations that are close to the atrium. This difference is still generated by the well-mixed consumption of MultiVent, which introduces uniform velocity boundary condition at the inlet between zone 5 and 6 (see Figure 6.10). Figure 6.12 shows the temperature comparison between the integrated simulation and full CFD simulation, which has a very good agreement between these two simulations. Therefore, the integrated simulation of wind-buoyancy ventilation validates the accuracy of this integration strategy, which includes the connected part of atrium and applies velocity boundary condition. Besides, it also validates the calculation method for wind pressure coefficients in the MultiVent are acceptable.

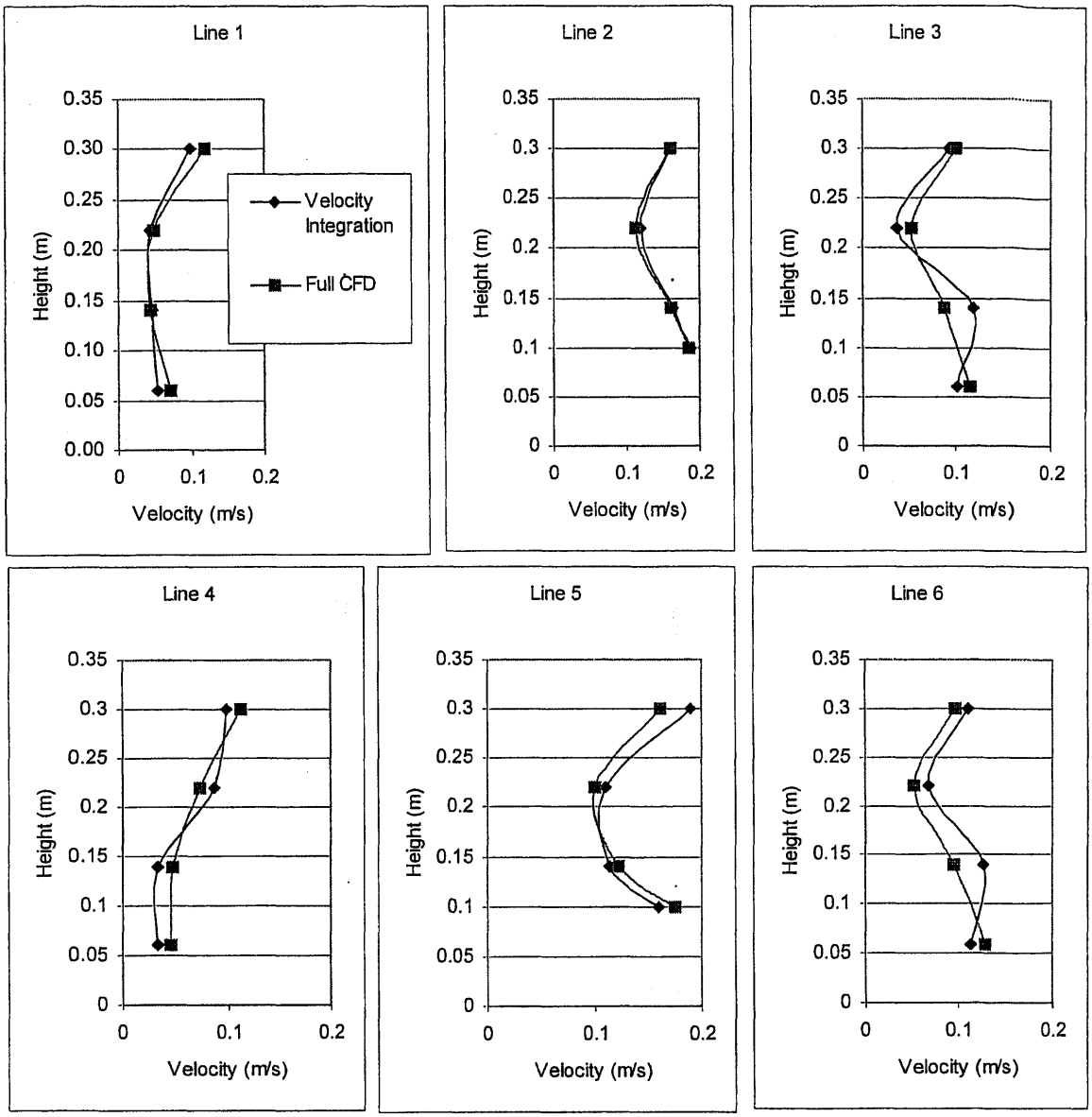

Figure 6.11 Velocity comparisons of velocity integration results and full CFD simulation results for wind-buoyancy ventilation

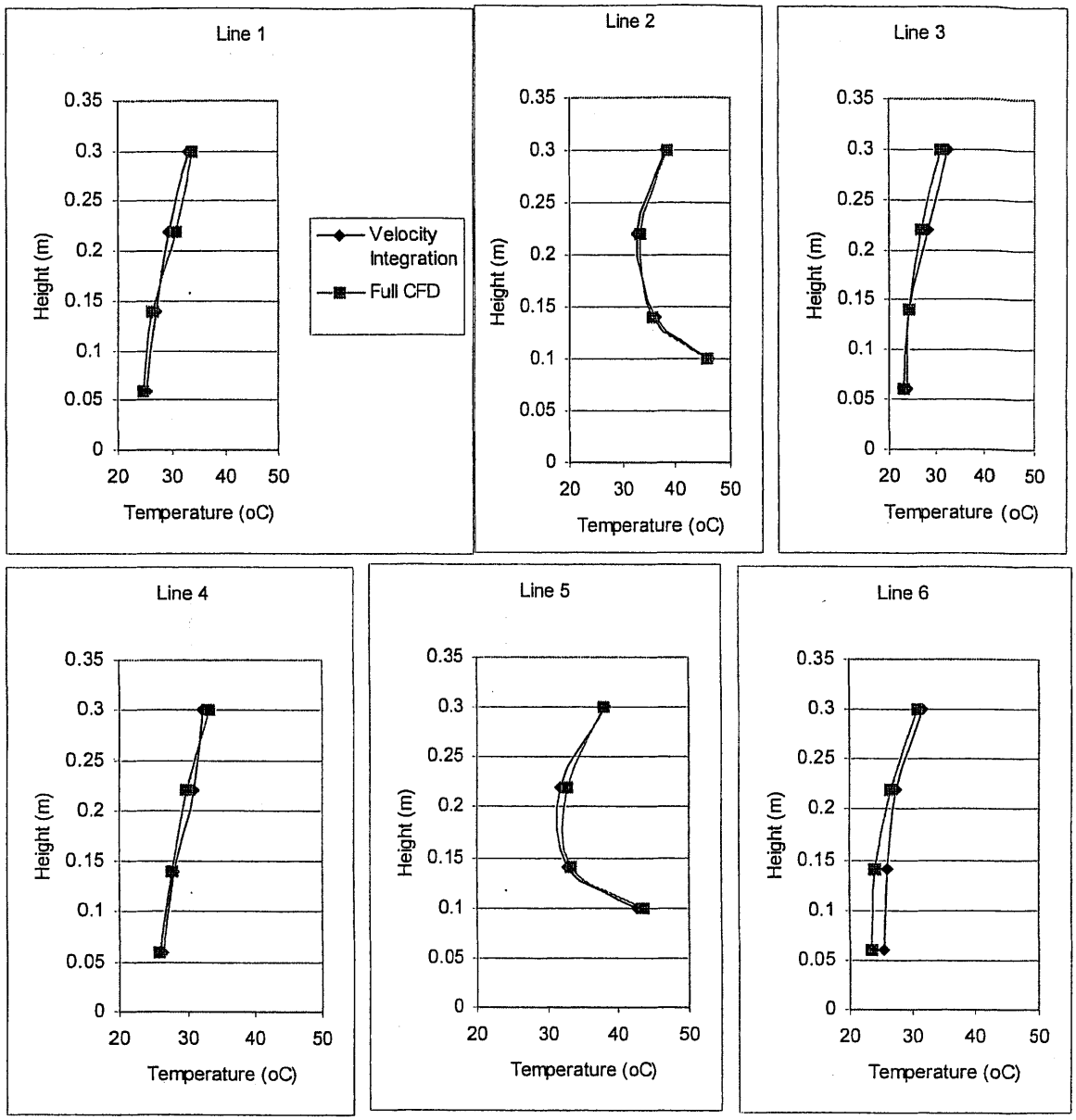

Figure 6.12 Temperature comparisons of velocity integration results and full CFD results for wind-buoyancy ventilation

6.5 Conclusions

In this chapter, the static integration strategy of MultiVent with CFD (PHOENICS) simulation is investigated. Because the complexity of naturally ventilated buildings limits the accuracy and application of the dynamic integration, we focused on static integration and studied the coupling strategy. Additionally, the boundary condition settings are also examined when we transfer the MultiVent calculation results to CFD simulation.

First, two integration strategies, single third floor north room or including part of atrium, are studied under buoyancy ventilation for the Luton model building. It seems that the strategy of including part of atrium can generate more accurate CFD simulation results because it gives a space for the airflow smoothing out the inaccuracy introduced by the uniform inlet boundary condition before the airflow enters the specific space.

Two boundary conditions, velocity or pure pressure boundary condition, are investigated with the integration strategy of including part of atrium under buoyancy ventilation. Simulation results showed that both of the boundary conditions can provide good CFD simulation results.

Finally, the integration simulation is also carried out under wind-buoyancy ventilation for the Luton model building. The results validate again that the integration strategy and velocity boundary condition can provide accurate CFD simulation in particular spaces.

Chapter 7

Generalize the Strategies of MultiVent Application and Integrated CFD Simulation for Natural Ventilation Prediction

7.1 Introduction

As discussed in Chapters 4 and 6, there are two main configurations that should be carefully considered in the prediction of natural ventilation: the atrium and large openings.

For buoyancy ventilation, two mechanisms can be applied to promote natural ventilation. One is solar radiation. For example, on hot sunny days the air temperatures in the atrium can rise to relatively high values, like a greenhouse. However, the air flow from atrium to occupied space should be avoided under this condition because the air in atrium is uncomfortably warm. This goal might be possible to achieve by ventilation. To avoid the additional costs associated with the ventilation of the atrium, buoyancy driven natural ventilation is desired, where the control possibilities are the location and size of openings in the walls of the atrium.

Another mechanism is to adopt internal heat sources inside the building. As we know, buoyancy results from differences in air density. Meanwhile, the density of air depends on temperature and humidity, although in MultiVent we do not consider the humidity difference between inside and outside environment. Cool air is heavier than warm air at the same humidity. Thus, heat given off by occupants and other internal sources tend to make air rise. The stale, heated air escapes from openings in the ceiling or roof, drawing fresher air in through lower openings to replace it.

Under this condition, the atrium and large opening are usually designed to increase the buoyancy force and reduce the air flow resistance inside the building. In this chapter, we will generalize the strategies of applying MultiVent to predict natural ventilation and integrating it with CFD (PHOENICS) to simulate the detailed information.

7.2 Generalization for MultiVent application in natural ventilation with the atrium and large openings

Most natural ventilation designs often simultaneously adopt the use of the atrium and large openings. Therefore, a case with both of these designed structures will be investigated to generalize the strategy for large openings and the atrium.

7.2.1 Case description

The Luton model building will be used to study the general rule for dealing with the large opening and atrium. Figure 7.1 shows the configuration of the model building. The third floor north room is the particular space that we will focus on. Three different sizes of openings between the middle atrium and the third floor north room will be investigated.

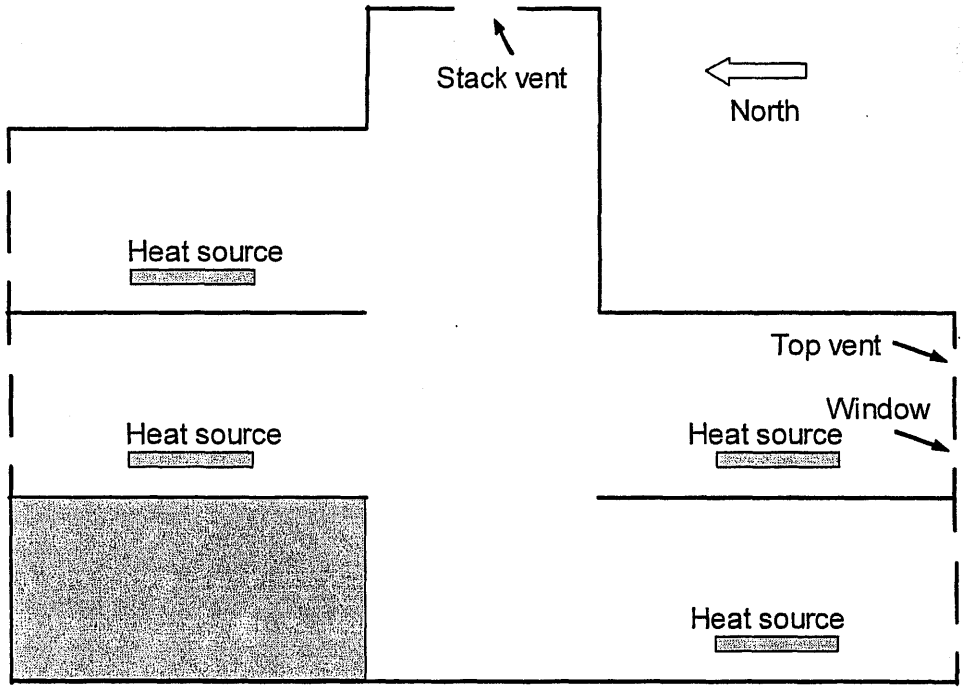

Figure 7.1 Configuration of the Luton model building

There are two optional MultiVent opening divisions for the three sizes of openings: dividing the large opening into two (see Figure 7.2, opening 'a' and 'b') or keeping single opening (see Figure 7.3, opening 'a'). If we apply the so-called Multiple Opening Model here, the problem may become confused because we cannot separate the effects of the

Multiple Opening Model from the effect of dividing the opening into two sub-openings. In fact, the strategy of dividing the large opening into two sub-openings can be viewed as an application of the Multiple Opening Model. The only difference is that the former is applied together with the atrium's zone divisions, while the latter doesn't require special zone divisions in the atrium. As we studied in Chapter 4, the Multiple Opening Model cannot significantly improve the natural ventilation prediction if we do not divide the connected atrium space into two zones. Therefore, in this case we will divide the vertical large opening between the third floor north room and the atrium into two sub-openings (opening 'a' and 'b' in Figure 7.2) and the connected atrium space into corresponding two zones shown in Figure 7.2 (zone 6 and 7).

In summary, in order to investigate whether the strategy of dividing the vertical large opening into two sub-openings and correspondingly splitting the connected atrium space into two zones works or not, we will compare the case shown in Figure 7.2 with the case shown in Figure 7.3. The case in Figure 7.3 has single opening between the third floor north room and the atrium where is only one zone (zone 6).

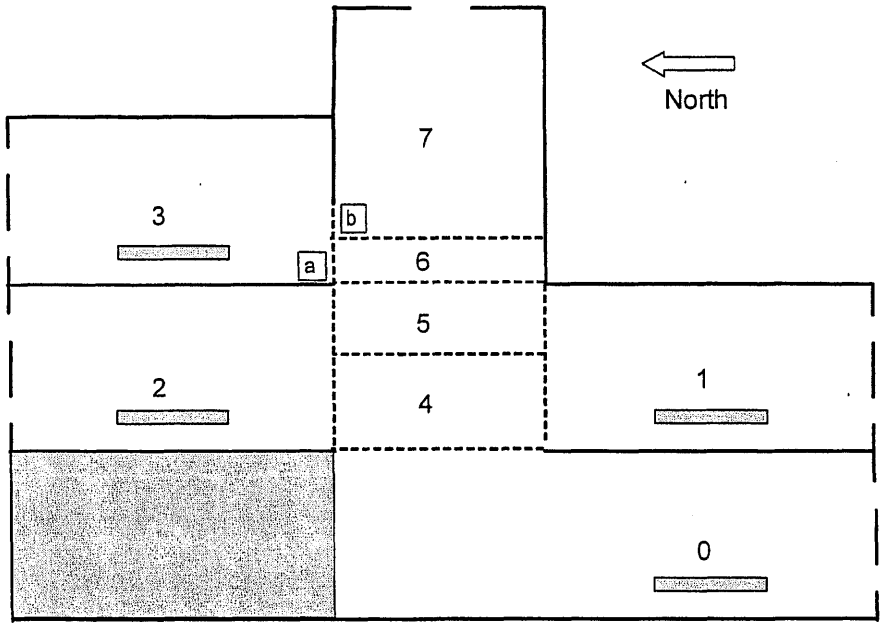

Figure 7.2 Two sub-opening ('a' and 'b') between the third floor north room and the atrium with two zones (6 and 7) in the connected atrium space

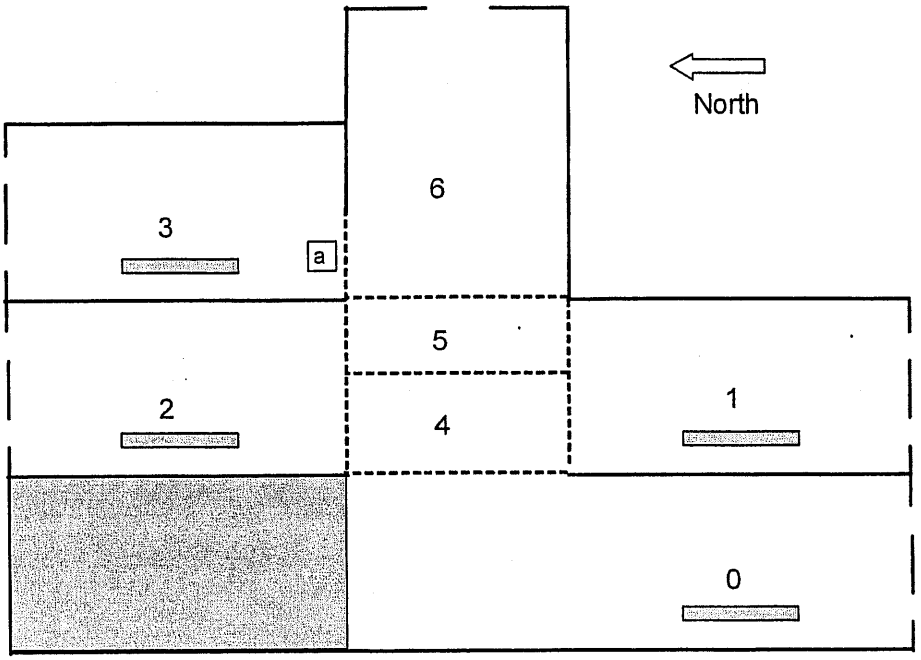

Figure 7.3 Single opening ('a') between the third floor north room and the atrium with one zone (6) in the connected atrium space

With the definitions of the strategy that has two/single sub-openings and two/single zones in connected atrium space, several cases with different sizes of the openings between the third floor north room (zone 3 in Figure 7.2 and 7.3) and the atrium (zone 6 and 7 in Figure 7.2, or zone 6 in Figure 7.3) can be studied. Table 7.1 summarizes the opening sizes corresponding to different opening and zone division strategies. In Table 7.1, the character 'Ho' is equal to the height of the opening between the third floor room and the atrium (combined height of openings 'a' and 'b' in Figure 7.2, or the height of opening 'a' in Figure 7.3), and the character 'H' is equal to the height of the third floor north room.

Table 7.1 Summary of opening sizes and zone divisions of the atrium for the six cases

Case Number	1	2	3	4	5	6
Two sub-openings and two corresponding atrium zones. (Figure 7.2)	Ho/H =40%		Ho/H =30%		Ho/H =20%	
Single opening and one corresponding atrium zone. (Figure 7.3)		Ho/H =40%		Ho/H =30%		Ho/H =20%

7.2.2 Buoyancy ventilation

The program MultiVent is applied to study the natural ventilation of six cases shown in Table 7.1. Due to the specific characteristics of this Luton model building, the opening discharge coefficients applied to the MultiVent calculation are listed as follows:

- The windows/vents on the exterior walls have Cd=0.7;
- The openings (vertical or horizontal) inside the building, except the vertical opening connecting the third floor north room and the atrium, have Cd=0.95;
- The vertical opening connecting the third floor north room and the atrium has Cd=0.75.

The zone air temperature results of MultiVent simulation for the six natural ventilation cases are shown in Table 7.2. The significant difference between the two cases with same opening size is highlighted in grey in the table.

Table 7.2 Zone air temperature summary and comparison between the six cases (oC)

Zones	Case 1	Case 2	Case 3	Case 4	Case 5	Case 6
0	26.63	26.66	26.67	26.66	26.66	26.66
1	33.04	33.08	33.08	33.06	33.07	33.04
2	33.04	33.08	33.08	33.06	33.07	33.04
3	45.79	48.44	48.63	48.44	48.43	48.30
4	29.68	29.70	29.74	29.70	29.74	29.67
5	33.04	33.05	33.02	33.02	33.02	33.01
6	33.06	33.06	33.03	33.03	33.02	33.01
7	34.01	-	33.04	-	33.03	-

Table 7.3 Summary of airflows through the opening 'a' (or opening 'b') and comparison between the six cases (kg/s)

Flow path	Case 1	Case 2	Case 3	Case 4	Case 5	Case 6
Opening 'a': airflow from zone 6 to zone 3 (Figure 7.2 and 7.3)	0.024	0.019	0.012	0.019	0.0168	0.019
Opening 'b': from zone 7 to zone 3 (Figure 7.2)	-0.0054	-	0.0072	-	0.0023	-

Note: The negative signal means the flow direction is reverse as the statement. That is, the airflow from zone 7 to zone 3 for case 1 through opening 'b' is -0.0054kg/s, of which the airflow direction is actually from zone 3 to zone 7.

From Table 7.2, we can see that the significant temperature difference between case 1 and case 2 happens at the air temperatures of zone 3. There is a 2.6°C difference between these two cases for zone 3. However, this difference is not so significant when it is compared with the air temperature difference of the outside air and the air leaving the building from zone 3, which is more than 25°C. Meanwhile, the other cases with 20% or 30% height openings have no significant air temperature differences between the two sub-opening case and single opening case in MultiVent calculation. The airflows in Table 7.3 illustrate why only case 1 and case 2 have significant air temperature differences in zone 3. For case 1, with 40% height opening (Ho/H=40%, see Table 7.1), there are reverse flows through opening 'a' and 'b' (see Figure 7.2). Although this reverse flow passing through the sub-opening 'b' is small, it affects the air exchange pattern and the air temperature of zone 3.

To validate the MultiVent's calculation, a full CFD simulation is carried out for case 1 that is buoyancy ventilation with 13°C ambient air temperature. Figure 7.4 shows the input definitions and boundary conditions of the full CFD simulation. As discussed in previous sections, we simulate the buoyancy ventilation's ambient environment by using a control volume that is set the surface temperature of the solid wall at constant temperature of 13°C. Additionally, the top outlet that is the boundary roof of the control volume can provide air mass exchange between the far ambient environment and the control volume (see Figure 7.4). Therefore, the exterior temperature of the top outlet is set equal to 13°C, with uniform zero pressure boundary condition at this top outlet.

The configuration of the control volume is 7m×5m×3m for length, width and height respectively. The height is specified as 'Hc' in Figure 7.4. In contrast, the size of the model building is 2.72m×1.76m×1.32m (Length×Width×Height). The height of the model building is specified as "Hm" in Figure 7.4. From comparison of these two configurations, we can see that the control volume should not affect the air flow around the model building because the solid boundary walls (or floor, outlet) are enough far away from the model building.

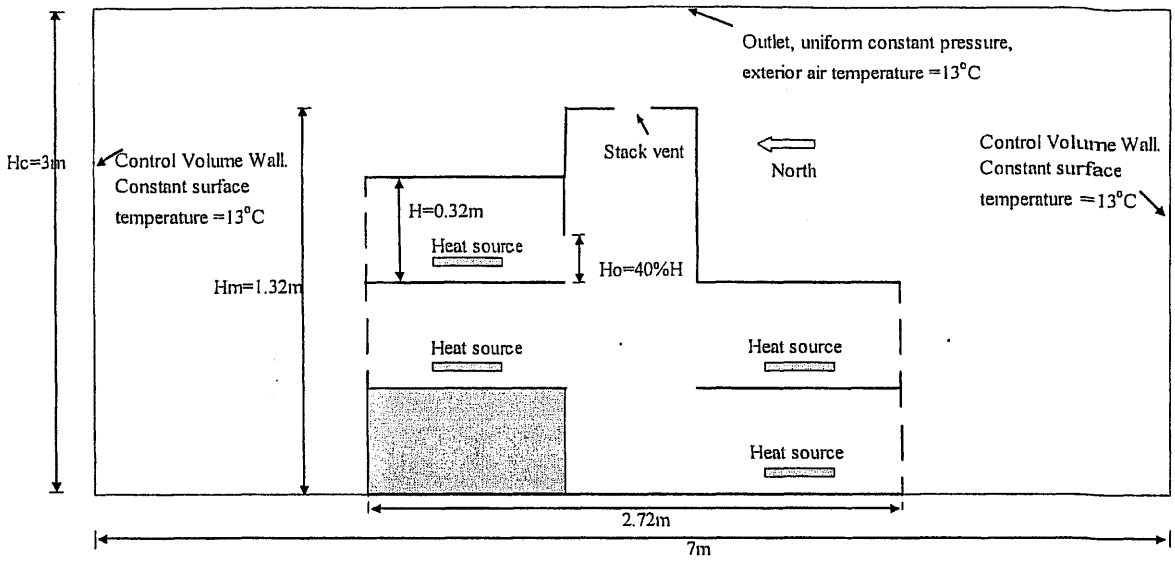

Figure 7.4 Sketch of the input and boundary conditions of the full CFD simulation

Similar to previous CFD simulations, the RNG k-ε model is applied here. In this full CFD simulation, the grid system is 64×49×73 for length, width and height with non-uniform grid sizes.

Figure 7.5 and 7.6 show the air flow distribution in the model building under the buoyancy ventilation condition. The main air flow pattern is the same as the MultiVent prediction. For example, from Figure 7.5, we find that the air enters the building from both upper vents and lower windows of the second floor rooms and leaves from the vents and windows of the third floor north room. If looking at the airflows at the opening that connects the third floor north room and the atrium, we also can find that there is a reverse flow (see Figure 7.6). Additionally, the airflow from the third floor north room (zone 3 in Figure 7.2) to atrium is much less than the airflow from atrium to the third floor north room, which matches very well with the MultiVent prediction of case 1 (see Table 7.1 and 7.3).

In addition to the good agreement between the airflow patterns, we also examined the average temperature comparison between the full CFD simulation and the MultiVent prediction for case 1 (see Table 7.4). The temperature comparison in Table 7.4 shows a good agreement between the full CFD simulation and MultiVent prediction. Although there is a small difference between the temperatures for the two calculations, this is generated by the well-mixed assumption of MultiVent zones. Each zone simply has a uniform air temperature and other physical parameters, such as pressure and density. This

assumption simplifies the problem but also incorporates approximations that will generate some internal errors. However, this small difference is acceptable for architectural design or general engineering applications. Thus, the full CFD simulation validates the accuracy of MultiVent calculation. Any conclusions obtained from MultiVent predictions for the six cases should stand firmly based on this validation.

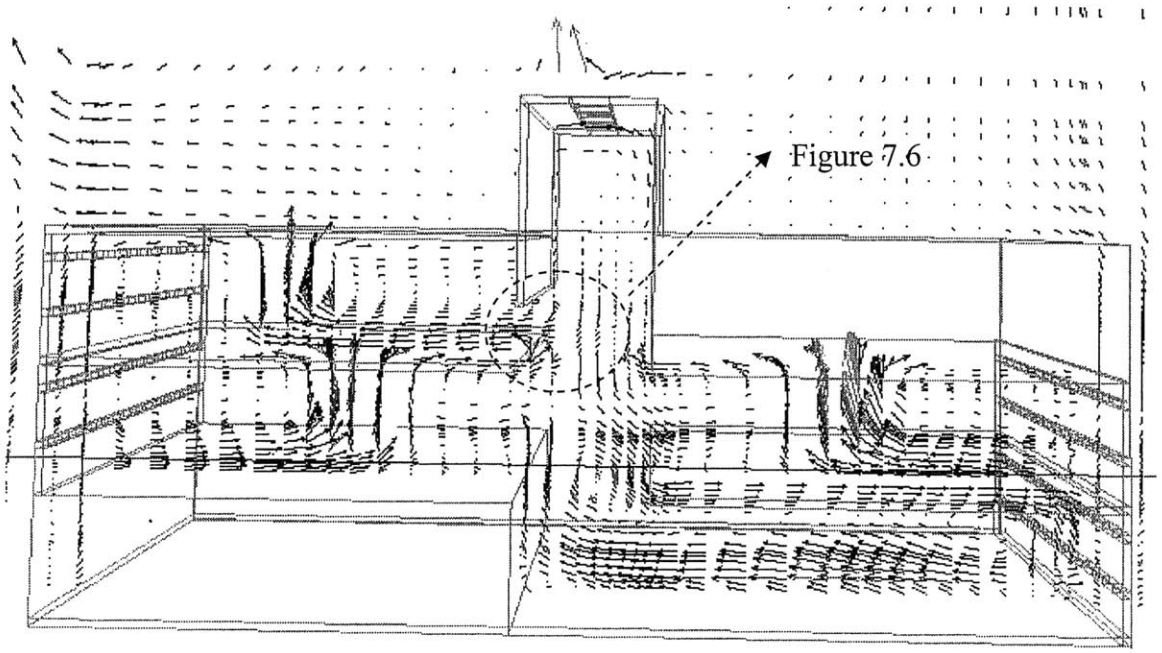

Figure 7.5 Full CFD simulation for the buoyancy ventilation case with Ho/H=40% value

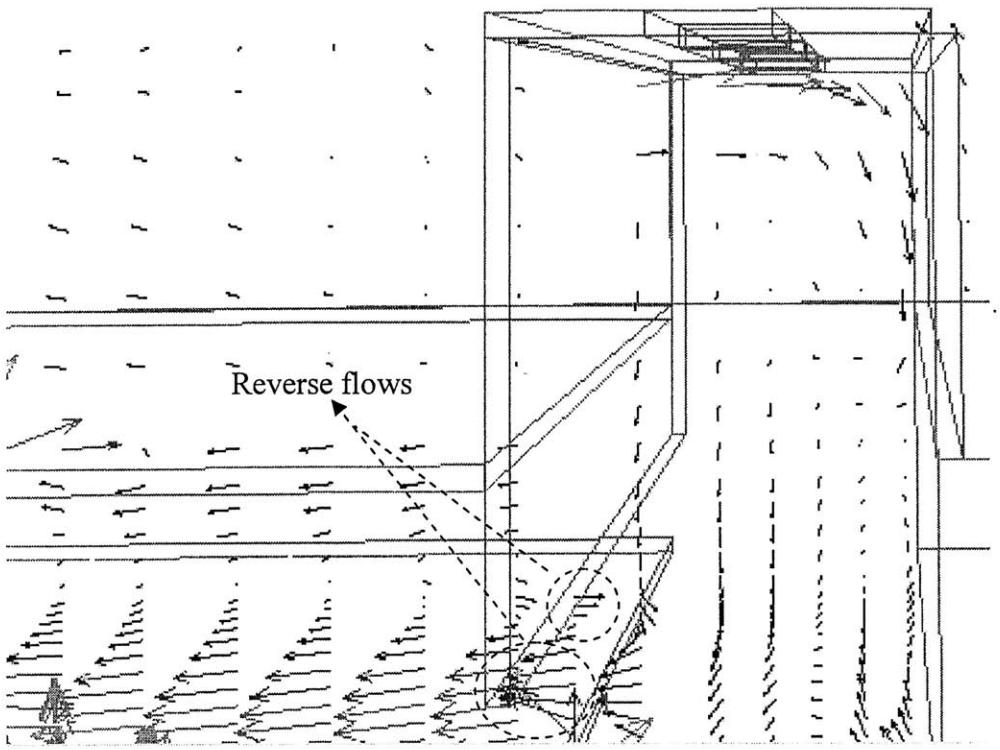

Figure 7.6 Detailed velocity distribution at the opening connected the third floor north room and atrium with Ho/H=40% value from full CFD simulation

Table 7.4 Temperature comparison between full CFD simulation and MULTIVENT prediction of buoyancy ventilation case 1 when Ho/H=40% (see Table 7.1 and 7.2)

	Zone 3	Zone 5	Zone 6	Zone 7
Full CFD simulation	44.55	30.95	31.47	32.29
MULTIVENT prediction*	45.79	33.04	33.06	34.01

Note: *The MULTIVENT prediction uses two sub-openings, same as case 1 in Table 7.2.

In Chapter 4, we found that the 100% height (Ho/H) opening should be divided into two sub-openings; otherwise MultiVent cannot accurately predict the air temperature of zone 3. It is reasonable that we can estimate that the air temperature prediction error for zone 3 will become greater with the opening height increasing to 60%, 80% or 100%, if we would not divide the vertical large opening between the third floor north room and the atrium into two sub-openings and correspondingly divide the connected atrium space into two zones. From this point of view, we can conclude that when an opening is greater than

40% of its connection to the occupied room (Ho/H>=40%), such as the third floor north room, we may need to divide the opening into two sub-openings and then divide the connected atrium space into two zones.

After we examined the cases when the large opening is located in the third floor north room, which only has an occupied room on one-side(zone 3 in Figure 7.7), we may need to investigate the conditions when the large opening locates in the second floor, where there are two occupied rooms on two-sides(zone 1 and 2 in Figure 7.7). If there are two occupied rooms on opposite sides such as Figure 7.7, we may predict that the MultiVent needs a different criterion for dividing the large opening and atrium because the air flow condition is different from the situation when there is only one occupied room on one-side shown in Figure 7.2.

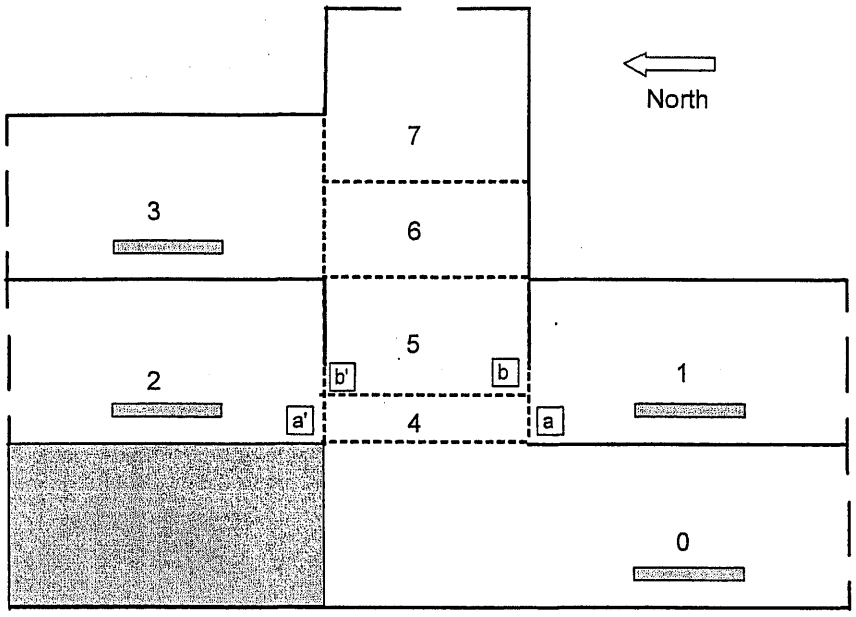

Figure 7.7 Two sub-openings ('a' and 'b') and two zones (4 and 5) in the connected atrium space of the second floor

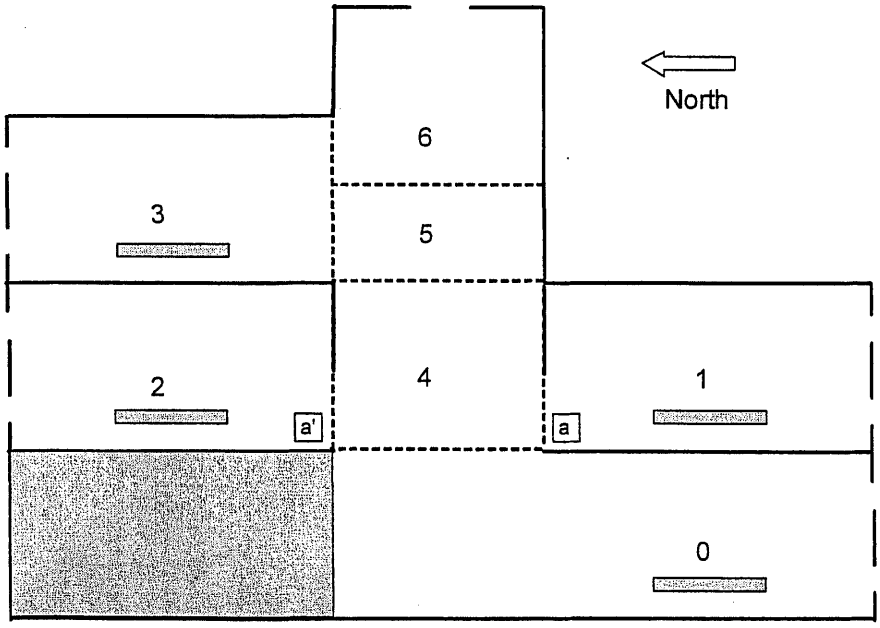

Figure 7.8 Single opening ('a') and one zone (zone 6) in the connected atrium space located of the second floor

For condition of the large opening located in the second floor, six cases with different heights of opening and zone divisions are studied via the MultiVent on-line calculation. Table 7.5 summarizes the cases' information.

Comparing the air temperatures of zone 1 and zone 2, we can see that there are significant differences between case 1 and case 2, and also between case 3 and case 4 (see Table 7.6). However, no large air temperature difference exists between case 5 and case 6. That is to say, with two-sided rooms, the openings with 30% or greater height of the occupied space (Ho/H>=30%), such as zone 1 and 2 in Figure 7.7, should be divided into two sub-openings.

We may consider that the Luton model building has a reasonable internal heat source when compared with the analogy of typical real buildings. Luton model building has 300W in a 1.92 m^2 area, which is approximately 156.3 W/m^2. This heat source is analogous to a heat source around $50W/m^2$ in office building. As we know, in typical full-scale buildings, the heat source in a market place is around $60\sim80W/m^2$, around $40\sim50W/m^2$ in an office space and much less in a residential space. Simply using the thermal theory, we know that the temperature stratification is positively correlated with the heat source strength, if the heat sources are mainly located in the lower part of space. Furthermore, the inverse flow is generated by the temperature stratification in the occupied space when the connected atrium space has smaller temperature stratification. Therefore, the conclusions from the Luton model building should cover the typical conditions of natural ventilation in full-scale typical buildings. In other word, the above 40% and 30% criteria for dividing the opening and connected atrium is a reasonable conclusion.

With above studying and discussion, we can reach following two strategies to applying MultiVent to the buoyancy ventilated buildings with a large opening connected with an atrium:

1. When the height of the opening equals or is above 40% of the connected occupied space (e.g. zone 3 in Figure 7.2), we should divide the opening into two sub-openings if the occupied spaces only locate at one side of the atrium.
2. When the height of the opening equals or is above 30% of the connected space, we should divide the opening into two sub-openings if the connected spaces locate at opposite sides of the atrium (e.g. zone 1 and 2 in Figure 7.7).

Of course, if we consider the typical heat strength in a full-scale building is analogous to the Luton model building, we may simplify the strategy to use MultiVent as: when the height of the opening (e.g. Figure 7.2 and 7.7) equals or is above 40% of the connected occupied space, we should divide the opening into two sub-openings. Correspondingly, the connected atrium space also needs to be divided into two small zones, which will improve the MultiVent simulation. The 40% criteria for the case when the occupied spaces locate on opposite sides of the atrium should not introduce big errors in Multivent calculation compared with the 30% criteria.

Table 7.5 Summary of cases and dealing method for the openings and zones for two opposite working space condition

Case Number	1	2	3	4	5	6
Two sub-openings and two corresponding atrium zones. (Figure 7.7)	Ho/H =40%		Ho/H =30%		Ho/H =20%	
Single opening and one corresponding atrium zone. (Figure 7.8)		Ho/H =40%		Ho/H =30%		Ho/H =20%

Table 7.6 Zone air temperature summary and comparison between the six cases for two opposite working space condition

Zones	Case 1	Case 2	Case 3	Case 4	Case 5	Case 6
0	26.40	25.94	26.21	25.82	25.74	25.63
1	35.14	41.35	37.51	42.01	42.75	43.06
2	35.14	41.35	37.51	42.01	42.75	43.06
3	40.17	40.29	40.36	40.41	40.71	40.64
4	26.43	33.18	26.23	33.28	25.74	33.45
5	33.09	-	33.25	-	33.55	-
6	33.16	33.27	33.32	33.33	33.60	33.51
7	39.51	39.71	39.74	39.86	40.22	40.17

7.2.3 Wind-buoyancy combined ventilation

After examining the Luton model building under buoyancy ventilation, we may need to investigate whether the above criteria could be suitable for natural ventilation when outside wind cannot be neglected. For example, when the wind velocity is around or greater than 1.0 m/s for Luton model building case, the wind pressure force may have the same order of magnitude as the buoyancy force. For the wind-buoyancy combined ventilation, we may only need to validate whether the above criteria obtained from pure buoyancy ventilation are suitable for cases with wind.

The opening that connects the third floor north room and the atrium will be taken as our objective to study the wind-buoyancy combined ventilation. Three opening sizes are examined for the two sub-opening cases and single opening cases: Ho/H=30%, Ho/H=40% and Ho/H=50% (see Table 7.7).

In this calculation, the outside wind velocity is equal to 1m/s at the height of 1.5 meters. The wind direction is exactly from south to north (see Figure 7.2 and 7.3). In comparison, we should notice that the Luton model building height is around 1.35 meters. The wind pressure coefficients are automatically predicted by MultiVent program according to the locations of the openings.

For the case with two sub-openings under wind-buoyancy combined ventilation, the zone divisions are the same as the case shown in Figure 7.2. Similarly, the case with a single opening has the same zone divisions as the case shown in Figure 7.3.

From the calculation results of MultiVent (see Table 7.8), it seems that the differences of the air temperature in the third floor north room between the corresponding two sub-opening case and the single opening case are smaller than the pure buoyancy ventilation cases. For instance, the temperature difference of 40% height opening is only 0.16°C compared with the pure buoyancy ventilation's 2.6°C. Even if the opening height is 50% of the third floor room's height, the temperature difference is only around 1.6°C. Although the temperature difference between the air entering the building and leaving the building is smaller than the pure buoyancy ventilation due to the existence of the wind, the ratio of these two cases' air temperature difference to the entering and leaving air temperature difference is slightly smaller or almost same as the pure buoyancy ventilation condition. Thus, we can conclude that the criteria strategies of dividing large openings for

applying MultiVent program achieved from pure buoyancy ventilation condition could be extended to all natural ventilation conditions.

Actually, this extension clearly obeys the physical theory. When the wind exists and cannot be negligible, the indoor air temperature should be closer to ambient than the pure buoyancy ventilation condition. The indoor air temperature stratification will be weaker than the pure buoyancy ventilation. Therefore we can see that the effects of the dividing two sub-openings will decrease and the criteria from buoyancy ventilation should be safely suitable for wind-buoyancy combined ventilation.

Table 7.7 Summary of cases for the different opening sizes under wind-buoyancy combined ventilation

Case Number	1	2	3	4	5	6
Two sub-opening and two corresponding atria zones. (Figure 7.5)	Ho/H =40%		Ho/H =50%		Ho/H =30%	
Single opening and one corresponding atria zone. (Figure 7.6)		Ho/H =40%		Ho/H =50%		Ho/H =30%

Table 7.8 Zone air temperature summary and comparison between the six cases under wind-buoyancy combined ventilation

Zones	Case 1	Case 2	Case 3	Case 4	Case 5	Case 6
0	22.35	22.34	22.33	22.35	22.34	22.34
1	23.38	23.36	23.34	23.37	23.36	23.35
2	29.36	29.35	29.33	29.35	29.35	29.35
3	40.25	40.09	38.53	40.15	40.12	40.10
4	22.85	22.83	22.82	22.84	22.83	22.84
5	26.99	26.98	26.97	27.0	26.99	26.99
6	26.99	27.01	26.97	27.0	27.02	27.01
7	27.02	-	28.35	-	-	27.02

7.3 Generalization of integrating the MultiVent with CFD simulation for natural ventilation with the atrium and large openings

When we apply MultiVent to predicting natural ventilation, it will generate some inaccuracy in the prediction results due to its simplified assumptions. For instance, the well-mixed zone assumption will create pressure errors for air flow calculation that then will result in temperature inaccuracy. Although this inaccuracy does not affect the application of MultiVent to natural ventilation prediction, CFD simulation may be required for some particular space in order to provide more accurate prediction. Besides the accuracy improvement, CFD simulation also can provide more detailed information for designers about the indoor thermal environment. Thus, designers can understand more about the future performance of natural ventilation in the designed building based on a more reliable prediction.

To integrate CFD simulation with MultiVent, two main problems arise:

- How to choose the integration zone and integration boundary surfaces.
- How to set boundary conditions for the integration boundary surfaces.

In Chapter 6, we have investigated the strategies of integrating CFD simulation with MultiVent. If we properly use MultiVent to predict the whole naturally ventilated building, the strategies of integrating MultiVent with CFD simulation can be concluded as following two methods:

- Choose the integration zone and integration boundary surfaces as follows:
  If the particular zone has a vertical opening (surface) to connect other interior zones, such as atrium, we should include part of the connected zone (e.g. atrium) to give a space to get rid of the effect of the uniform parameters of the connected zone due to the well-mixed assumption. However, for the vertical exterior openings and horizontal interior openings, it is not necessary to include part of the connected zone in CFD simulation.

- Set boundary conditions for the integration boundary surfaces as follows:
  Generally, the pure pressure boundary conditions and velocity (mass) boundary conditions could generate good results in CFD simulation. The velocity (mass) boundary condition is recommended because pressure does not directly interact with the mass and energy conservation.

7.4 Summary and conclusions

In this chapter, we investigated the strategies of applying MultiVent to natural ventilation prediction and integrating it with CFD simulation for a particular space. We focused on the main obstacles that make natural ventilation prediction difficult: the atrium and large openings.

First, the method of applying MultiVent to buoyancy ventilation is studied. Two conditions are examined: one-side occupied rooms connected with the atrium and opposite-side occupied rooms connected with the atrium. There is a slight difference for the criteria on the size of the large opening when we need to divide the opening into two sub-openings. However, if we consider the analogy of the heat source in the Luton model building, it is reasonable to choose Ho/H>=40% as the criteria to determine whether we should divide the opening into two sub-openings for design and engineering applications. The wind-buoyancy combined ventilation has slightly smaller temperature stratification than the pure buoyancy ventilation. Therefore, we can conclude that the benchmark of Ho/H>=40% is suitable for most of natural ventilation with an atrium and large openings.

After studying the strategies of applying MultiVent, we also summarized the method of how to integrate MultiVent results to CFD simulation for a particular space. Two problems were analyzed: choosing integration zone and setting boundary conditions.

Chapter 8

Conclusions and Recommendations

8.1 Conclusions

Natural ventilation is widely applied in newly designed buildings because it has the potential to significantly reduce the energy cost required for mechanically ventilated buildings. Natural ventilation does have many advantages to cool buildings; however, it also has some disadvantages when compared with the mechanical ventilation. The main shortcoming of natural ventilation is that it is difficult to control. Wind direction, wind velocity, heat sources and size of opened windows introduce uncertainties to natural ventilation airflow rates. Natural ventilation relies on the wind force and the buoyancy force to keep a building cool. In buoyancy ventilation, in order to prevent hot air moving into the upper level rooms, which may generate poor indoor thermal environment, we need to carefully design the height of the atrium/chimney and the areas/distribution of the windows in the building. Several methods provide quantitative predictions of the performance of the natural ventilation design: experiment measurement, analytical model [56], multi-zone model, and computational fluid dynamics (CFD) method. The objective of this work is to combine the advantages of both the multi-zone model and the CFD simulation in order to accurately and quickly assess the natural ventilation design. The contributions of this thesis include two main parts:

- Develop a new program by coupling the multi-zone airflow and thermal model for natural ventilation prediction.
- Investigate the strategies of how to integrate the multi-zone model with the CFD simulation.

1. A newly developed multi-zone model program for natural ventilation, MultiVent

The MultiVent program couples the multi-zone airflow and thermal model, which can be used to simultaneously iterate the indoor air temperature and airflows. At the early design stage, the designer may not have detailed configuration data about the designed building. Therefore, the multi-zone model rather than the CFD simulation can fit the prediction task and provide whole-building analysis to improve the design [67]. In addition, instead of requiring the user to estimate and set the indoor air temperature, the coupling method

of MultiVent program only asks the user to estimate a physically reasonable indoor heat source.

The numerical solution method of the coupled multi-zone airflow and thermal model has adopted the so called quasi-implicit difference method and the Newton-Raphson method. The quasi-implicit difference method has advantages of stability, convergence and quickness with a relatively larger time step compared with the explicit method.

The MultiVent program was validated for the buoyancy and combined wind-buoyancy ventilation by comparing it with the full CFD simulation. In order to properly use the MultiVent program in natural ventilation predictions, two structure factors were carefully examined: large openings and atria. The general method to deal with these two factors was investigated and it was concluded that: if the opening between the room and the connected atrium is higher than 40% of the height of the room, it is recommended to divide the opening into two sub-openings and divide the connected atrium space correspondingly into two sub-zones. When dividing the opening, we may simply divide it into two equal sub-openings. For general applications, the MultiVent program can provide prediction for natural ventilation design with accuracy of no more than 10% error in temperature and airflow (see cases in Chapter 4 and 6).

Besides the cases under general conditions, the extreme cases with plume re-entering into higher floor rooms were also studied by applying the MultiVent program and a two-step method was developed to handle these cases. Although these extreme cases can be avoided by adding some structures and may not happen when the ambient wind velocity is relatively high, the two-step method provides an example of how to deal with the cases under extreme conditions.

In order to provide the convenient way for users to use the MultiVent program, a web-server was developed during this thesis research. Four typical building scenarios were designed for a user's choice: atrium aided, wind-scoop aided, single-sided and cross ventilation buildings. Table 8.1 summarizes the strength of natural forces used in each type of the four typical natural ventilation adopted by MultiVent. The MultiVent program will automatically generate the zone division and the network before it operates the calculation. After the calculation, the MultiVent program provides virtual graphs for user to examine the calculation results. In addition to the building scenarios, the user also can define a more complicated case using user-self-designed case function.

Table 8.1 Application of natural forces adopted in the MultiVent natural ventilation types

Ventilation Type	Buoyancy Force	Wind Force
Atrium-aided natural ventilation	*****	**
Wind-scoop aided natural ventilation	***	****
Single-sided natural ventilation	***	-
Cross natural ventilation	-	*****

Note: The mark '*' in Table 8.1 shows the strength of the natural forces applied in the natural ventilation.

2. Strategies to integrate the MultiVent with the CFD simulation

The purpose of developing the integrating technique is to take advantages of both the multi-zone model and the CFD simulation. With the accurate prediction of the MultiVent, a static integration method was applied in current research to study the integrating strategies. That is to say, the CFD boundary conditions are supplied by the MultiVent simulation. The CFD simulation for a particular space can provide detailed information for users to understand the exact performance of the natural ventilation in this space.

To integrate the CFD simulation with the MultiVent, two main problems arise:

- How to choose the integration zone and integration boundary surfaces.
- How to set boundary conditions at the integration boundary surfaces.

This thesis has investigated the strategies for integrating CFD simulation with MultiVent and concluded the following integrating strategies:

- If the particular space (zone) has a vertical opening (surface) to connect other interior zones, such as atrium, we may need to include part of the connected zone (e.g. atrium) to allow an entrance zone to minimize errors introduced by the assumption of uniform parameters at the connecting surface.
- Generally, both the pure pressure boundary conditions and velocity (mass) boundary conditions can generate good results in the CFD simulation. The velocity (mass) boundary condition is recommended because pressure does not directly interact with the mass and energy balance.

8.2 Recommendations

In addition to the limitations that were discussed in previous chapters, the current work is still subject to further improvements or extensions in several areas.

1. For wind-buoyancy ventilation design, the wind pressure coefficients are automatically calculated by MultiVent program. However, the wind pressure coefficients applied in MultiVent program needs further validation via CFD simulation and thus we can improve the estimation of wind pressure coefficients.

2. MultiVent provides a visualization of simulation results for the four building scenarios. Up to now, MultiVent hasn't provided a visual view of results for a user self-designed case that differs from the four building scenarios. The algorithm to create the geometry connections between the zones and to supply enough information to the user design is still being developed.

3. For natural ventilation, MultiVent has been validated by full CFD simulation, for simultaneous buoyancy and wind-buoyancy ventilation. Due to the limitation of the available data, MultiVent hasn't been thoroughly validated by experiment measurements.

4. Night ventilation of thermal mass is a fundamental method to save energy with natural ventilation. In MultiVent, thermal mass transients are not included in the thermal model. Thus, MultiVent cannot provide the performance of transient thermal mass temperatures in natural ventilation design. In the future, the simple transient modeling for the thermal mass should be developed in MultiVent program, which would deal with simple thermal mass using a fast calculation method that is not be as complicated as other energy simulation programs (e.g. TRNSYS).

5. The strategies of integrating MultiVent with CFD have been investigated and summarized. Unfortunately, the automatically integrating function hasn't been implemented in current work due to the huge volume and complexity of the PHOENICS program.

8.3 Future prospective

Natural ventilation techniques can offer an important contribution to building design, in conformity with the criteria of sustainability. However, natural ventilation systems are more difficult to design in comparison with the traditional mechanical systems. These difficulties are increased by the conceptual problems from the non-linearity of physical processes of air movement in rooms. Therefore, natural ventilation is a very complex phenomenon that needs a lot of further studies. Several related areas that may need to be investigated in future are:

1. Include mechanical ventilation module into MultiVent

The current version of MultiVent is focused on the applications in natural ventilation. To meet more complex requirements, the mechanical ventilation module may need to be included in the MultiVent program.

2. Integrate multi-zone model with the zonal model

For architectural or simple engineering applications, the detailed and accurate prediction of CFD simulation may not be strongly necessary. Therefore, integrating the multi-zone model with the zonal model can provide a much faster and simpler strategy to evaluate the thermal and indoor air quality performance. The zonal model[30] is an alternative to CFD. In zonal models a room is divided into a relatively small number of zones, typically on the order of tens to hundreds, compared to thousands and more for typical CFD simulations. The zonal model lies between the multi-zone model and the CFD simulation. It may have more complicated thermal/airflow/contaminant/envelope sub-models compared with the multi-zone model, and then it can provide detailed information for the indoor environment predictions.

3. Develop automatically integrated program between MultiVent and CFD simulation

In order to provide a more convenient simulation service for architects, the automatic integration between MultiVent and CFD simulation is required. Some simple CFD programs, such as the MIT CFD program, may be chosen as the integrated code.

References:

1. Sustainable building technical manual: green building design, construction, and operations. Public technology, Inc., 1996. Web link: http://www.sustainable.doe.gov/pdf/sbt.pdf
2. Y. Gao, Q. Chen, Coupling of a multi-zone airflow analysis program with a computational fluid dynamics program for indoor air quality studies, *Proceedings of the 4th International Symposium on Heating Ventilating and Air Conditioning*, pp 236-242, 2003, Beijing, China.
3. P. Heiselberg, et al, Principles of hybrid ventilation, Hybrid Ventilation Center, Annex 35 IEA ECB BCS *Hybrid Ventilation*, Aalborg University, ISSN 1395-7953 R0207, Aalborg Univ., AUC, August 2002.
4. M. Deru, P. Burns, Infiltration and natural ventilation model for whole-building energy simulation of residential buildings, *Proceedings of the ASHRAE conference*, Kansas city, Missouri, June 28-July 2, 2003.
5. F. Haghighat, J. Rao, and P. Fazio, The influence of turbulent wind on air change rates - a modeling approach. *Building and Environment*, Vol. 26(2), pp 95-109, 1991.
6. J.D. Holmes, Mean and fluctuating internal pressures induced by wind, *Proceedings of the 5th International Conference of Wind Engineering*, pp 435-450, Fort Collins, Colombia, 1979.
7. A. Okamoto, T. Hasegawa, and S. Togari, Air-conditioning system of the KI Building. *ASHRAE Journal*, pp 32-37, Aug. 1992.
8. K.M. Musha, 1/f fluctuation of heartbeat period. *IEEE Transactions on Biomedical Engineering*, Vol. BME-29 (6), pp 456-457, 1982.
9. Y.Z. Xia, J.L. Niu, and R.Y. Zhao, Effects of turbulent air on human thermal sensations in a warm isothermal, *Indoor Air--International Journal Of Indoor Air Quality And Climate*, Vol.10 (4), pp 289-296, 2000.
10. Q.X. Jia, R.Y. Zhao, Simulation of natural wind with a new method, *Proceedings of the 3rd international symposium on heating, ventilation and air conditioning*, Shenzhen, China, pp154-158, Nov. 1999.
11. A.H.C. van Paassen, P.J. Lute, Energy saving through controlled ventilation windows, *The proceedings of the 3rd European conference on architecture*, Florence, Italy, 1993.
12. R. M. Aynsley, A resistance approach to analysis of natural ventilation airflow networks, *Journal of wind engineering and industrial aerodynamics*, Vol 67&68(1997), pp711-719.

13. J. Tsutsumi, T. Katayama, et val., Investigation and numerical simulation of the wind effects on thermal comfort in a house, *Journal of wind engineering and industrial aerodynamics*, Vol 60(1996), pp267-280.
14. R. Jozwiak, J. Kacprzyk, J.A. Zuranski, Wind tunnel investigations of interference effects on pressure distribution on a building, *Journal of wind engineering and industrial aerodynamics*, Vol 57(1995)., pp159-166.
15. F. Flourentzou, J. Van der Maas, C.A. Roulet, Natural ventilation for passive cooling: measurement of discharge coefficients, *Energy and Buildings*, Vol 27 (1998), pp 283-292.
16. Z.D. Chen, Y. Li, J. Mahoney, Natural ventilation in an enclosure induced by a heat source distributed uniformly over a vertical wall, *Building and Environment*, Vol 36 (2001), pp 493-501.
17. R.Y. Pelletret, W.P. Keilholz, COMIS 3.0-a new simulation environment for multi-zone air flow and pollutant transport modeling, *Building Simulation' 97-5th International IBPSA Conference, Prague*, 1997.
18. W. Dols Stuart, G. Walton, K. Denton, CONTAMW 1.0 User Manual, Gaithersburg, MD, NIST, 1997
19. T.P. McDowell, J.W. Thornton, S. Emmerich, and G. Walton, Integration of airflow and energy simulation using CONTAM and TRANSYS, *ASHRAE Transactions*, Vol. 109, No.1. pp 1-14, 2003.
20. S. Klein, TRNSYS-A transient system simulation program, Engineering Experiment Station Report 38-13. Solar Energy Laboratory, University of Wisconsin-Madison, 2000.
21. J.H. Ferziger, M. Peric, Computational methods for fluid dynamics, Spriner-Verlag, New York, 1996.
22. J.Y. Tsou, Strategy on applying computational fluid dynamic for building performance evaluation, *Automation in Construction*, Vol. 10 (2001), pp327-335.
23. Y. Jiang, Study of natural ventilation in buildings with large eddy simulation, Ph.D. thesis, Massachusetts Institute of Technology, Cambirdge, MA, USA, 2002.
24. Z.Q. Zhai, Q. Chen, Performance of coupled building energy and CFD simulations, *Energy and Buildings*, Vol. 37(2005), pp333-344.
25. D.B. Crawley, L.K. Lawrie, C.O. Pedersen, F.C. Winkelmann, EnergyPlus: energy simulation program, *ASHRAE Journal*, Vol. 42 (4) (2000), pp49-56.
26. C. Negrao, Conflation of Computational Fluid Dynamics and building thermal simulation, Ph.D. Thesis, University of Strathclyde, Glasgow, UK, 1995

27. A. Shaelin, V. Dorer, et al., Improvement of multizone model predictions by detailed flow path values from CFD calculation, *ASHRAE Transactions*, 93-7-4 (1993), pp 709-720.
28. Y. Gao, Q. Chen, Coupling of a multi-zone airflow analysis program with a computational fluid dynamics program for indoor air quality studies, *Proceedings of the 4th International Symposium on Heating Ventilating and Air Conditioning*, pp 236-242, Beijing, China, 2003.
29. G. Walton, AIRNET-A computer program for building airflow network modeling. NISTR, 89-4072, National Institute of Standards and Technology, 1988.
30. C. Inard, H. Bouia, P. Dalicieux, Prediction of air temperature distribution in buildings with a zonal model, *Energy and Buildings*, Vol. 24(1996), pp 25-132.
31. Y. Lin, POMA-A zonal model for airflow and temperature distribution analysis, Master thesis, Concordia, University of Montreal, Canada 1999.
32. J. Furbringer, C. Roulet, R. Borchiellini, et al., Evaluation of COMIS: final report, IEA Annex 23, 1996.
33. H.E. Feustel, A. Rayner-Hooson, et al., COMIS Fundamentals, Lawrence Berkeley Laboratory, report LBL-28560.
34. W. Stuart Dols, George N. Walton, Kevin R. Denton, CONTAMW 1.0 User Manual-Multizone Airflow and Contaminant Transport Analysis Sofware, National Institute of Standards and Technology, NISTIR 6476, 2000.
35. W.J. Layton, 2002, A mathematical introduction to Large Eddy Simulation, Research report, Department of Mathmatics, Unversity of Pittsburgh, Pittsburgh, PA 15260, USA. URL link: http://www.math.pitt.edu/techrep/0303.pdf
36. W. Zhang, Q. Chen, Large eddy simulation of indoor airflow with a filtered dynamic subgrid scale model, *Inter. J. of Heat and Mass Transfer*, Vol. 43 (17), pp 3219-3231, 2000.
37. Q. Chen, Prediction of room air motion by Reynolds-stress models, *Building and Environment*, Vol. 31(3), pp 233-244, 1996
38. P.K. Kundu, I.M. Cohen, Fluid Mechanics, Elsevier Academics Press, San Diego, California, 2004.
39. O. Reynolds, On the extent and action of the heating surface of steam boilers; Proc. Manchester Lit Phil Soc, Vol. 8, 1874.
40. L. Prandtl, Bericht ueber Untersuchungen zur ausgebildeten Turbulenz, ZAMM Vol. 3, pp 136-139, 1925.
41. A.N. Kolmogorov, Equations of motion of an incompressible turbulent fluid, Izv Akad Nauk SSSR Ser Phys VI No 1-2, pp56, 1942.

42. D.B. Spalding, Mixing and chemical reaction in confined turbulent flames, *The proceedings of the 13th International Symposium on Combustion*, pp 649-657, The Combustion Institute, 1971.
43. B.F. Magnussen, B.H. Hjertager, On mathematical modelling of turbulent combustion with special emphasis on soot formation and combustion, *The proceedings of the 16th Int. Symposium on Combustion*, pp 719-729, The Combustion Institute, 1976.
44. D.B. Spalding, A turbulence model for buoyant and combusting flows, *International J. for Numerical Methods in Engineering*, Vol. 24, pp 1-7, 1987.
45. D.B. Spalding, Multi-fluid models of Turbulence; Progress and Prospects, lecture CFD 96, the Fourth Annual Conference of the CFD Society of Canada, Ottawa, Ontario, Canada, June 2 - 6, 1996.
46. CHAM, "Phoenics-VR 3.5 reference guide", CHAM Ltd., London, UK, 2002.
47. B.E. Launder, D.B. Spalding, The numerical computation of turbulent flows, *Comp. Meth. in Appl. Mech. & Eng.*, Vol.3, pp269, 1974.
48. B.E. Launder, C.H. Priddin, and B.R. Sharma, The calculation of turbulent boundary layers on spining and curved surfaces, *ASME J Fluids Eng.*, Vol.99, pp321, 1977.
49. V. Yakhot, S.A. Orszag, Renormalization group analysis of turbulence, *J.Sci.Comput.*, Vol.1, pp3, 1986.
50. J.O. Hinze, Turbulence, McGraw Hill Book Company, Chapter 3, p181-190, 1959.
51. L.M. Smith, W.C. Reynolds, On the Yakhot-Orszag Renormalization group method for deriving turbulence statistics and models, *Phys. Fluids A.*, Vol.4, No.2, pp364, 1992.
52. V. Yakhot, L.M. Smith, The Renormalization group, the eps- expansion and derivation of turbulence models, *J.Sci.Comput.*, Vol.7, No.1, 1992.
53. V. Yakhot, S.A. Orszag, S. Thangam, et al., Development of turbulence models for shear flows by a double expansion technique, *Phys.Fluids A.*, Vol.4, No.7, 1992.
54. X. Yuan, Q. Chen, L.R. Glicksman, Y. Hu, and X. Yang , Measurements and computations of room airflow with displacement ventilation, *ASHRAE Transactions*, Vol. 105 (1), pp340-352, 1999.
55. N. Kobayashi, Q. Chen, Floor-supply displacement ventilation in a small office, *Indoor and Built Environment*, Vol. 12, No. 4, pp 281-291, 2003.
56. J.P. Lau, J.L. Niu, Measurement and CFD simulation of the temperature stratification in an atrium using a floor level air supply method, *Indoor and Built Environment*, Vol. 12, No. 4, pp 265-280, 2003.

57. J. Srebric, Simplified methodology for indoor environment design, Ph.D degree thesis, Massachusetts Institute of Technology, Cambridge, MA, United States, 2000.
58. Q. Chen, L.R. Glicksman, X. Yuan, S. Hu, Y. Hu, and X. Yang, Performance evaluation and development of design guidelines for displacement ventilation, Final report of ASHRAE RP-949, MIT, Cambridge, MA, 1998.
59. Q. Chen, Comparison of different k- ε models for indoor air flow computations, *Numerical Heat Transfer Part B: Fundamentals*, Vol. 28, pp353-369, 1995.
60. J.A. Clarke, Energy simulation in building design, Adam Hilger Ltd., Briston and Boston, pp 204, 1985.
61. Y.L. Wang, P. Gao, Study on effects of the wind pressure coefficients in infiltration calculation, *Journal of Harbin University of C. E. & Architecture*, Vol. 34 No. 4, 2001.
62. N. Heijmans, Technical report: Impact of the uncertainties on wind pressures on the prediction of thermal comfort performance (Annex 1: Wind profile models), IEA-ECB&CS Annex 35 HybVent.
63. C.F. Gerald, P.O. Wheatley, Applied Numerical Analysis, 3rd edition, Addison-Wesley Publishing Company, USA, 1985.
64. Z. Guan, J.F., Lu, Fundamental Numerical Analysis, 1st edition, High Education Publishing Company, Beijing, China, 1998.
65. C.E. Walker, et al., Building performance: analysis of naturally ventilated UK office building, Proceeding of Roomvent 2004, Coimbra, Portugal, September 5-8, 2004.
66. M. Grosso, Wind pressure distribution around buildings: a parametrical model, *Energy and Buildings*, 1992 (2), pp101-131.
67. D.M. Lorenzetti, Assessing multizone airflow simulation software, Proceedings of the 9th international conference on indoor air quality and climate (Indoor Air 2002), v.1 (2002), pp267-271.